LAMINAR BURNING VELOCITY OF MIXTURES OF AIR

WITH INDOLENE, ISOOCTANE, METHANOL AND PROPANE

by

Mohamad Metghalchi

B.S., Oklahoma University
(1975)

M.S., Massachusetts Institute of Technology
(1977)

SUBMITTED IN PARTIAL FULFILLMENT
OF THE REQUIREMENTS FOR THE
DEGREE OF

DOCTOR OF SCIENCE

at the

MASSACHUSETTS INSTITUTE OF TECHNOLOGY

February 1980

Signature of Author.. _ ......
Department of Mechanical Engineering
September 28, 1979

Certified by...
James C. Keck
Thesis Supervisor

Accepted by..
Warren M. Rohsenow
Chairman, Department Chairman

LAMINAR BURNING VELOCITY OF MIXTURES OF AIR

WITH INDOLENE, ISOOCTANE, METHANOL AND PROPANE

by

Mohamad Metghalchi

Submitted to the Department of Mechanical Engineering
on October 1, 1979, in partial fulfillment of the
requirements for the degree of Doctor of Science.

ABSTRACT

A facility for measuring the laminar burning velocity of fuel-air-residual gas mixtures has been constructed. It consists of a spherical combustion bomb in an oven which can be heated up to 500 K. The bomb is equipped with ionization probes to measure the arrival time of the flame at the wall and check the spherical symmetry of flame, a piezoelectric pressure transducer to measure pressure during the combustion process, and a balanced pressure indicator to calibrate the transducer. A laser shadowgraph system was used to measure the arrival time of the flame front at a known radius, and also to check the assumption of negligible pre-flame reaction.

A thermodynamic analysis was used to calculate laminar burning velocities from the pressure time history obtained during the combustion process. The burned gas properties were computed using an equilibrium assumption for the burned gas, and the unburned gas properties were computed using thermodynamic data from JANAF tables and assumption of frozen composition.

Laminar burning velocities of propane-air, isooctane-air, methanol-air, and a multicomponent hydrocarbon fuel similar to commercial gasoline (indolene)-air mixtures were measured in the pressure range of 0.4 to 40 atm and temperature range 298 to 750 K for fuel-air equivalence ratios from 0.8 to 1.5. The results are presented graphically and fitted to power law and exponential relations.

In addition, the effects of residual gases on the laminar burning velocity of stoichiometric isooctane-air mixtures were studied. The residual gases were simulated by a mixture of carbon dioxide in nitrogen (15% V/V with residual fraction of 10 and 20 percent by mass were used). The autoignition of end gases for isooctane-air mixtures were observed, and corresponding thermodynamic states are reported.

Thesis Supervisor: James A. Keck
          Title: Ford Professor of Engineering

ACKNOWLEDGMENT

It is my extreme pleasure to thank Professor James C. Keck for his guidance, patience, encouragement and inspiration that he provided generously during the entire course of this work. It has been my great privilege to work with him.

Other members of the thesis committee, Professors John B. Heywood, James A. Fay, Adel F. Sarofim, and Dr. Dirk Appel are also sincerely thanked for their valuable help both in private consultation and in committee meetings.

The author would like to thank Mr. Bob Dezmelyk and Professor William Unkel for invaluable assistance with the construction and installation of the on-line computer used in this work.

Next, I must thank Mr. Fee Yee, our Assistant Engineer in the Energy and Chemical Dynamics Laboratory for his assistance with the bomb hardware and electronics.

My next thanks goes to Mr. Mark Sellnau for his assistance in setting up the experimental facility.

Appreciation is also expressed to Ms. Sandra Williams for her excellent effort in typing this thesis.

Particularly, I would like to thank my wife, Flora for her understanding, patience, and sacrifices during the past two years. Sincere thanks also to my parents, my sisters, and my brothers for their constant encouragement, and most importantly, their unfailing moral support.

DEDICATED TO

MY WIFE, FLORA METGHALCHI,

and

KAZEM and KHORSHID METGHALCHI

TABLE OF CONTENTS

LIST OF TABLES

LIST OF FIGURES

13

CHAPTER 1

INTRODUCTION

The laminar combustion properties of fuels at high pressures and temperatures are of fundamental importance for analyzing and predicting the performance of internal combustion engines and power plants. Of practical interest is the laminar burning velocity, which is also called normal combustion velocity, flame velocity, or laminar flame speed. The laminar burning velocity is a physicochemical constant for a given combustible mixture, and is defined as the velocity, relative to the unburned gas, at which a plane flame front propagates into the mixture.

As a result of recent analyses carried out in connection with efforts to improve the efficiency and reduce the pollutants of automotive engines and burners, the importance of laminar flame speed data has become more evident. Among the parameters related to laminar flame speed are:

The thickness of the wall quench layers that are a primary source of unburned hydrocarbons and carbon monoxide [1], [2].

The minimum ignition energy required to ignite the charge. This in turn affects the range of equivalence ratios over which an engine can be operated [3], [4].

In addition the laminar flame speed is an important parameter in various turbulent combustion models [5] - [7] and can be used in con-

junction with basic combustion models to deduce activation energies
and reaction rates.

At the present time there is only limited information about the
laminar burning velocities of different fuel-air mixtures; this infor-
mation is mainly for gaseous fuel at low temperatures and pressures.
There is very little information for liquid fuels at the high tempera-
tures and pressures of importance for practical engines and burners.

This thesis is concerned with experimental and analytical work
using a heated spherical constant-volume combustion bomb to measure
the laminar burning velocities of several practical fuel-air mixtures
at different equivalence ratios, temperatures, and pressures encountered
in internal combustion engines and burners. The fuels studied were
propane, isooctance, methanol and an unleaded multi-component hydro-
carbon fuel similar to commercial gasoline.

In the approach taken here, the pressure record is the primary
measurement. A thermodynamic analysis of the pressure-time data was
performed to calculate laminar burning velocity as a function of
temperature, pressure and equivalence ratio. The effect of residual
gases on the flame speed for isooctance-air mixtures was also studied
and the spontaneous ignition limits for isooctance-air mixtures was
determined.

Chapter 2 discusses thermal, diffusion, and comprehensive theories
for calculating laminar burning velocity as well as different types of
experimental approaches to the problem. Chapters 3 and 4 describe the
experimental apparatus used in this study and the experimental procedure

for laminar burning velocity measurement. Analysis of the data is discussed in Chapter 5. Chapter 6 contains the experimental results and the laminar burning velocities for different fuel-air mixtures. Conclusion and suggestions for further work are offered in Chapter 7.

CHAPTER 2

LAMINAR FLAME PROPAGATION

Laminar flame propagation has been the subject of interest of many scientists and has been studied for over a century. Some researchers have studied the subject from a theoretical point of view while others have tried to understand this phenomenon by using an experimental approach to the measurement of laminar flame speed.

2.1 Theoretical Approaches

There are three theoretical approaches to laminar flame propagation: a) thermal theories, b) diffusion theories, and c) comprehensive theories.

The problem of determining the propagation velocity of a deflagration wave was first studied by Mallard and LeChatelier [8], who employed the thermal theory. They assumed that the flame consists of a preheat zone and a reaction zone and that the heat conducted from the reaction zone is the amount necessary to bring the unburned gases to the ignition temperature. With this postulation the energy equation becomes

$$\dot{m} \, C_p(T_i - T_u) = k(T_f - T_i)/\delta \tag{1}$$

where

k = thermal conductivity

C_p = specific heat at constant pressure

δ = thickness of the reaction zone

$\dot{m}$ = mass flow rate of combustible mixture into the flame

T_u = unburned gas temperature

T_i = ignition temperature

T_f = flame temperature

By substituting $\rho_u S_u$, where ρ_u is the unburned gas density and S_u is the laminar burning velocity, for $\dot{m}$ for a unit area Mallard and LeChatelier derived the following relation for laminar burning velocity

$$S_u = \frac{k}{\rho_u C_p} \frac{T_f - T_i}{T_i - T_u} \frac{1}{\delta} \tag{2}$$

By relating the thickness of the reaction zone to reaction time and reaction rate they came to the conclusion that laminar flame speed is proportional to the square root of the reaction rate.

Zeldovich, Frank-Kamenetski, and Semenov later improved the thermal theory of laminar flame propagation [9]. They included the diffusion of molecules as well as of heat but not that of free radicals or atoms. They derived the following relation for laminar flame speed

$$S_u = [(2k/\rho_u C_p)(I/(T_f - T_u))]^{1/2} \tag{3}$$

where

$$I = \frac{1}{a_o} \int_{T_u}^{T_f} \omega dT \tag{4}$$

a_o = number of mole of reactant per volume

ω = reaction rate

$$\omega = Z \exp(-E/RT) \tag{5}$$

Z = pre-exponential term in the Arrhenius expression

E = activation energy

R = universal gas constant

In this theory it was assumed that the total number of moles of mixture did not vary during the reaction and that the Lewis number was 1. Later Zeldovich et al. removed those restrictions and derived the following relation for laminar flame speed for a first order reaction [10]

$$S_u = [\frac{2k_f C_{pf} Z}{\rho_0 \bar{C}_p} (\frac{T_u}{T_f})(\frac{n_r}{n_p}) (Le)(\frac{R T_f^2}{E}) \frac{\exp(-E/RT_f)}{(T_f - T_u)}]^{1/2} \tag{6}$$

where

k_f = thermal conductivity evaluated at T_f

C_{pf} = specific heat evaluated at T_f

$\bar{C}_p$ = average specific heat between T_u and T_f

n_r/n_p = ratio of the number of moles of reactants to products

Le = Lewis number = $k/\rho D C_p$

D = diffusivity

VonKarman and Millan [11] also solved the mass, momentum, and energy equations neglecting diffusion and derived an integral relation for flame speed measurement.

The diffusion theory was used by Tanford and Pease [12]. They suggested that the diffusion of active particles from the flame front is the controlling factor in combustion, and they derived the following relation for laminar flame speed

$$S_u = [\sum_i \frac{k_i C x_i D_i}{Q B_i}]^{1/2} \tag{7}$$

where

k_i = rate constant appropriate to the ith active species

C = concentration of combustible

D_i = diffusion coefficient of the active particle into unburned gas

Q = mole fraction of potential combustion product

B_i = a factor usually close to unity, which corrects for the loss of radicals due to chemical processes.

x_i = calculated equilibrium mole fraction at the flame front

Many investigators have developed comprehensive theories of laminar flame propagation. The equations that describe a deflagration wave can be summarized as follows [8]:

Conservation of mass:

$$\rho v = m = constant \tag{8}$$

$$d \, \varepsilon_i/dx = \omega_i/m \tag{9}$$

Conservation of momentum

$$\rho v^2 + p - (\frac{4}{3} \mu + \kappa)dv/dx = constant \tag{10}$$

Diffusion equation

$$\frac{dX_i}{dx} = (\frac{m}{\rho}) \sum_{j=1}^{n} \frac{X_i X_j}{D_{ij}} (\frac{\varepsilon_j}{Y_j} - \frac{\varepsilon_i}{Y_i}) \tag{11}$$

Conservation of energy

$$m(\sum_{i=1}^{N} h_i \varepsilon_i + \frac{v^2}{2} - K \frac{dt}{dx} - (\frac{4}{3} \mu + \kappa)v \frac{dv}{dx}$$

$$\tag{12}$$

$$= constant$$

where:

v = velocity of gas mixture

X_i = mole fraction of species i

Y_i = mass fraction of species i

ω_i = rate of production of species i by chemical reaction

μ = coefficient of (shear) viscosity

κ = bulk viscosity coefficient

K = thermal conductivity

ε_i = $\rho Y_i (v + V_i)/\rho v$ is the mass flux fraction of chemical species i

V_i = diffusion velocity of species i

D_{ij} = binary diffusion coefficient for species i and j .

Hirschfelder et al. [13] were among the first investigators who tried to include both thermal and diffusion theories. In order to solve the set of nonlinear equations, Hirschfelder had to assume heat sink boundary conditions on the cold side. Von Karman and Penner [14] later simplified the governing equations (Eqs. (9) through (13)) by introducing the fact that the eigenvalue solution of the equations is the same for all ignition temperatures whether it be near T_f or not.

Since then many investigators have solved the governing equations for laminar flame propagation using various assumptions [8]. These solutions can not be used for complicated fuel where much essential information such as reaction rates, multicomponent diffusion coefficients, and diffusion velocity are not available to date. Because it is not yet possible to calculate the laminar flame speed of different fuel oxidant mixtures, it must be determined experimentally.

2.2 Experimental Approaches

2.2.1 Tube Method

In this method a tube is closed at one end and the gas is ignited at the open end. The combustion wave propagates from the open end to the closed end of the tube. Gerstein et al. [15] used the tube method to measure flame speed, and they used the following relation for determining laminar burning velocity

$$S_u = \frac{\pi R^2}{A} (S_s - S_g) \tag{13}$$

where:

R = flame radius

A = tube area

S_s = flame front speed with respect to tube

S_g = gas velocity in front of flame.

Gerstein et al. used photocells to measure the flame front speed S_s , and measured the gas velocity S_g , from the growth of a soap bubble blown from a tube connected to the flame tube.

2.2.2 Bunsen Burner Method [16]

This method has been used by many investigators. In this method, premixed gases flow up a cylindrical tube that is long enough to ensure streamline flow at the mouth. The gas burns at the mouth of the tube and the shape of the Bunsen cone is recorded and measured by various means.

The laminar flame speed can be measured using the following relation

$$S_u = V_0 \sin \alpha \tag{14}$$

where:

V_0 = velocity of the unburned gas

α = the cone apex angle

2.2.3 Flat Flame Burner

A flat flame can be created by placing a porous metal disk or a series of small tubes of 1mm or less in diameter at the exit of a larger flow tube. At low velocities, a flat stationary flame can be obtained a short distance above the burner matrix, whereas at high gas

velocities, a conical flame is produced. The burning velocity can then be calculated by dividing the gas volume flow rate by the flat flame area.

Since in this method there is an excessive heat loss from the flame to the burner matrix, the flame cannot be considered adiabatic. Botha and Spalding [17] utilized heat removal by the burner matrix, to stabilize the flat flame. They calculated the burning velocity for different flow rates by the area method. They plotted the burning velocity against the heat extraction rate, and then extrapolated back to zero heat extraction, to obtain the adiabatic burning velocity.

2.2.4 Soap Bubble Method

In this method the gas mixture is contained in a soap bubble and ignited at the center by a spark, and a spherical flame spreads outwards. The pressure remains constant in this experiment. Strauss and Edse [18] used the soap bubble method to measure the laminar burning velocity of methane-oxidant mixtures. They used the following relation for determining the flame

$$S_u = \frac{S_s}{E} \tag{15}$$

where S_s is spatial velocity which was determined photographically, and E is the expansion ratio, which represents the ratio of burned gas volume to unburned gas volume. The expansion ratio was determined from calculation of adiabatic flame temperature and combustion gas composition, assuming that complete chemical and thermodynamic equilibrium prevails in the burned gas.

2.2.5 Constant Volume Combustion Bomb

In this method the gas mixture is contained in a constant volume combustion bomb, and it is ignited centrally. This method measures the adiabatic flame speed, and one of its advantages is that the laminar burning velocity can be measured over a range of temperature and pressure in each experiment. Other advantages of this method are that the experimental facilities are easy to build and that experimentation is also easy.

Many investigators have tried to derive an explicit formula for the laminar burning velocity given the pressure history and the flame-front radius of the combustion process. Lewis and Von Elbe [19] assumed that the mass fraction burned is proportional to the pressure of the combustion process and derived the following relation

$$S_u = (1 - \frac{R^3 - R_f^3}{3p\gamma_u R_f^2} \frac{dp}{dR_f}) \frac{dR_f}{dt} \tag{16}$$

where:

R = radius of the combustion bomb

R_f = radius of flame front

p = pressure inside the combustion bomb

γ_u = unburned gas specific heat ratio

Subsequent workers have developed improved expressions for laminar flame speed. Garforth and Rallis [20] have derived the following relation for flame speed calculation.

$$S_u = (\bar{\alpha}/\beta)[F^2 + (\bar{\epsilon}/\bar{\alpha})(1 - F^2)]S_s + (1/\beta)\{(r_f F^3/3)(d\bar{\alpha}/dt)$$

(17)

$$+ [r_f(1 - F^3)/3] (d\bar{\epsilon}/dt) - (\bar{\alpha} - \bar{\epsilon})F^2(d\tau/dt)\}$$

where:

$\bar{\alpha} = \bar{\rho}_b/\rho_0$ ratio of average burned gas density to initial density

$\beta = \rho_u/\rho_0$

$\tau =$ flame front thickness

$F = 1 - \tilde{\tau}$

$\bar{\epsilon} = \bar{\rho}_f/\rho_0$ ratio of average density of gas within the flame front to initial density

$r_f =$ flame front radius

$\tilde{\tau} = \tau/r_f$

For a thin flame, Eq. (17) reduces to the following relation:

$$S_u = \frac{\bar{\rho}_b}{\rho_u} S_s + \frac{r_f}{3\rho_u} \frac{d\bar{\rho}_b}{dt}$$

(18)

which Garforth and Rallis [20] call the burnt gas equation for buning velocity. Equation (16) is referred to as the unburnt gas equation for burning velocity.

Other investigators such as Bradley and Mitcheson [21] and Ryand and Lestz [22] have recently measured the flame speed in a constant volume combustion bomb, and have reported measurements for different fuel-air mixtures which will be discussed in a later chapter.

CHAPTER 3

EXPERIMENTAL APPARATUS

3.1 Combustion Bomb

A schematic diagram of the combustion bomb used for the measure-
ments reported in this thesis is shown in Fig. 1. The combustion bomb
is spherical and has an inside diameter of 152.4 mm with a 19 mm wall
thickness, and was designed to withstand a pressure of 700 atm. The
combustion bomb material is 4150 FM alloy steel in the annealed condi-
tion. The two halves are held together by 6 clamp bolts and sealed by
a fluorocarbon o-ring. The combustion bomb is located in a 400mm × 400mm ×
460mm glass wool oven and can be heated electrically to a temperature
$\approx 700K$. However, because of the temperature limitations of the Kistler
pressure transducer and the o-ring, the maximum temperature at which
measurements could be made was 500°K.

3.2 Gas and Fuel Manifold

The gas and fuel handling system is shown in Fig. 2. The bomb
is located inside the oven. A thermocouple gauge is used to measure
the vacuum pressure. Three bourdon tube gauges with different ranges
are used to read the pressure of the system. An oil manometer and a
dead weight tester are connected to the system in order to calibrate
the pressure gauges. A mercury manometer is placed inside an oven
directly beneath that containing the bomb. It can be heated up to 400°K
and is used to measure the pressure of the fuel when the combustion bomb
is at elevated temperatures. Liquid fuel is injected through a septum.

A detail of the fuel injection system is shown in Fig. 3. The system consists of a high temperature silicone compound under compression. Liquid fuels are injected using syringes sized according to the amount of fuel injected.

3.3 Electrodes and Ignition System

Standard 14 mm spark plugs with extended stainless steel electrodes that were tapered to a point at their tips were used to form the spark gap at the center of the bomb. Figure 4 shows a spark plug with its extended electrode. The gap between two electrodes was set at 0.5 mm. A standard capacitive discharge ignition system in which the energy stored in the capacitors can be varied from a few millijoules to 2 joules was used for producing the spark. Figure 5 shows the electrical circuit for the ignition system.

3.4 Dynamic Pressure Measurement

The dynamic pressure inside the combustion bomb was measured with a piezoelectric Kistler pressure transducer, Model 603B1, coated with Dow Corning high-vacuum grease and calibrated against a balanced-pressure indicator.

Figure 6 shows a schematic diagram of the balanced-pressure indicator that screws into the combustion bomb. At its inner end it carries a 0.001 inch steel diaphragm between two 0.002 inch steel rings, supported by two heavy disks. In operation, a steady gas pressure, called the "balancing pressure", is applied to the outer side of the diaphragm, whose inner side is exposed to combustion bomb pressure. As the pressure inside the combustion bomb passes through

equilibrium with the balancing pressure, the diaphragm is deflected one way or the other, and makes or breaks an electrical contact wit- a center conductor. This conductor is connected to the sensing circuit shown in Fig. 7 which produces an output pulse when the contact is made or is broken. This pulse is fed into the CRT cathode of an oscilloscope, and causes a bright spot to appear on the pressure trace at a point corresponding to the balancing pressure. This pulse also stops a counter, recording the precise time at which the pressure inside the combustion bomb equals the balancing pressure. This infor- mation is used to calibrate the Kistler transducer on each run and effectively minimizes errors due to the thermal sensitivity of the Kistler transducer.

3.5 Ionization Probes

The arrival time of the flame front at the wall was measured using ionization probes. There are three ionization probe positions on the perimeter of the combustion bomb, two of which are diametrically opposed. All are flush with the spherical inner surface of the combus- tion bomb. These probes are used to check for spherical symmetry of the flame propagation.

The details of the probes are given in Fig. 8. The insulation gap on the probe was 0.025 mm. This prevented significant penetration of the electric field beyond the interior wall and eliminated the problem of premature signals [23]. The electrical circuit which was used with the ionization probes is shown in Fig. 9. Three counters

were used to read the time at which each of the three ionization probe pulses occurred.

3.6 Laser Shadowgraph

The arrival time of the flame front at a known radius was measured using the laser shadowgraph system shown in Fig. 10. A 5 milliwatt He-Ne laser with a wavelength of 6328Å was used. The beam diameter was 1.8 mm and the intensity distribution inside the beam was Gaussian. The distance from the center of the combustion bomb to the laser beam was 64.64 mm. The window inserts were made of stainless steel and are shown in Fig. 11. Since the ports are used for fine optical measurements, quartz windows were used in the apparatus.

When the flame front passes through the laser beam a diffraction pattern similar to that produced by a knife edge is produced. Using this system the time when the flame front cuts the laser beam can be measured to ± 0.1 msec and the radius of the flame front can be measured to ± 0.15 mm. A comparison of this radius with the corresponding value from the pressure measurement is used to check the assumption of negligible preflame reactions.

3.7 Data Recording Equipment

Figure 12 shows the data handling and processing equipments used in the experiment. It consists of a two-channel 12-bit analog-to-digital converter controlled by a microcomputer. The maximum number of digitized points per channel is 256 and the time increment between points is 0.25 msec. The instrumentation also includes four counters which are used to read the time at which the ionization probe

pulses occur and that at which the balanced-pressure switch closes.
An oscilloscope is used to monitor all inputs. The experimental
procedure will be discussed in the next chapter.

CHAPTER 4

EXPERIMENTAL PROCEDURE

The bomb was first heated to the desired temperature which was monitored by four thermocouples. The first thermocouple was welded to a washer and a small socket screw was used to hold the washer on the top of the combustion bomb. The second thermocouple was welded to a washer placed under one of the clamp bolts that holds the two halves of the combustion bomb together. The third one was hung loose in the oven one inch above the combustion bomb, and the fourth one was located close to the injection septum. The accuracy of an individual measurement was $\pm$ 3°C, and the maximum spread in temperature among four thermocouples was $\pm$ 10°C. The time required for the temperature to stabilize under heated conditions was 45 minutes at most.

In order to prepare a fuel-air mixture, first the combustion bomb was pumped down to a pressure less than 30 millitorr. For gaseous fuel the bomb was filled to the desired pressure and 5 minutes settling time was allowed to elapse. Statistical studies described in Chapter 6 showed this time to be adequate. Then the plumbing lines were evacuated till pressure was less than 30 millitorr, and air was introduced into the bomb up to the desired pressure. A waiting time of 5 minutes permitted the fuel and air to mix completely and become quiescent.

For liquid fuels the amount of liquid necessary to make the desired fuel-air mixture was calculated and then injected through the septum in the manifold. It was noticed that the measured pressure of

the fuel was not the same as the calculated pressure based on the ideal gas calculation of the fuel vapor and the assumption that all the fuel evaporates. This phenomenon was observed for all fuels and is discussed in Appendix A. In order to achieve the desired pressure, more fuel was injected into the manifold and the pressure was read with the mercury manometer. Again, the plumbing lines were pumped down, air was introduced into the combustion bomb, and 5 minutes waiting time was allotted to permit the fuel and air to mix completely.

Next the question of charge stratification was considered. The density ratio of two different heights was calculated by the following relation

$$\frac{\rho_2}{\rho_1} = \exp(\frac{-g(Z_2 - Z_1)}{RT})$$ (19)

where ρ_1 and ρ_2 are densities at two heights of Z_1 and Z_2. The ratio of densities at the top and bottom of the combustion bomb was 0.99998 for air and 0.99993 for isooctane which was the heaviest fuel studied. The equivalence ratio variation in the combustion bomb is $\leq$ .05%, which is negligible compared to measurement errors.

After the filling procedure was completed, the pressure transducer was zeroed and the mixture ignited. Figure 13 shows a typical oscillogram for a stochiometric propane-air mixture having initial conditions of 1 atm and 300K. The horizontal scale is 10 msec/div. for pressure and ionization probe-signals. The vertical scale for the pressure signal is 1.36 atm/div. The balancing time of the pressure inside the bomb with the pressure on the balancing side of the balanced-pressure

indicator is represented by a dot before maximum pressure. The laser signal is delayed 22 msec and the sweep rate is 1 msec/div. It can be seen that the laser signal has the same characteristics of a signal produced by a sharp edge.

The analog signals from the pressure transducer and the laser were fed directly to the microcomputer and the digitized data were transferred automatically from the microcomputer to the host computer. Times from the ionization probe and balanced-pressure indicator were input manually to the host computer. The data could be processed immediately or stored in the memory for later analysis.

CHAPTER 5

ANALYSIS OF DATA

In the data reduction process the dynamic pressure record was first calibrated. This was necessary since the calibration curve of a piezoelectric transducer is temperature sensitive. There are three options available for calibration of a piezoelectric transducer. One method is to accept the piezoelectric pressure transducer signal and calculate flame speed based on that signal. A second method is to use the balanced-pressure indicator. For this method the following relation was used

$$p_i = p_o + \frac{p_b - p_o}{p_{k,b} - p_o} (p_i - p_o) \qquad (20)$$

where:

p_i = pressure of the mixture

p_o = initial pressure of the mixture

p_b = balancing pressure

$p_{k,b}$ = pressure of the mixture at the time when balanced-pressure switch closes

The third method is to match the final mass fraction burned to the desired value. For this method the following relation was used:

$$p_i = p_o + \frac{x_d}{x_f} (p_i - p_o) \qquad (21)$$

where p_i and p_o are the same as Eq. (21), x_d is the desired final mass fraction burned and x_f is the mass fraction burned

calculated at the maximum pressure measured by the Kistler pressure transducer.

In the analysis of the data it is assumed that for a flame radius greater than a centimeter or two it is a good approximation to assume that the thickness of the flame front is negligible and that the gas within the bomb consists of a burned fraction x at thermodynamic equilibrium and an unburned fraction $1-x$ frozen at its original composition. The unburned gas itself consists of two parts. The first part consists of the portion of unburned gas which is compressed isentropically, and the second part is the portion of the unburned gas contained in the thermal boundary layer at the combustion bomb wall, which conducts heat to the bomb wall. It is further assumed that the pressure p is uniform, there is no stratification of the charge and the flame front is smooth and spherical although cellular flames have been observed for rich fuel-air mixtures by Babkin et al. [37].

Under these conditions and using one-dimensional heat conduction from the unburned gas to the bomb wall it is shown in Appendix B that the equations for the conservation of volume and energy can be written as follows:

$$V/M + A\delta/M = \int_0^x v_b dx' + \int_x^1 v_u dx' \qquad (22)$$

$$E/M - (A/M) \int_0^\delta p d\delta' = \int_0^x e_b\, dx + \int_x^1 e_u dx' \qquad (23)$$

where:

V = combustion bomb volume

M = mass of gas in the bomb

E = total initial energy of gas in the bomb

v = specific volume

e = specific internal energy

δ = displacement thickness

A = combustion bomb wall area

x = mass fraction burned

x' = integration variable

and the subscripts b and u refer to burned and unburned gas respectively. The displacement thickness is defined as

$$\delta = (1/\rho_\infty) \int_0^\infty (\rho - \rho_\infty)dr \qquad (24)$$

where:

ρ = density of unburned gas within the thermal boundary layer

ρ_∞ = density of that portion of unburned gas that compresses isentropically

It is shown in Appendix C that

$$\delta(t) = (\frac{\mu_0}{\pi \rho_0})^{1/2} (\frac{p_0}{p})^{1/\gamma_u} \int_0^t [((\frac{p'}{p_0}) \\ - (\frac{p'}{p_0})^{1/\gamma_u}) (\int_{t'}^t \frac{p''}{p_0} dt'')^{-1/2}]dt'$$

(25)

where:

μ_0 = viscosity of unburned gas at the initial temperature and pressure

γ_u = specific heat ratio of unburned gas

t = time

p_0 = initial pressure of gas mixture

ρ_0 = initial density of gas mixture

t', t'' = integration variables

For slowly varying specific heats of burned gas, $v_b(T_b, p)$ and $\rho_b(T_b, p)$ may be expanded in a Taylor series about the mean gas temperature:

$$\bar{T}_b = \frac{1}{x} \int_0^x T_b(x', x) dx' \qquad (26)$$

Neglecting terms of order $(T_b - \bar{T}_b)^2$ and higher, Eqs. (22) and (23) become

$$V/M + A\delta/M = x v_b(p, \bar{T}_b) + (1-x) v_u (p, s_{uo}) \qquad (27)$$

$$E/M - (A/M) \int_0^\delta p d\delta' = x e_b(p, \bar{T}_b) + (1-x) e_u(p, s_{uo}) \qquad (28)$$

where s_{uo} is the initial entropy.

The fraction error in x introduced by this approximation is derived in Appendix D, and is

$$\frac{\delta x}{x} \approx \frac{(\delta T_b)^2}{24 C_{vb}(\bar{T}_b - T_u)} \left(\frac{\partial C_{vb}}{\partial T} \right)_p \tag{29}$$

where C_{vb} is the equilibrium specific heat of the burned gas at constant volume and δT_b is the spread in burned gas temperature. For the range of conditions investigated, $\delta T \approx 500$ K and the corresponding value of $\delta x/x \lesssim 0.002$, which is negligible compared to measurement errors.

Equations (27) and (28) were solved for two unknowns $\bar{T}_b$ and x using the Newton-Raphson iteration method. The burned gas properties were computed using an approximation to equilibrium properties developed by Martin and Heywood [24] and the unburned gas properties were computed using thermodynamic data from JANAF tables [25] for the individual species in the mixture and the assumption of frozen composition. The calculation procedure is along the line suggested by Lorusso [26]. This procedure is outlined in Table 1 and fuel thermodynamic properties are described in Appendix E.

Figure 14 shows the relationship between the temperature distributions in the fuel-air mixtures as a function of mass fraction burned. It can be seen that first the unburned gas is compressed isentropically. It then burns at constant enthalpy, as shown in Appendix F, to reach the adiabatic flame temperature. Finally, the burned gas is compressed isentropically to the final state.

The following definitions result from the assumption of spherical symmetry and mass conservation.

$$V_b = x \tilde{v}_b \ M = (4/3)\pi \ R_f^3 \qquad (30)$$

$$R_f = [3V_b/4\pi]^{1/3} \qquad (31)$$

$$A_f = 4\pi R_f^2 \qquad (32)$$

$$S_u = M \ \dot{x}(t)/\rho_u A_f \qquad (33)$$

$$S_f = \dot{R}_f(t) \qquad (34)$$

$$S_g = S_f - S_u \qquad (35)$$

where:

R_f = radius of flame

A_f = area of flame

S_u = laminar burning velocity

$\dot{x}$ = rate of mass fraction burned

S_f = flame front velocity

S_g = unburned gas velocity

The following relation was used to calculate x:

$$\dot{x} = \frac{dx}{dp} \ \dot{p} \qquad (36)$$

where:

$\dot{p}$ = rate of pressure rise

It is shown in Appendix G that

$$\frac{dx}{dp} = \frac{v_0(1-(1-x) \frac{v_u}{v_0} (1 - \frac{\gamma_b}{\gamma_u}) + \frac{A}{v_0} (\gamma_b p \frac{d\delta}{dp} + \delta))}{\gamma_b(R_b T_b^{\circ} - R_u T_u)} \qquad (37)$$

where:

γ = specific heat ratio of gas

T_b° = adiabatic flame temperature

R = $\tilde{R}/\bar{M}$

$\tilde{R}$ = universal gas constant

$\bar{M}$ = mean molecular weight of gas mixture

v_0 = specific volume of gas mixture at initial state

The two terms $\gamma_b p \frac{d\delta}{dp}$ and δ in Eq. (37) are the consequences of including the thermal boundary layer at the combustion bomb wall and are shown graphically in Fig. 15 as a function of normalized pressure for stochiometric propane-air mixtures having an initial pressure of 1 atm and an initial temperature of 296K. It can be seen that the values for both terms have the same order of magnitude and both should be considered in the calculation.

All parameters on the right hand side of Eq. (37) are known from the calculation outlined in Table 1. Thus dx/dp can be evaluated readily. The rate of pressure rise is obtained by numerical differentiation of the pressure data. Using this information, the adiabatic flame speed can be calculated from Eq. (33). A FORTRAN

computer program was used to calculate the laminar burning velocity

(Appendix I).

CHAPTER 6

EXPERIMENTAL RESULTS AND DISCUSSION

6.1 Mixing Time

Before undertaking extensive measurements, studies were made to check the reproducibility of the data. First, the effect of waiting time on the combustion process was studied. Tests were run involving waiting times of 2, 5, and 10 minutes with stoichiometric propane-air mixtures having initial conditions of 1 atm and 298 K temperature. Figure 16 shows the time deviation of the ionization probe pulses from the mean time $t_i - \bar{t}$. Also shown is the distance the flame traveled in that time. Figure 16 shows no measurable bouyancy effect. Figure 17a shows the difference of the time when peak pressure occurred and the mean time of the ionization probe pulses as a function of waiting time. The distance which the flame had travelled at that time is also shown in this figure. Figure 17b shows the ratio of the pressure inside the combustion bomb at the average arrival time of the flame for three ionization probes to the maximum pressure as a function of waiting time. As a result of these studies it was concluded that 2 to 10 minutes of waiting time before combustion did not have any effect on the measurement. Five minutes was then chosen as a reasonable waiting time to allow for fuel and air to mix completely and become quiescent.

Using this five-minute waiting time tests were done to check the reproducibility of the data. Four identical runs were made for

stoichiometric propane-air mixtures at the initial temperature of 298 K and the initial pressure of 1 atm. and the laminar burning velocity was calculated along the isentropes for each. Figure 18 shows the results plotted as a function of temperature and pressure. It can be seen that the data are very reproducible.

Further evidence of this reproducibility is given in Table 2. The parameters shown are peak pressure p_p , time at which peak pressure occurs t_p , the time deviation of the ionization probe pulse from the mean time $t_i - \bar{t}$, the standard deviation of flame radii deduced from the ionization probe pulses δR_{rms} , the deviation of the calculated flame front radius from that given by the laser beam and the unburned mass fraction at the end of combustion δx_u . As can be seen, the maximum pressure and the time at which maximum pressure occurred are very close for all four runs. Although there is some evidence of a systematic variation in the arrival times of the flame front at the ionization probes, which might indicate a small asymmetry, it should be noted that since the flame speed is less than 100 cm/sec, the displacements involved are only fractions of a milli-meter. This is smaller than the accuracy with which the probes could be positioned and is not considered to be significant. The other quantities in Table 2, δR_{rms} , δR_{laser} and δx_u , are all well within the accuracy of the measurements.

6.2 Parametric Fit of Measured Burning Velocity

The measured laminar burning velocities for different fuel-air mixtures have been fitted to two different functional forms. The

first is the simple power law relation

$$S_u = S_{uo} \left(\frac{T_u}{T_{uo}} \right)^\alpha \left(\frac{p}{p_o} \right)^\beta \qquad (38)$$

where

S_u = laminar burning velocity cm/sec

S_{uo} = laminar burning velocity at reference point cm/sec

T_u = temperature of unburned mixture K

T_{uo} = reference temperature 298K

p = pressure of gas mixture atm

p_o = reference pressure 1 atm

α, β = constants

The constants α and β as well as S_{uo} were determined by fitting the data to the power law expression using the least square method.

The second relation to which the data has been fitted is that used by Lavoie [29] to correlate data from previous experiments. It is

$$V_{STP} = \frac{\rho_u S_u}{\rho_{STP}} = A \left(\frac{p}{p_o} \right)^\beta \exp(-E/2RT_b^\circ) \qquad (39)$$

where:

V_{STP} = mass average burning velocity cm/sec

ρ_u = density of gas mixture

ρ_{STP} = density of gas mixture at standard temperature and pressure condition (T = 273 K, p = 1 atm)

T_b^o = adiabatic flame temperature K

R = gas constant 1.987 cal/(gm.mole.K)

A, B, and E are fitted constants

6.3 Propane-Air Mixtures

Systematic measurements of laminar burning velocities for propane-air mixtures were made at equivalence ratios of 0.8, 1.0 and 1.2. At each equivalence ratio, initial pressures of 0.4, 1.0 and 2.0 atm at room temperature were chosen. Measurements were first made along the isentropes starting with these initial conditions. Measurements at higher temperatures and pressures were made by heating the bomb to 400 K and 500 K and choosing initial pressures which lay on the same isentropes. Using this method laminar burning velocities were obtained for the pressure range 0.4 - 40 atm. and the temperature range 298 to 750 K.

Figure 19 shows the laminar burning velocity along one of these isentropes for a stoichiometric propane-air mixture having initial conditions of 296 K and 1 atm. Three overlapping runs are shown: the circle points indicate atmospheric initial conditions; the triangular points indicate initial conditions of 400 K and 3.13 atm, and the square points indicate initial conditions of 500 K and 7.6 atm. The scatter in the data is less than ± 2% and can be attributed to round-off error in the analog-to-digital converter.

The temperatures at which ionization probe pulses occur are shown in the figure, and it can be seen that these probe pulses occur very close to each other.

The laminar burning velocity increases along an isentrope, peaks a little before peak pressure and then falls off as the flame travels the last millimeter to the wall. The fall-off is most likely due to heat loss to the windows and the electrodes that protrude into the bomb. The solid and dashed curves are exponential and power law fits to the data.

Figure 20 shows data for 9 different isentropes. The top set is for propane-air mixtures with an equivalence ratio of 0.8, the second set is for stoichiometric mixtures and the bottom set is for an equivalence ratio of 1.2. These data show that laminar burning velocity decreases with increasing initial pressure at constant temperature and increases with the increasing initial temperature at constant temperature.

Figure 21 shows laminar burning velocity as a function of equivalence ratios for propane-air mixtures at a temperature of 298 K and pressure of 1 atm. The laminar burning velocity peaks for an equivalence ratio of 1.1 and falls off for both the rich and lean mixtures. The smooth curve is the best fit of the data to a second degree polynomial. The equation for this curve is

$$S_{uo} = 38.31 + 24.84(\phi - 1) - 153(\phi - 1)^2 \qquad (40)$$

where ϕ is the fuel-air equivalence ratio.

The burning velocities obtained for propane-air mixtures were fitted to the power law relation (Eq. (38)). The values of S_{uo}, α, and β thus found are given in Table 3. In this table the percentage of data points falling within $\pm$ 5% of the fitted curve is also given.

Note that the values of S_{uo} given in Table 3 and by Eq. (40) differ about 9 to 16 percent.

The calculated burning velocity data were also fitted to the exponential form. The values of A, B, and E are given in Table 4 along with the percentage of data points falling within $\pm$ 5% of the fitted curve.

The exponential fits (40) are shown graphically by the solid curves in Figures 19 and 20. It can be seen from these Figures and from the last columns in Tables 3 and 4 that the overall fit of the power law and exponential relations are equally good. The exponential relation appears to be slightly better at pressures below 2 atm but it is sensitive to the calculation of the adiabatic flame temperature and is less convenient to use than the power law relation. There has been a preference for the exponential relation on fundamental ground. However, in view of the strong variation of both the pre-exponential coefficient A and the apparent activation energy E with the equivalence ratio, the physical significance of these quantities is doubtful.

There have been previous measurements of laminar burning velocity for propane-air mixtures, but most of the data are for low temperatures and pressures [25 through 31]. Comparison of the data in Table 4 with the corresponding values obtained by Lavoie from previous data (Table 5) shows reasonable agreement for the pressure exponent but significant disagreement in the values of A and E. The most probable reason for this is the limited amount of high pressure and temperature data with which Lavoie had to work.

Figure 22 shows laminar burning velocities measured in this study as a function of unburned gas temperature for stoichiometric propane-air mixtures at atmospheric condition compared with those measurements reported by Kuehl [28]. It can be seen that the differences are less than 8 percent. Table 6 shows laminar burning velocity at 1 atm pressure and 311 K temperature as a function of the equivalence ratio compared with Kuehl's measurements. The laminar burning velocity at 311 K is calculated using Eq. (40) and Table 3. It can be seen that the differences are less than 7 percent.

Recent measurements of the burning velocity of propane-air mixtures made in a spherical bomb similar to that used in this study have also been reported by Ryan and Lestz [22]. Their results agree with those measured in this study at a temperature of 500 K and a pressure of 6 atm, as shown in Fig. 23, but show a significantly steeper temperature dependence of the laminar burning velocity. One possible reason for this is the assumption made by Ryan and Lestz that the unburned mass consumed in each time step of their numerical integration burns at constant volume. Since the combustion actually occurs at constant pressure, this leads to an incorrect value of the entropy for the burned gas which could in turn affect the calculated flame speeds.

6.4 Isooctane-Air Mixtures

Laminar burning velocities of isooctane-air mixtures were measured for different equivalence ratios in the pressure range of 0.4 - 40 atm and the temperature range of 298 - 750 K. The same

procedure used for propane-air mixtures was employed here for setting the initial temperature and pressure of the mixtures. At some points autoignition was observed, as will be discussed later. As a result of this it was not possible to gather as much data as in the case of propane-air mixtures. The effects of residual gases on the laminar burning velocity of isooctane-air were also studied and will be discussed later.

The measured values of laminar flame speed for isooctane-air mixtures were fitted to both power law and exponential relations. Table 7 shows values for S_{uo}, α, β, and the percentage of data points falling within $\pm$ 5% of the fitted curve as a function of the equivalence ratio. The power law fit is shown graphically by the dashed curves in Fig. 24. The power law fit is quite good except for low pressure and temperature data.

The values of A, β, and E for the exponential fit are given in Table 8 along with the percentage of data points falling within $\pm$ 5% of the fitted curve. The exponential fits are shown graphically by the solid curves in Fig. 24. It can be seen from Fig. 24 and the last column of Tables 7 and 8 that the exponential fit is slightly better than the power law fit, but the power law relation is much easier to use.

The laminar burning velocities of isooctane-air mixtures were measured at room pressure and temperature for different equivalence ratios. These measurements are shown in Fig. 25. As in the case of propane-air mixtures it was observed that flame speed peaks for an

equivalence ratio of 1.1 and falls off for both rich and lean mixtures.
The data are fitted to second and third degree polynomials. The
equations for these polynomials are

$$S_{u_0} = 31.97 + 23.24(\phi - 1) - 91.46(\phi - 1)^2 \qquad (41)$$

$$\delta = 1.57$$

and

$$S_{u_0} = 32.57 + 20.62(\phi - 1) - 139.12(\phi - 1)^2 + 104.8(\phi - 1)^3 \qquad (42)$$

$$\delta = 1.28$$

where

$$\delta = \sqrt{\sum \frac{(S_{u_f} - S_{u_m})^2}{N}}$$

and S_{u_f}, S_{u_m}, and N are fitted burning velocity, measured
burning velocity, and number of data points respectively. The smooth
curve in Fig. 25 is the second degree polynomial (Eq. 41).

The effects of residual gases on the flame speed were studied.
A mixture of nitrogen and carbon dioxide, which is described in
Appendix H, was used to simulate residual gases. The mixture was
composed of 15% carbon dioxide and 85% nitrogen based on the volume
and had a molecular weight of 30.4. The residual fraction was cal-
culated as the ratio of mass of diluent to the total mass of gas mix-
ture. Two different residual fractions of 10 and 20 percent were used.
The effects of the residual fraction on flame speed were studied for
stoichiometric mixtures having an initial temperature of 298 K and

three different initial pressures of 1, 2, and 4 atm. These measured values were fitted into the power law relation (Eq. (38)). Table 9 gives the values of S_{uo}, α, and β, for stoichiometric mixtures as a function of the residual fraction along with the percentage of data points falling within ± 5% of the fitted curve.

Figure 26 shows flame speed data for three different isentropes having the same initial conditions but with a varied percentage of diluent. The three different ratios used were 0, 10, and 20 percent. The points indicate the measured data and the solid curves indicate the corresponding power fits. Figure 27 shows flame speed normalized with respect to the flame speed with no diluent as a function of unburned gas temperature. It can be seen that flame speed decreases about 20% for each 10% of diluent.

Autoignitions occurred as the initial temperature and pressure of isooctane-air mixtures were increased, making it impossible to gather more flame speed data. Figure 28 shows the oscillogram for stoichiometric isooctane-air mixtures with initial conditions of 500 K temperature and 15.1 atm pressure. The ionization probe signals and the laser signal are also shown. The horizontal scale is 10 msec/div. and the vertical scale is 13.6 atm/div. for the pressure signal. It can be seen that autoignition occurred about 35 msec after the ignition, and that ionization probe pulses occurred at the same time as was expected.

The values of pressures and temperatures at which autoignition occurred as a function of the equivalence ratio are shown in Table 10.

The pressure and temperature history of the combustion process of isooctane-air mixtures in which autoignition occurred are shown in Tables 11, 12, and 13 for three different ratios of 0.8, 1.0, and 1.2.

Different authors have measured the laminar burning velocity of isooctane-air mixtures for a variety of conditions. Dugger and Graab [34] used a bunsen-burner for measuring flame speed at atmospheric pressure and at temperatures of 311 and 422 K. They varied the mole fraction of oxygen in an oxygen-nitrogen mixture from 0.21 to 0.50. Heimel and Weast [35] also used a bunsen burner to measure the laminar flame speed for stoichiometric isooctane-air mixtures at atmospheric pressure for temperatures from 298 K to 707 K. They fitted their flame speed data with the equation

$$S_u = 12.1 + 8.362 \times 10^{-5} \, T_u \, 2.15 \tag{43}$$

where T_u is in K . Figure 29 shows a comparison of the laminar burning velocities measured in this study with those measured by Dugger and Graab [34] and Heimel and Weast (Eq. (43)) for stoichiometric isooctane-air mixtures at atmospheric conditions. It can be seen that the agreement is quite close.

In an earlier work this author and Keck [36] suggested the following relation for laminar burning velocity of stoichiometric isooctane-air mixtures

$$S_u = 35.25 \left(\frac{T_u}{T_{uo}} \right)^{1.97} \left(\frac{p}{p_o} \right)^{-0.12} \tag{44}$$

where T_{uo} and p_o are the same as in Eq. (38). Equation (44) predicts a value of flame speed about 10 - 15 percent higher than those predicted by this study. The reason for this is that in the earlier work [36] the measured pressures were read from oscillograms with a manual digitizer. In this study an analog-to-digital converter was used to digitize the pressure signals. The error in digitization has most likely propagated into flame speed measurement and has caused a 10 - 15 percent error.

For high pressure and temperature data Babkin et al. [37] fitted their data for stoichiometric isooctane-air mixtures with the equation

$$S_u = (404 \log T_u - 1008) \, p^{-0.39 + 0.40(T_u/1000)} \tag{45}$$

where p, T_u and S_u are in atm., K , and cm/sec . Ryan and Lestz [22] fitted their data with the equation

$$S_u = 7,452 \, (p)^{-.25} \exp(-2123.3/T_u) \tag{46}$$

Figure 30 shows a comparison of the laminar burning velocities measured in this study with those measured by Babkin et al. (Eq. 45) and Ryan and Lestz (Eq. 46) for stoichiometric isooctane-air mixtures at 6 atm. pressure. It can be seen that, as in the case of propane-air mixtures, Ryan and Lestz found a significantly steeper temperature dependence for the laminar burning velocity (see explanation above). The values predicted by Babkin et al. differ by less than 8 percent from values predicted by this study.

6.5 Methanol-Air Mixtures

Laminar burning velocities for methanol-air mixtures at different equivalence ratios were measured and the results were fitted to power law and exponential relations. Because of low vapor pressure at room temperature it was not possible to measure flame speeds along an isentrope with the initial pressure of 2 atm. Therefore there are fewer data points than for propane-air mixtures. Figure 31 shows the measured burning velocities of methanol-air mixtures at the three different equivalence ratios of 0.8, 1.0, and 1.2 in the range of 298 - 750 K and 0.4 - 40 atm.

The values of S_{uo}, α, β, and the percentage of δ_5 data points falling within $\pm$ 5% of the fitted curves for the power law fit are given in Table 14 as a function of the equivalence ratio. The power law fit is shown by dashed curves in Figure 31.

The values of A, β, and E for the exponential fit are shown in Table 15 along with the percentage of data points falling within $\pm$ 5% of the fitted curve as a function of equivalence ratio. The exponential fits are shown graphically by the solid curves in Fig. 31. Both fits are quite good but the exponential fit is better than the power law fit for low pressure and temperature data.

The laminar burning velocity of methanol-air mixtures was measured as a function of the equivalence ratio at room temperature and pressure. Because of the low vapor pressure of methanol at room temperature the maximum equivalence ratio was 1.2. These data are shown in Fig. 32, and have been fitted to second and third degree poly-

nomials. The equations for these polynomials are

$$S_u = 42.29 + 42.86(\phi - 1) - 107.14(\phi - 1)^2$$

$$\hat{\delta} = 1.57 \tag{47}$$

$$S_u = 43.40 + 62.76(\phi - 1) - 176.59(\phi - 1)^2$$
$$- 462.96(\phi - 1)^3$$

$$\hat{\delta} = 0.38 \tag{48}$$

The third degree polynomial is shown in Fig. 32. It can be seen that the laminar burning velocity for a methanol-air mixture peaks at an equivalence ratio of 1.1 and falls off for both rich and lean mixtures.

Ryan and Lestz [22] fitted their measurements of the laminar burning velocity for stoichiometric methanol-air mixtures with the equation

$$S_u = 8517.6 \ p^{-0.15} \ \exp(-2172.8/T_u) \tag{49}$$

Figure 33 shows a comparison of the laminar burning velocities measured in this study with those measured by Ryan and Lestz (Eq. 49). As in the case of propane and isooctane Ryan and Lestz found a significantly steeper temperature dependence for the laminar burning velocity.

Gibbs and Calcoate [38] have measured the laminar burning velocities for methanol-air mixtures using a bunsen burner. Their data are for atmospheric pressure and temperatures of 298 K and 373 K. Wiser and Hill [39] have measured the flame speed using a horizontal tube. The measured velocities are for room temperature and 0.86 atmospheric pressure. Figure 34 shows a comparison of the values of flame speed

measured by Gibbs and Calcoate [38] and Wiser and Hill [39] with

those measured in this study. Considering the relatively weak pressure

dependence found for laminar flame speed, it can be seen that the re-

sults of Wiser and Hill [39] are in excellent agreement with those of

this study. The results of Gibbs and Calcoate are systematically high-

er, the difference increasing from 5% at ϕ = 1.2 to 20% at ϕ = 0.8 .

The reason for this difference could not be ascertained.

For high temperature data Table 16 shows a comparison of the

values of laminar burning velocities measured by Gibbs and Calcoate

[38] and the power law relation of this study for atmospheric pressure

and a temperature of 375 K as a function of the equivalence ratio. It

can be seen that the predicted values for the equivalence ratios of 1.0

and 1.2 are within 10% of each other, but that the values predicted for

equivalence ratios of 0.8 deviate about 29%.

6.6 RMFD 303-Air Mixtures

RMFD 303 is a wide-boiling-range multicomponent hydrocarbon pre-

pared by Howell Hydrocarbon. It is a standard gasoline used for knock

rating. The average molecular formula of the fuel is $C_{7.8}H_{13.214}$.

Table 17 shows the physical properties and chemical analysis of RMFD

303 [40].

RMFD 303 does not evaporate completely at room temperature. This

can be seen in Fig. 35 where the ratio of measured pressure over cal-

culated pressure in the manifold is shown as a function of calculated

pressure at room temperature. Calculated pressure is based on the

assumption of the ideal gas for the fuel vapor and the assumption that

all the fuel evaporates. The circle points indicate 300 K temperature. It can be seen that the ratio decreases from 62% to 52%. The reason for this is that some components of the fuel have very low vapor pressure at room temperature, and as pressure increases they saturate. This problem is also encountered during an engine cold-starting where fuel does not evaporate because the engine is cold and a rich mixture is used to start the engine. This evaporation problem is discussed in Appendix A. In order to overcome the problem, initial temperatures were increased from 298 K to 350 K. The square points in Fig. 35 represent the corresponding pressure ratios at 350 K. It can be seen that as the temperature increased the ratio of measured pressure over calculated pressure increased. This is because at 350 K the saturation pressures of different components exceeded the pressure required to make the desired mixture.

Figure 26 shows laminar burning velocity measured at room temperature and pressure as a function of the equivalence ratio. There are two different scales for equivalence ratios. One is based on the vapor pressure of the fuel inside the combustion bomb and the other is based on the mass of fuel injected into the manifold. These measurements have been fitted to second and third degree polynomials and the corresponding δ are:

$$S_u = 31.83 + 28.87(\phi - 1) - 85.61(\phi - 1)^2 \tag{50}$$

$$\delta = 1.97$$

$$S_u = 33.9 + 31.96(\phi - 1) - 193.75(\phi - 1)^2 + 174.48(\phi - 1)^3 \tag{51}$$

$$\delta = 0.74$$

where ϕ is the equivalence ratio based on the vapor pressure of the fuel in the combustion bomb. The smooth curve in Fig. 36 represents the third degree polynomial.

Measurements of laminar burning velocities for RMFD 303-air mixtures were made at equivalence ratios of 0.8, 1.0 and 1.2. At each equivalence ratio, initial pressures of 0.4, 1.0 and 2.0 atm were used. Measurements then were made for higher temperatures and pressures. Using this method laminar burning velocities were obtained for the pressure range of 0.4 - 34 atm and the temperature range of 298 to 750 K.

The laminar burning velocities for RMFD 303-air mixtures are shown in Fig. 37. The dashed curves indicate the power law fit. Table 18 shows the values S_{uo}, α, and β as well as the percentage of data points falling within $\pm$ 5% of the fitted curve as a function of the equivalence ratio.

The measured burning velocities for RMFD 303-air mixtures were also fitted to the exponential relation. The values for A, β, E, and the percentage of data points falling within $\pm$ 5% of the fitted curve are shown as a function of the equivalence ratio in Table 19.

The laminar burning velocity of RMFD 303-air mixtures as a function of the equivalence ratio at 350 K and 1 atm were measured and are shown in Fig. 38. The laminar burning velocity peaks for an equivalence ratio of 1.1 and falls off for both rich and lean mixtures. The measured flame speeds have been fitted to both second and third

degree polynomials. The equations of these polynomials with corres-
ponding δ are:

$$S_u = 39.76 + 27.58(\phi - 1) - 105.58(\phi - 1)^2 \qquad (52)$$

$$\delta = 1.38$$

and

$$S_u = 40.59 + 23.38(\phi - 1) - 124.48(\phi - 1)^2 + 42.47(\phi - 1)^3 \qquad (53)$$

$$\delta = 1.18$$

The smooth curve in Fig. 36 is Eq. (52).

6.7 Comparison of Values of Burning Velocity for Different Fuel-Air Mixtures

The parameters S_{uo}, α, and β for the power law relation for different fuel-air mixtures are shown in Tables 20 and Fig. 39 as a function of equivalence ratios. Flame speed is a very weak function of pressure and at a given equivalence ratio the burning velocity does not vary much for the four fuel-air mixtures studied. The temperature exponent α varies only about 8% at a given equivalence ratio. The pressure exponent β increases as the equivalence ratio increases while α decreases as the equivalence ratio increases. The burning velocity is fastest for methanol-air mixtures and slowest for RMFD 303-air mixtures. This might suggest that as the complexity of fuel increases the burning velocity decreases.

CHAPTER 7

CONCLUSION AND SUGGESTIONS

A facility for measuring the laminar burning velocity of fuel-air-residual gas mixtures was constructed. A thermodynamic analysis was used to calculate laminar burning velocities from the pressure time history obtained during the combustion process.

Laminar burning velocities for propane-air, isooctane-air, methanol-air and RMFD 303 (a primary reference gasoline)-air mixtures were measured in the pressure range of 0.4 to 40 atm and temperature range 298 to 750 K for fuel-air equivalence ratios from 0.8 to 1.5. The measured values of flame speed were fitted to both power law relation and to an exponential expression to provide correlations of the data for use in combustion models. The exponential expression was derived from Semenov's [9] theory. An apparent activation energy E was calculated from the exponential expression. Both the pre-exponential coefficient A and the apparant activation energy E was found to depend strongly on the equivalence ratio. Thus the physical significance of A and E is doubtful. The following conclusions can be drawn on the basis of the flame speed measurements:

1) Methanol-air mixtures have the highest flame speed among the fuel-air mixtures studied, followed by propane-air, isooctane-air and RMFD 303-air mixtures.

2) The laminar burning velocitiy peaks at an equivalence ratio of about 1.1 and falls off for both rich and lean mixtures

3)　The laminar burning velocity is a strong function of unburned gas temperature and increases as the unburned gas temeprature increases.

4)　The laminar burning velocity decreases as the pressure of the gas mixture increases.

On the basis of the results obtained it is concluded that the constant volume combustion bomb is a useful device for measuring adiabatic flame speed. In addition to the test performed the following studies could also be made without modification of the apparatus:

1)　Measure the laminar burning velocities of different multi-component hydrocarbon fuels .

2)　Investigate the effects of residual gases on laminar-burning velocities of different fuel-air mixtures at pressures and temperatures up to 40 atm and 750 K.

3)　Analyze combustion products to check unburned mass fraction and measure the mass of hydrocarbon per unit area, as well as carbon monoxide and nitric oxides in the combustion product.

Suggestions for future experiments which would require modifications to the experimental facilities include:

1)　Use the shadowgraph technique to phtotgraph the flame to see if it is smooth or wrinkled.

2)　Use laser scattering to measure flame thickness, especially for low burning velocity mixtures

3)　Make heat transfer measurements to check the theory used, and study the quench layer structure.

REFERENCES

[1] Ferguson, C.R. and Keck, J.C., "On Laminar Flame Quenching and Its Application to Engine Combustion", Combustion and Flame, 28, 197-205 (1977).

[2] Ferguson, C.R. and Keck, J.C., "Stand-Off Distance on a Flat Flame Burner", Combustion and Flame, 34, 85-98 (1979).

[3] DeSoete, G.G., "The Influence of Isotropic Turbulence on the Critical Ignition Energy", Thirteenth Symposium on Combustion, p. 735.

[4] Van Tiggelen, A., and Deckers, J., "Chain Branching and Flame Propagation", Sixth Symposium on Combustion, p. 61.

[5] Blizard, N.C. and Keck, J.C., "Experimental and Theoretical Investigation of Turbulent Burning Model for Internal Combustion Engines", SAE Paper 740191, February 1974.

[6] Tabaczynski, R.J. et al., "A Turbulent Entrainment Model for Spark Ignition Engine Combustion", SAE Paper 770647, June 1977.

[7] Groff, E.G., General Motors Research Center, Personal Communication, July 1979.

[8] William, F.A., "Combustion Theory", (Addison-Wesley Publishing Company, Inc. 1965, p. 95).

[9] Semenov, N.N., "Thermal Theory of Combustion and Explosion, III. Theory of Normal Flame Propagation", N.A.C.A. Tech. Memo No. 1026, 1942.

[10] Glassman, Irvin, "Combustion" (Academic Press), 1977.

[11] Von Karman, T. and Millan, G., "The Thermal Theory of Constant Pressure Deflagration," C.B. Biezeno, Anniversary Volume on Applied Mechanics, pp. 55-69; N.V. DeTechnische Uitgererij H. Stam. Haarlem, March 1953.

[12] Tanford, C. and Pease, R.N., "Theory of Burning Velocity, II. The Square Root Law for Burning Velocity", Journal of Chemical Physics 15, p. 861 (1947).

[13] Hirschfelder, J.O., Curtis, C.F., and Bud, R.B., "The Molecular Theory of Gases and Liquids", (Wiley, New York), 1954, Chapter 11.

[14] Von Karman, T., and Penner, S.S., "Selected Combustion Problems",
        (AGARD Combust. Colloq.), pp. 5-40, Butterworths, London
        (1954).

[15] Gerstein, M., Levine, O., and Wong, E.L., "Flame Propagation
        II. The Determination of Fundamental Burning Velocities
        of Hydrocarbons by a Revised Tube Method", Journal of
        American Chemical Society 73-418 (1951).

[16] Andrews, G.E., and Bradley, D., "Determination of Burning
        Velocity: A Critical Review", Combustion and Flame 18,
        113-153 (1972).

[17] Botha, J.P., and Spalding, D.B., "The Laminar Flame Speed of
        Propane/Air Mixtures with Heat Extraction from the
        Flame", Proc. Roy. Soc. (London), Ser. A, 225-71 (1954).

[18] Strauss, W.A. and Edse, R., "Burning Velocity Measurements by
        the Constant-Pressure Bomb Method", Seventh Symposium
        (International) on Combustion, pp 377-385 (1957).

[19] Lewis, B. and von Elbe, G., "Combustion, Flames and Explosions
        of Gases", 2nd Edition, Academic Press, p. 396.

[20] Garforth, A.M. and Rallis, C.J., "Laminar Burning Velocity of
        Stoichiometric Methane-Air Pressure and Temperature
        Dependence", Combustion and Flame 31, 53-68 (1978)

[21] Bradley, D. and Mitcheson, A., "Mathematical Solution for
        Explosions in Spherical Vessels", Combustion and Flame
        26, 201-217 (1976)

[22] Ryan, T.W. and Lestz, S.S., "The Effects of Fuel Composition
        and Charge Dilution on the Laminar Burning Velocity as
        Determined in a Constant Volume Combustion Bomb",
        Technical Paper CSS/CI-79-02, Central State Section of
        the Combustion Institute, April 1979.

[23] Metghalchi, M., "Laminar Burning Velocity of Isooctane-Air,
        Methane-Air, and Methanol-Air Mixtures at High Temperature
        and Pressure", S.M. Thesis, M.I.T., October 1976.

[24] Martin, M.K., and Heywood, J.B., "Approximate Relationships
        for the Thermodynamic Properties of Hydrocarbon-Air
        Combustion Products", Combustion, Science and Technology,
        Vol. 15, pp. 1-10, 1977.

[25] JANAF Thermochemical Tables, Dow Chemical Company, Clearinghouse,
        Springfield, Va.

[26] LoRouso, J., "Combustion and Emissions Characteristics of
      Methanol, Methanol-Water, and Gasoline Blends in a
      Spark Ignition Engine", Masters Thesis, Dept. of
      Mechanical Engineering, M.I.T., May 1976.

[27] Lavoie, G.A., Paper 780229, presented at Automotive
      Engineering Congress, Detroit, February-March, 1978.

[28] Kuehl, D.K., "Laminar-Burning Velocities of Propane-Air
      Mixtures", Eighth Symposium on Combustion, 1960, p. 510.

[29] Brokaw, R.S. and Gerstein, M., "Correlation of Burning
      Velocity, Quenching Distances, and Minimum Ignition
      Engines for Hydrocarbon-Oxygen-Nitrogen System", Sixth
      Symposium (International) on Combustion, 1956, p. 66.

[30] Kaskan, W.E., "The Dependence of Flame Temperature on Mass
      Burning Velocity", Sixth Symposium (International) on
      Combustion, 1956, p. 134.

[31] Agnew, J.T. and Gariff, L.B., "The Pressure Dependence of
      Laminar Burning Velocity by the Spherical Bomb Method",
      Combustion and Flame, Vol. 5, 209, 1961.

[32] Chase, J.D. and Weinberg, F.J., "The Acetylen Decomposition
      Flame and the Deduction of Reaction Mechanism from 'Global'
      Flame Kinetics", Proc. Royal Soc. A275, 1963, p. 411.

[33] Raezer, S.D. and Olsen, H.L., "Measurement of Laminar Flame
      Speeds of Ethylene-Air and Propane-Air Mixtures by the
      Double Kernel Method", Combustion and Flame, 6, 227, 1962.

[34] Dugger, G.L. and Graab, D.D., "Flame Velocities of Hydrocarbon-
      Oxygen-Nitrogen Mixtures", Fourth Symposium (International)
      on Combustion, 1952, p. 302.

[35] Hiemel, S. and Weast, R.C., "Effect of Initial Mixture
      Temperature on Burning Velocity of Benezene-Air, n-Heptane-
      Air, and Isooctane-Air Mixtures", Sixth Symposium
      (International) on Combustion, 1957, p. 37.

[36] Metghalchi, M., and Keck, J.C., "Laminar Burning Velocity of
      Isooctane-Air, Methane-Air, and Methanol-Air Mixtures
      at High Temperature and Pressure", Presented at the Fall
      Meeting of the Eastern Section of the Combustion Institute,
      November 10-11, 1977, Hartford, Connecticut.

[37] Babkin, V.S., V'yun, A.V., and Kozachenko, L.S., "Determination
      of Burning Velocity from the Pressure Record in a Constant
      Volume Vessel," Combustion, Explosion, and Shock Waves,
      Vol. 3, No. 3, pp. 362-370, 1967.

[38] Gibbs, G.J. and Calcoate, H.F., "Effect of Molecular Structure
      on Burning Velocity", Journal of Chemical and Engineering
      Data, 4, 226-237 (1957).

[39] Wiser, W.H. and Hill, G.R., "A Kinetic Comparison of the
      Combustion of Methyl Alcohol and Methane", Fifth Symposium
      (International) on Combustion, 553-558, 1955.

[40] By, A.B., "Spark Ignition Engine Knock as Related to End Gas
      Pressure-Temperature Histories", Master's Thesis,
      Department of Mechanical Engineering, M.I.T., May 1979.

[41] Hildebrand, F.B., "Advanced Calculus for Application, (Prentice-
      Hall Inc., Englewood Cliffs, N.J.) 1976, Second Ed.

TABLE 1

The Calculation Procedure for Laminar Burning Velocity
from the Pressure-Time History Obtained During the
Combustion Process

```
┌─────────────────────┐        ┌─────────────────────┐
│   Initial State     │        │   Measure p(t)      │
│   p₀, T₀, φ         │        │                     │
└─────────────────────┘        └─────────────────────┘
```

$$p_0,\ T_0,\ \phi$$

```
┌─────────────────────┐        ┌─────────────────────┐
│ Isentropic Compression │     │   Use of Eq.(26)    │
│ of unburned gas     │        │    to Calculate     │
│                     │        │       δ(t)          │
└─────────────────────┘        └─────────────────────┘
```

$$T_u = T_0 (p/p_0)^{\gamma-1/\gamma}$$

$$\gamma = \gamma(T_u)$$

```
┌─────────────────────┐
│ JANAF Table to Calculate │
│ Unburned Gas Properties │
└─────────────────────┘
```

```
┌──────────────────┐   ┌──────────────────┐   ┌─────────────────────┐
│ Martin & Heywood │   │  Burned Gas      │   │ Solve Eqs. (28) and (29) │
│ Model of Equili- │   │  Properties for  │   │ for  x  and  T_b  Using │
│ brium            │   │  Given φ, p, T_b │   │ Newton-Raphson Itera- │
│                  │   │                  │   │ tion Method         │
└──────────────────┘   └──────────────────┘   └─────────────────────┘
```
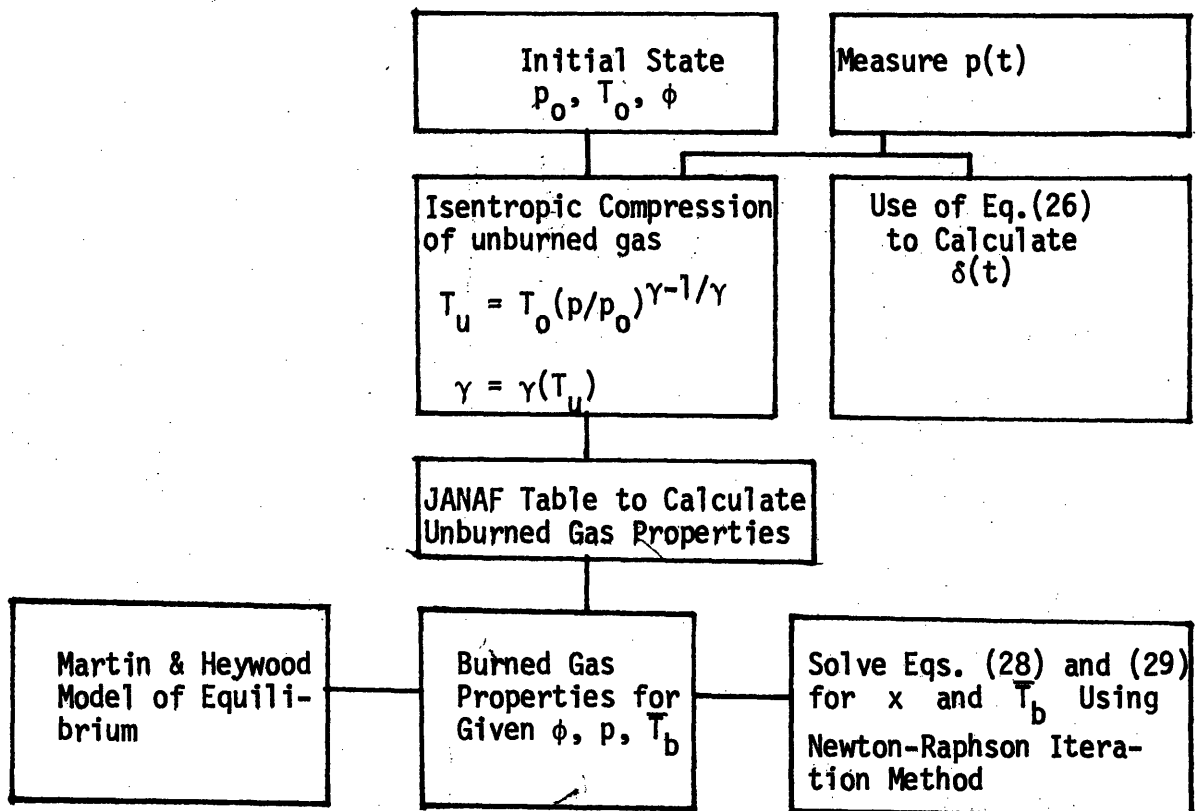
TABLE 2

REPRODUCIBILITY OF DATA

Run No.	p_p (atm)	t_p (msec)	$t_1 - \bar{t}$ (msec)	$t_2 - \bar{t}$ (msec)	$t_3 - \bar{t}$ (msec)	δR_{rms} (mm)	δR_{Laser} (mm)	δx_u
1	9.327	38.95	-0.32	0.68	-0.36	0.24	+0.004	0.001
2	9.135	39.21	-0.58	0.32	0.25	0.23	-0.069	0.025
3	9.210	39.21	-0.26	0.38	-0.11	0.15	-0.021	0.008
4	9.221	38.95	-0.49	0.45	0.04	0.21	+0.019	0.015

p_p : Max. Pressure

t_p : Time of p_p

$$\bar{t} = \frac{t_1 + t_2 + t_3}{3}$$

δR_{rms} : STD Deviation of I.P.

$$\delta R_{Laser} = R_{Calc} - 64.64$$

TABLE 3

Parameters S_{uo}, α, β, and δ_5 Used in the Power Law Relation for

Propane-Air Mixtures as a Function of the Equivalence Ratio

$$\left(S_u = S_{uo}\left(\frac{T_u}{T_{uo}}\right)^\alpha \left(\frac{p}{p_o}\right)^\beta , \quad T_{uo} = 298 \text{ K}, \quad p_o = 1 \text{ atm}\right)$$

	S_{uo} cm/sec	α	β	% of the data within $\pm$ 5%
0.8	23.3	2.27	-0.23	63
1.0	31.9	2.13	-0.17	74
1.2	33.8	2.02	-0.17	76

TABLE 4

Parameters A, β, E, and δ_5 Used in the Exponential Relation

for Propane-Air Mixtures as a Function of the Equivalence Ratio

$$\left(V_{STP} = \frac{\rho_u S_u}{\rho_{STP}} = A \left(\frac{p}{p_o} \right)^{\beta} \exp(- E/2RT_b^o) \quad , \quad p_o = 1 \text{ atm} \right)$$

	A cm/sec	β	E (cal/gm. mole)	% of the Data Within ± 5%
0.8	17.1×10^4	0.757	72,500	62
1.0	136.8×10^4	0.713	95,600	74
1.2	6.98×10^4	0.803	66,900	88

TABLE 5

Parameters A, β, and E Used in the Exponential Relation for Propane-
Air Mixtures as a Function of the Equivalence Ratio Calculated by
Lavoi [27]

	A cm/sec	β	E cal/gm. mole
0.8	2.44×10^4	0.8	54,348
1.0	29.00×10^4	0.8	80,566
1.2	4.10×10^4	0.8	61,355

TABLE 6

Comparison of Laminar Burning Velocity of Propane-Air
Mixtures at 1 Atm Pressure and 311 K Temperature as a
Function of the Equivalence Ratio with Kuehl's
Measurement

	S_u(cm/sec) Kuehl	Sm(cm/sec) This Study
0.8	31.8	30
0.9	38.5	37.7
1.0	40	41.9
1.1	42.86	42.9
1.2	43	40.6

TABLE 7

Parameters S_{uo}, α, β, and δ_5 Used in the Power Law Relation for
Isooctane-Air Mixtures as a Function of the Equivalence Ratio

$$\left(S_u = S_{uo}\left(\frac{T_u}{T_{uo}}\right)^{\alpha}\left(\frac{p}{p_o}\right)^{\beta} \quad T_{uo} = 298 \text{ K}, \quad p_o = 1 \text{ atm}\right)$$

ϕ	S_{uo} cm/sec	α	β	% of the Data within $\pm$ 5%
0.8	19.25	2.36	-0.22	63
1.0	27.00	2.26	-0.18	58
1.2	27.63	2.03	-0.11	75

TABLE 8

Parameters A, β, E, and δ_5 Used in the Exponential
Relation for Isooctane-Air Mixtures as a Function
of the Equivalence Ratio

$$(V_{STP} = \frac{\rho_u}{\rho_{STP}} \quad S_u = A(\frac{p}{p_o})^\beta \exp(-E/2RT_b^o) \ , \ p_o = 1 \ atm)$$

φ	A cm/sec	β	cal/gm. mole	% of the Data Within ± 5%
0.8	36.2×10^4	0.745	79,700	71
1.0	454×10^4	0.693	107,500	71
1.2	4.46×10^4	0.848	63.800	81

TABLE 9

Parameters S_{uo}, α, β, and δ_5 Used in the Power Law
Relation for Stoichiometric Isooctane-Air Mixtures
as a Function of the Residual Friction

$$(S_u = S_{uo} \left(\frac{T_u}{T_{uo}} \right)^{\alpha} \left(\frac{p}{p_o} \right)^{\beta} \, , \quad T_{uo} = 298K \, , \quad p_o = 1 \text{ atm})$$

Residual Fraction	S_{uo} cm/sec	α	β	% of the Data Within ± 5%
0	27.00	2.26	-0.18	58
0.10	23.71	1.99	-0.23	71
0.20	18.50	2.39	-0.37	93

TABLE 10

Values of Pressures and Temperatures for Isooctane-
Air Mixtures at which Autoignition Occurred as a
Function of the Equivalence Ratio

ϕ	p atm	T_u K
0.8	73	738
1.0	66	698
1.2	47	645

TABLE 11

Pressure and Temperature History of the Combustion Process for Isooctane-Air Mixture $\phi = 0.8$, in which Autoignition Occurred (T_i = 500 K, p_i = 14.5 atm)

Pressure (atm)	Temperature (K)	
15.33	507	
17.15	521	
19.05	535	
21.11	549	
23.39	563	
25.86	577	
28.526	591	
31.437	605	
34.60	619	
38.03	633	
41.74	647	
45.68	661	
49.94	675	
54.57	689	
59.46	703	
64.89	717	
70.73	731	
73.00	738	autoignition

TABLE 12

Pressure and Temperature History of Combustion Process
for Stoichiometric Isooctane-Air Mixtures in Which
Autoignition Occurred (p_i = 15.1 atm, T_i = 500 K)

Pressure (atm)	Temperature (K)
16.00	507
17.94	521
19.98	535
22.17	549
24.72	563
27.42	577
30.28	591
33.484	605
36.92	619
40.70	633
44.78	647
49.13	661
53.85	675
59.01	689
66.00	698 autoignition

TABLE 13

Pressure and Temperature History of Combustion Process
for Isooctane-Air Mixture ϕ = 1.2, Which Autoignition
Occurred (P_i = 6.26 atm, T_i = 400 K)

Pressure (atm)	Temperature (K)	
6.81	409	
7.85	423	
8.97	437	
10.20	451	
11.59	465	
13.12	479	
14.79	493	
16.66	507	
18.67	521	
20.89	535	
23.34	549	
25.99	563	
28.88	577	
32.07	591	
35.62	605	
39.37	619	
43.62	633	
47.00	645	autoignition

TABLE 14

Parameters S_{uo}, α, β and δ_5 Used in the Power Law
Relation for Methanol-Air Mixtures as a Function of
Equivalence Ratio

$$(S_u = S_{uo} \left(\frac{T_u}{T_{uo}} \right)^{\alpha} \left(\frac{p}{p_o} \right)^{\beta} , T_{uo} = 298 \text{ K}, p_o = 1 \text{ atm})$$

ϕ	S_{uo} cm/sec	α	β	% of the Data Within $\pm$ 5%
0.8	23.58	2.47	-0.21	60
1.0	32.69	2.11	-0.13	60
1.2	38.11	1.98	-0.11	76

TABLE 15

Parameters A, β, E, and δ_5 Used in the Exponential
Relation for Methanol-Air Mixtures as a Function
of the Equivalence Ratio

$$\left(V_{STP} = \frac{\rho_u S_u}{\rho_{STP}} = A\left(\frac{p}{p_0}\right)^{\beta} \exp(-E/2RT_b^o) \ , \quad p_0 = 1 \ atm \right)$$

ϕ	A cm/sec	β	E cal/gm. mole	% of the Data Within ± 5%
0.8	55×10^4	0.751	77,200	66
1.0	578×10^4	0.732	105,900	74
1.2	1.05×10^4	0.896	45,700	73

TABLE 16

Comparison of Laminar Burning Velocity of Methanol-
Air Mixtures of 1 atm Pressure and 311 K Temperature
as a Function of the Equivalence Ratio with the
Measurements Reported by Gibbs and Calcoate [38]

ϕ	S_u Gibbs & Calcoate cm/sec	S_u This Study cm/sec
0.8	58.5	41.05
1.0	71.2	63.16
1.2	66.4	59.44

TABLE 17

Physical Properties and Chemical Analysis of RMFD 303 (Indolene)

Stoichiometric Fuel-Air Ratio	0.06988
Lower Heat of Combustion (Kcal/gm)	10.15
Motor Octane Rating	88.3
Research Octane Rating	101.4
Specific Gravity	0.765
Average Molecular Formula	$C_{7.8}H_{13.214}$

Component Weight Percent

Aromatic	45.3%
Olefin	13.9%
Parafin	40.8%

Component Molecular Percents

Aromatic	52.49%
Olefin	9.36%
Parafin	38.16%

Component Typical Hydrocarbon

Aromatic	Toluene
Olefin	Undecene
Parafin	Isooctane

TABLE 18

Parameters S_{uo}, α, β, and δ_5 Used in the Power Law
Relation for RMFD 303-Air Mixtures as a Function of
the Equivalence Ratio

$$\left(S_u = S_{uo} \left(\frac{T_u}{T_{uo}}\right)^{\alpha} \left(\frac{p}{p_o}\right)^{\beta}, \quad T_{uo} = 298 \text{ K}, \quad p_o = 1 \text{ atm}\right)$$

ϕ	S_{uo} cm/sec	α	β	% of the Data Within $\pm$ 5%
0.8	19.15	2.27	-0.17	76
1.0	25.21	2.19	-0.13	74
1.2	28.14	2.02	-0.087	80

TABLE 19

Parameters A, β, E, and δ_5 Used in the Exponential
Relation for RMFD 303-Air Mixtures as a Function
of the Equivalence Ratio for the Exponential Relation

$$\left(V_{STP} = \frac{\rho_u S_u}{\rho_{STP}} = A \left(\frac{p}{p_0}\right)^\beta \exp(-E/2RT_b^\circ) \quad , \quad p_0 = 1 \text{ atm}\right)$$

ϕ	A (cm/sec)	β	E cal/(gm.mole)	% of the Data Within ± 5%
0.8	10.9×10^4	0.807	70,400	70
1.0	51.7×10^4	0.795	88,800	64
1.2	2.9×10^4	0.884	60,400	84

TABLE 20

Parameters S_{uo}, α, and β for Mixtures of Air with Indolene
(RMFD 303), Isooctane, Methanol, and Propane as a Function
of the Equivalence Ratio for the Power Law Relation

$$S_u = S_{uo}\left(\frac{T_u}{T_{uo}}\right)^{\alpha}\left(\frac{p}{p_o}\right)^{\beta} \quad , \quad T_{uo} = 298 \text{ K}, \ p_o = 1 \text{ atm}$$

Fuel	$\phi = 0.8$	$\phi = 1.0$	$\phi = 1.2$
		S_{uo}	
Methanol	23.58	32.69	38.11
Propane	23.20	31.90	33.80
Isooctane	19.25	27.00	27.63
RMFD 303	19.15	25.21	28.14
		α	
Methanol	2.47	2.11	1.98
Propane	2.27	2.13	2.06
Isooctane	2.36	2.26	2.03
RMFD 303	2.27	2.19	2.02
		β	
Methanol	-0.21	-0.13	-0.11
Propane	-0.23	-0.17	-0.17
Isooctane	-0.22	-0.18	-0.11
RMFD 303	-0.17	-0.13	-0.087

PRESSURE TRANSDUCER PORT

VALVE PORT

IONIZATION GAGE
PORT

PORT FOR WINDOW
INSERT →

PORT FOR WINDOW
INSERT ←

1.4 KW ELECTRICAL
HEATER

20° 20°

O-RING

22°

22°

SPARK PLUG
PORT

SPARK PLUG
PORT

IONIZATION GAGE PORT

I cm
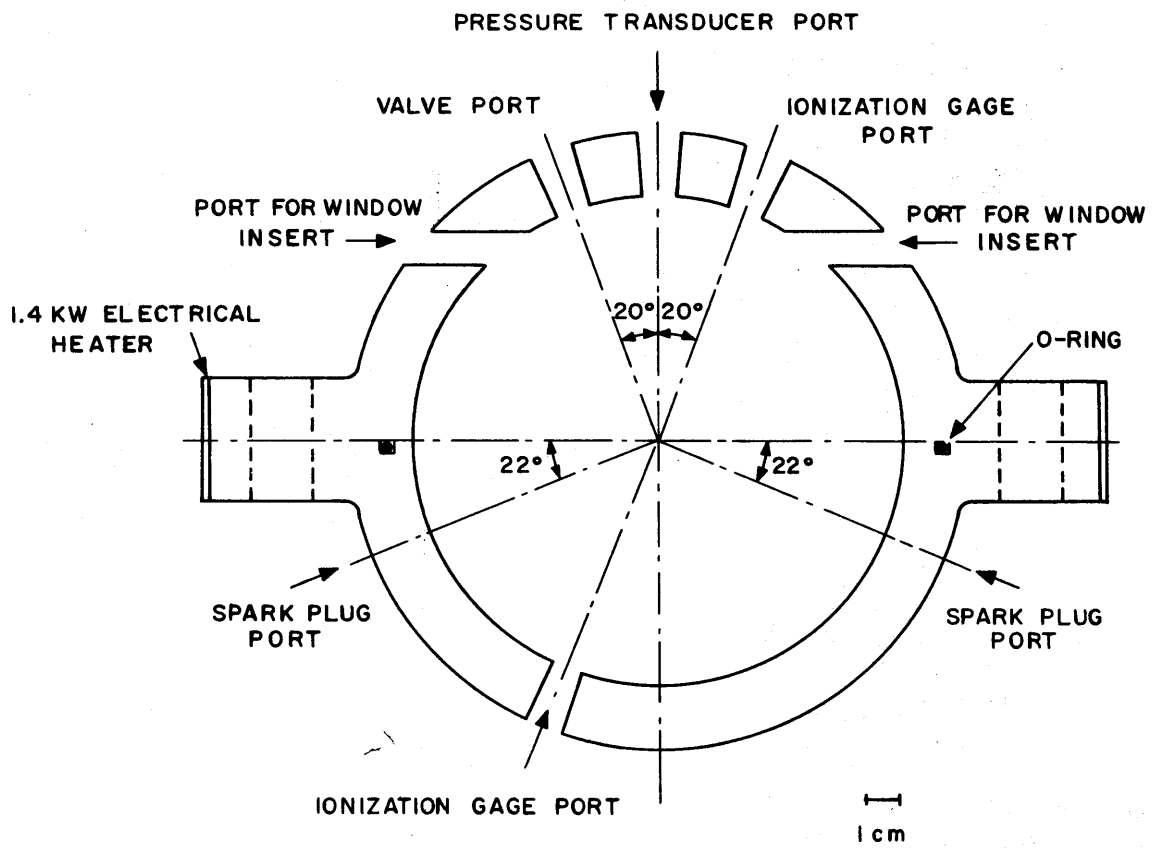
FIG. 1   Schematic Diagram of the
Combustion Bomb

FIG. 2 Gas and Fuel Handling System

EXTERIOR WALL
OF OVEN

HIGH TEMPERATURE
SILICONE COMPOUND
UNDER COMPRESSION

TO COMBUSTION BOMB

FUEL INJECTING
SYRINGE

TO VACUUM PUMP

TO MANOMETER

89
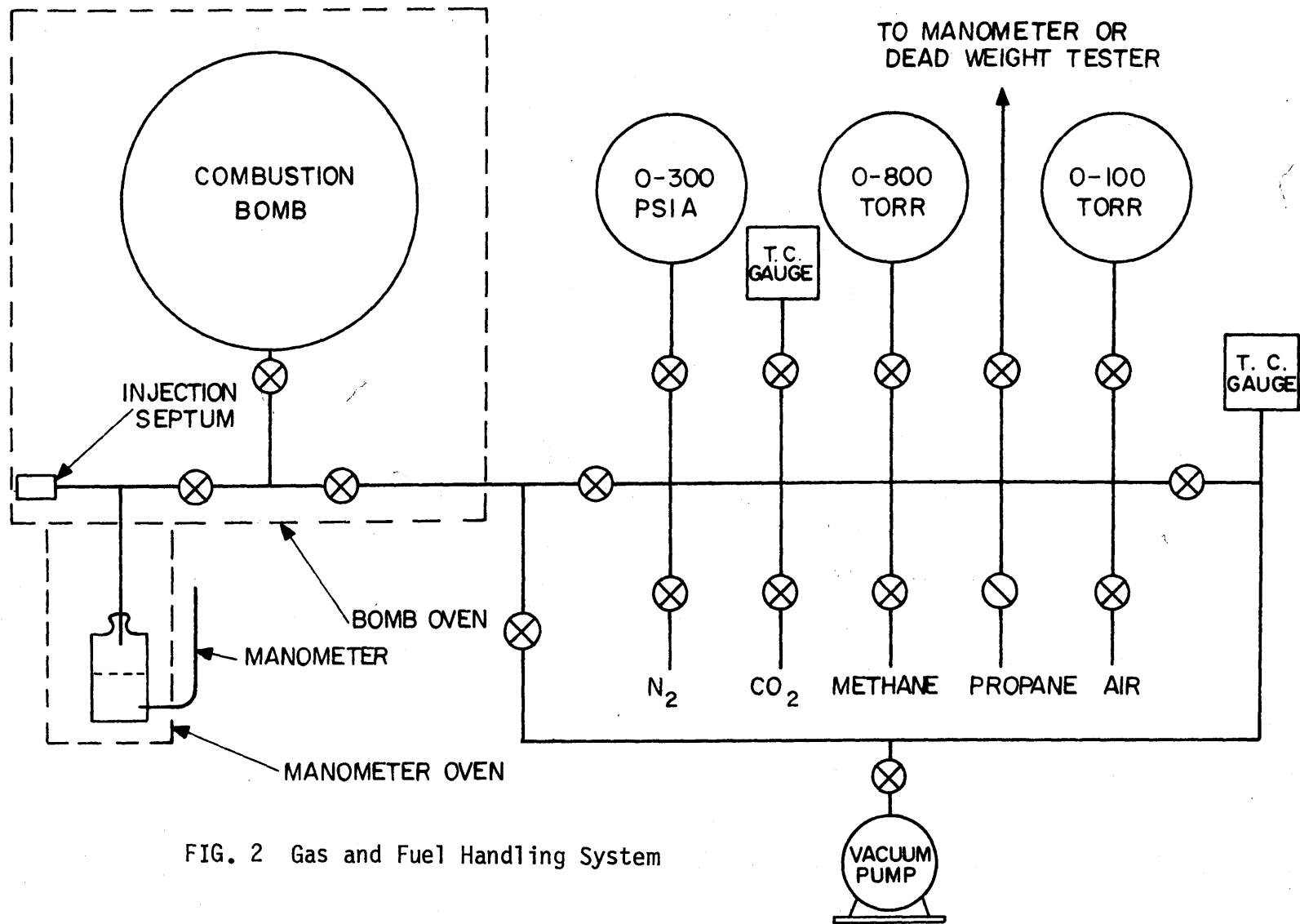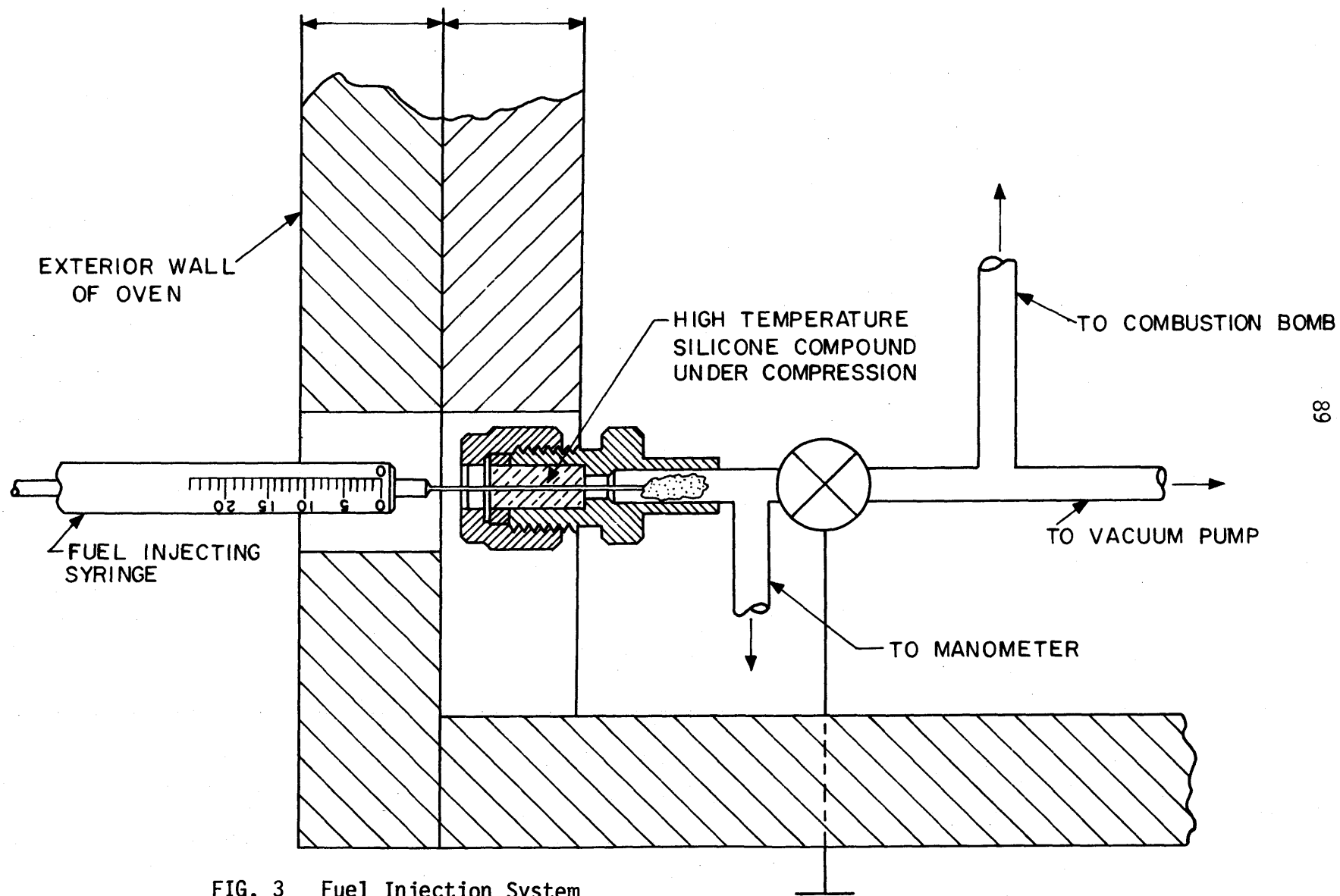
FIG. 3   Fuel Injection System
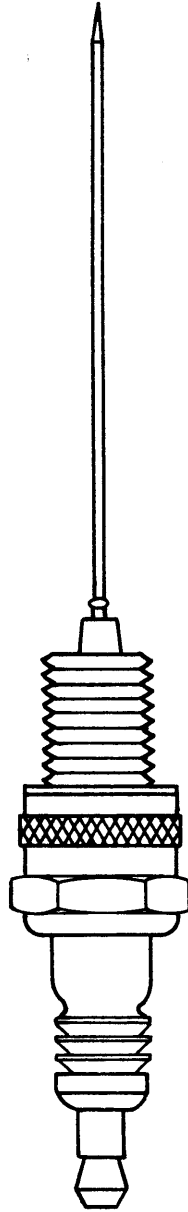
FIG. 4 Schematic Diagram of the Spark Plug
with its Extended Electrode

FIG. 5   Electrical Circuit for Ignition
System

BOMB SIDE

MICA INSULATOR   DIAPHRAGM
                        .OOI INCH

STEEL SHIM
O.OO2 INCH

TEFLON
INSULATOR

ELECTRODE
BALANCING SIDE
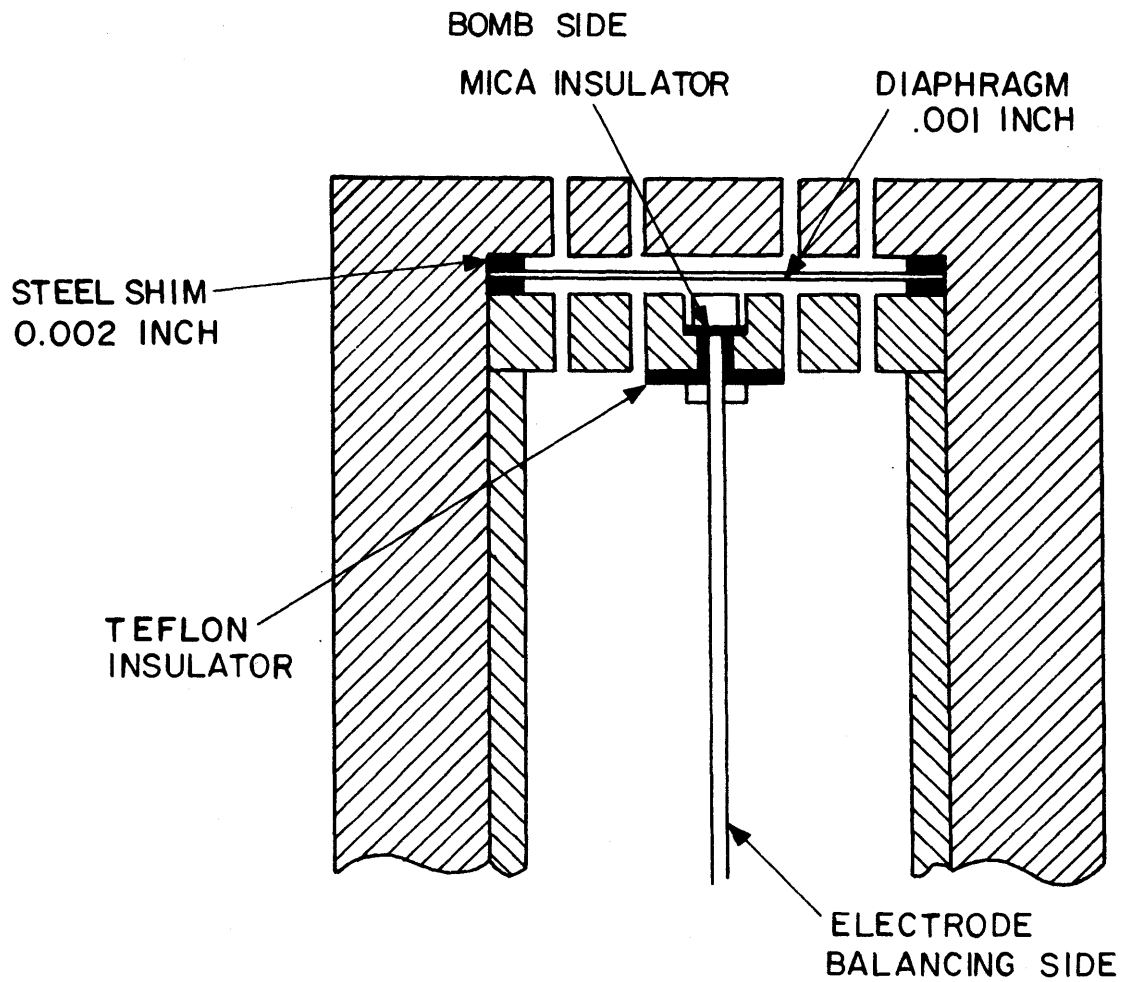
FIG. 6   Schematic Diagram of the Balanced-
          Pressure Indicator
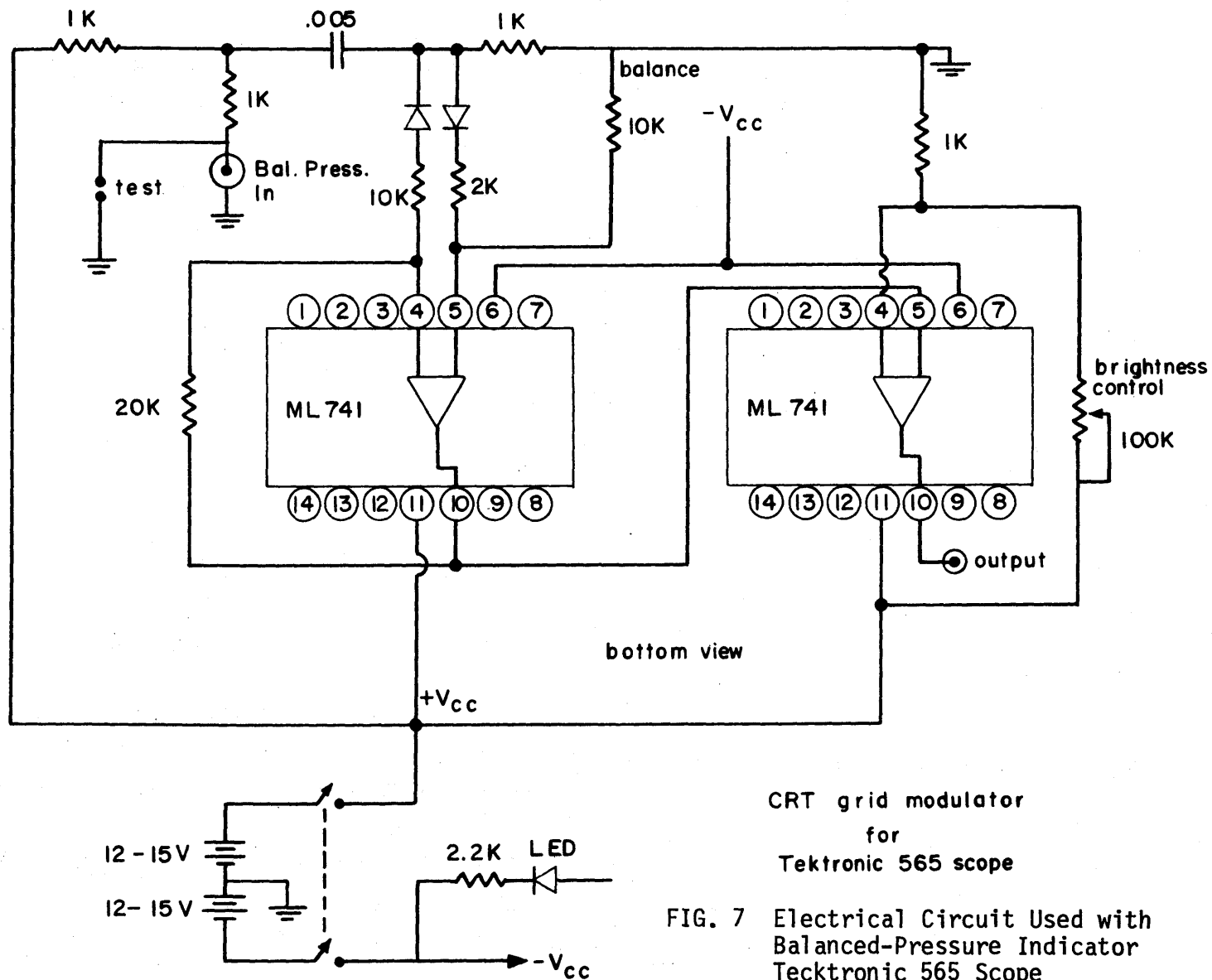
CRT grid modulator
for
Tektronic 565 scope

FIG. 7 Electrical Circuit Used with
Balanced-Pressure Indicator
Tecktronic 565 Scope
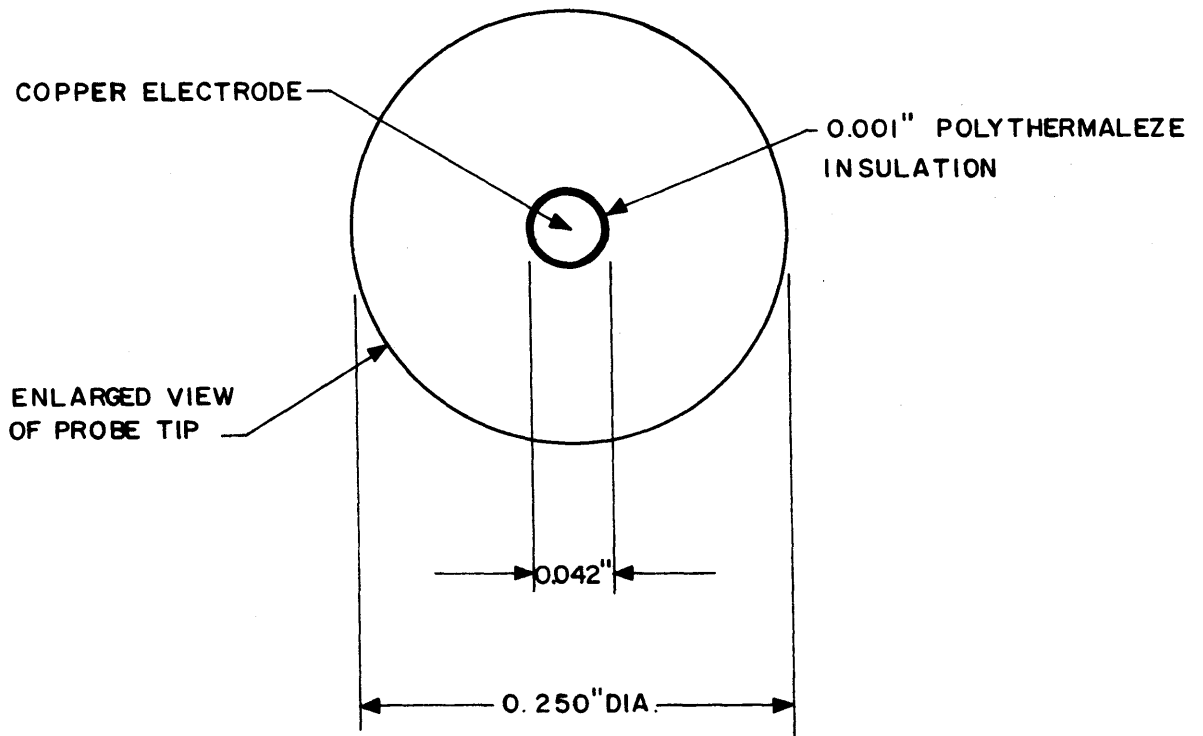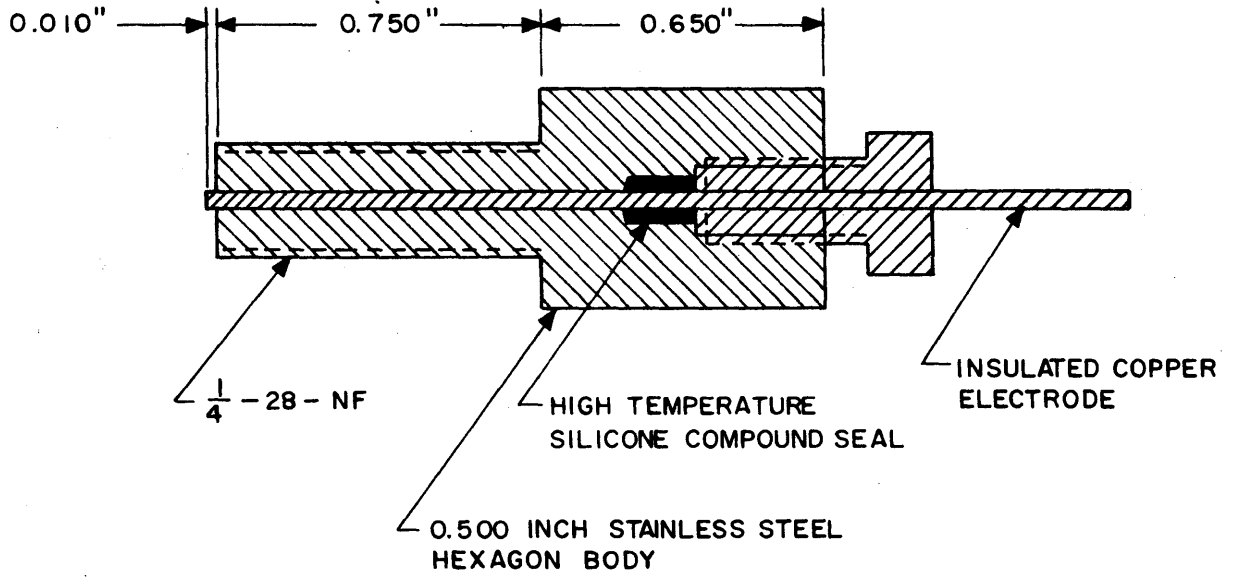
FIG. 8   Schematic Diagrams Showing Construction of
Ionization Probes
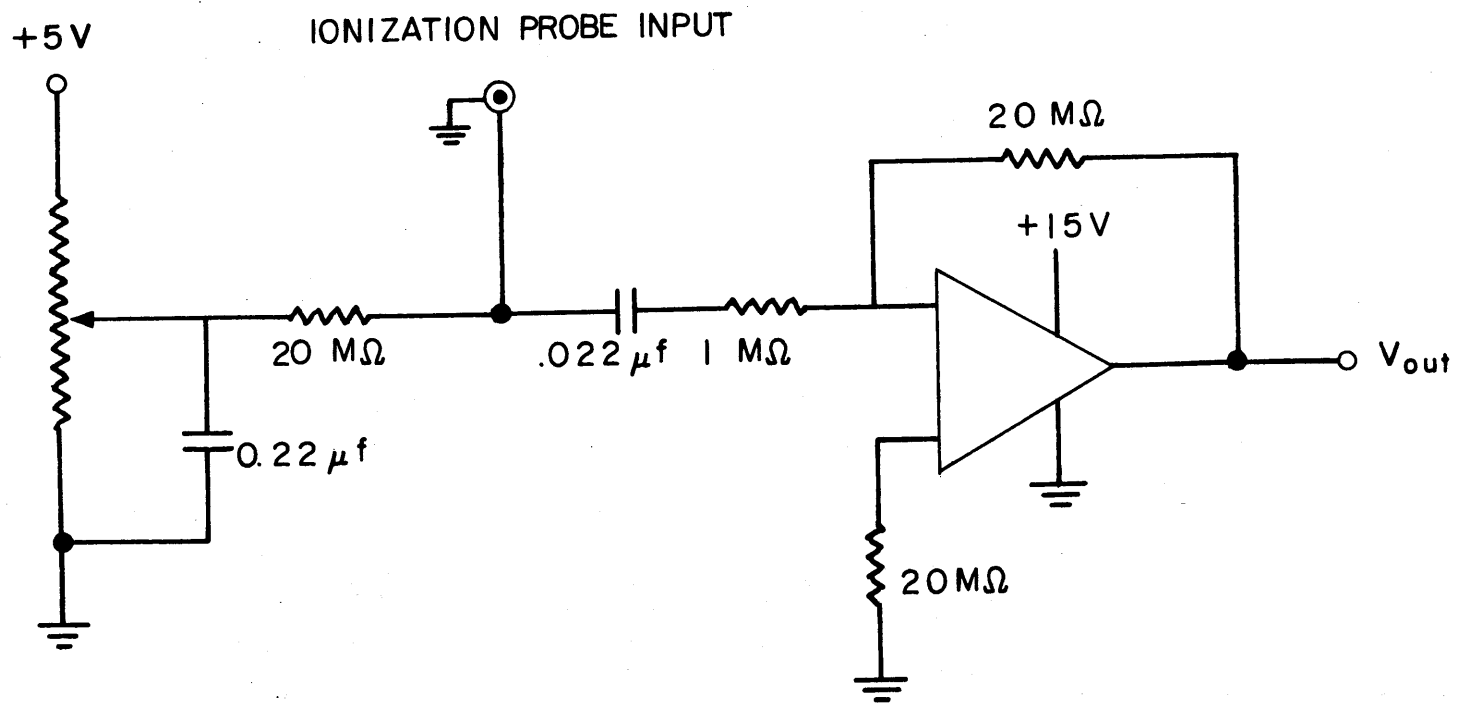
FIG. 9   Schematic Diagram of Ionization
          Probe Circuit

COMBUSTION
BOMB

7.62 CM

6.464 CM

DETECTOR

0.05 mm Slit

1.8 mm Diameter Beam

MIRROR

LASER

MIRROR
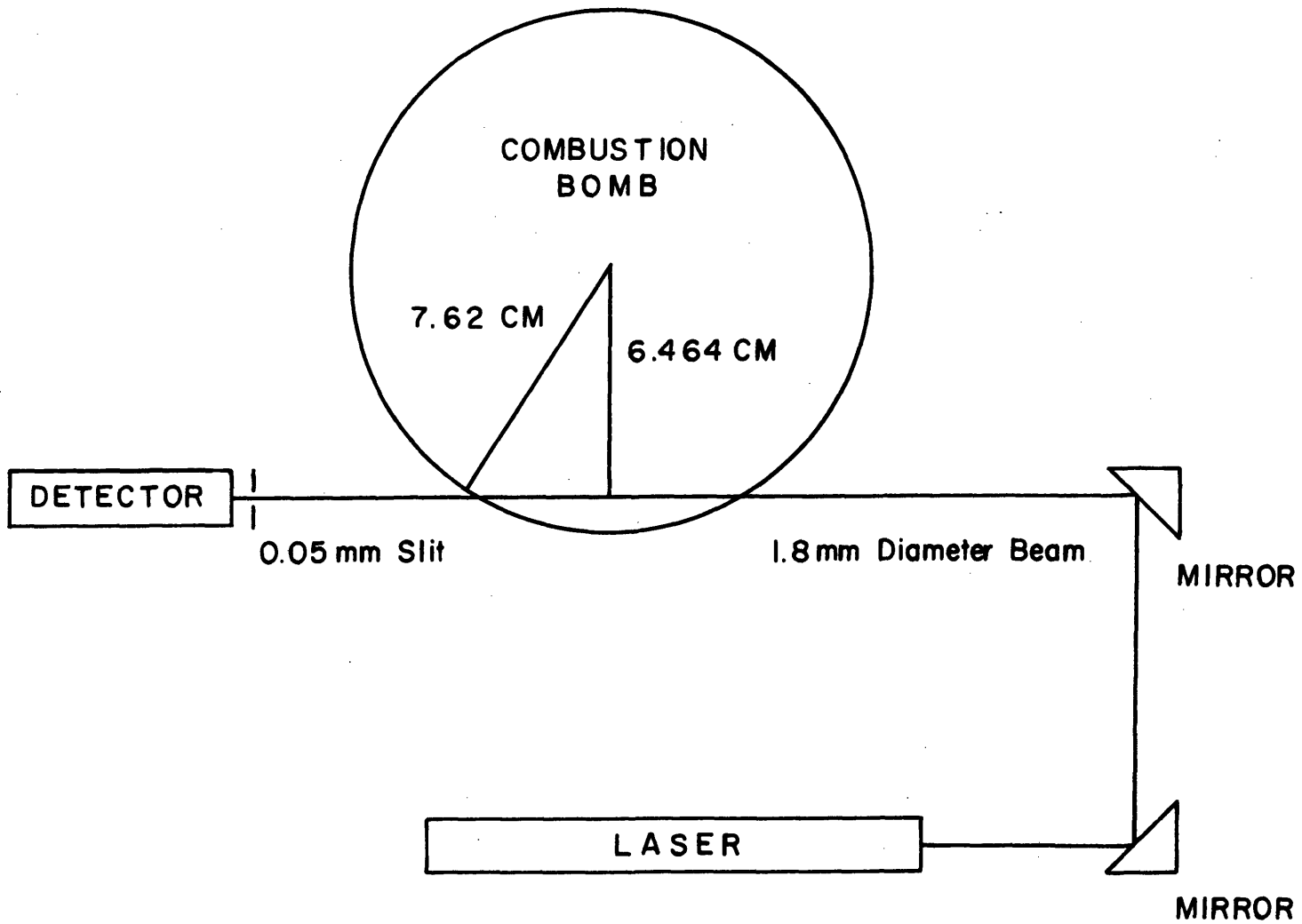
FIG. 10   Schematic Diagram of Laser System

0.560" O. D.

COPPER GASKET

QUARTZ WINDOW

TEFLON GASKETS

WALL OF COMBUSTION BOMB

0.400"

0.280"

0.750"

0.250"

0.600"

0.600"

0.750"

97
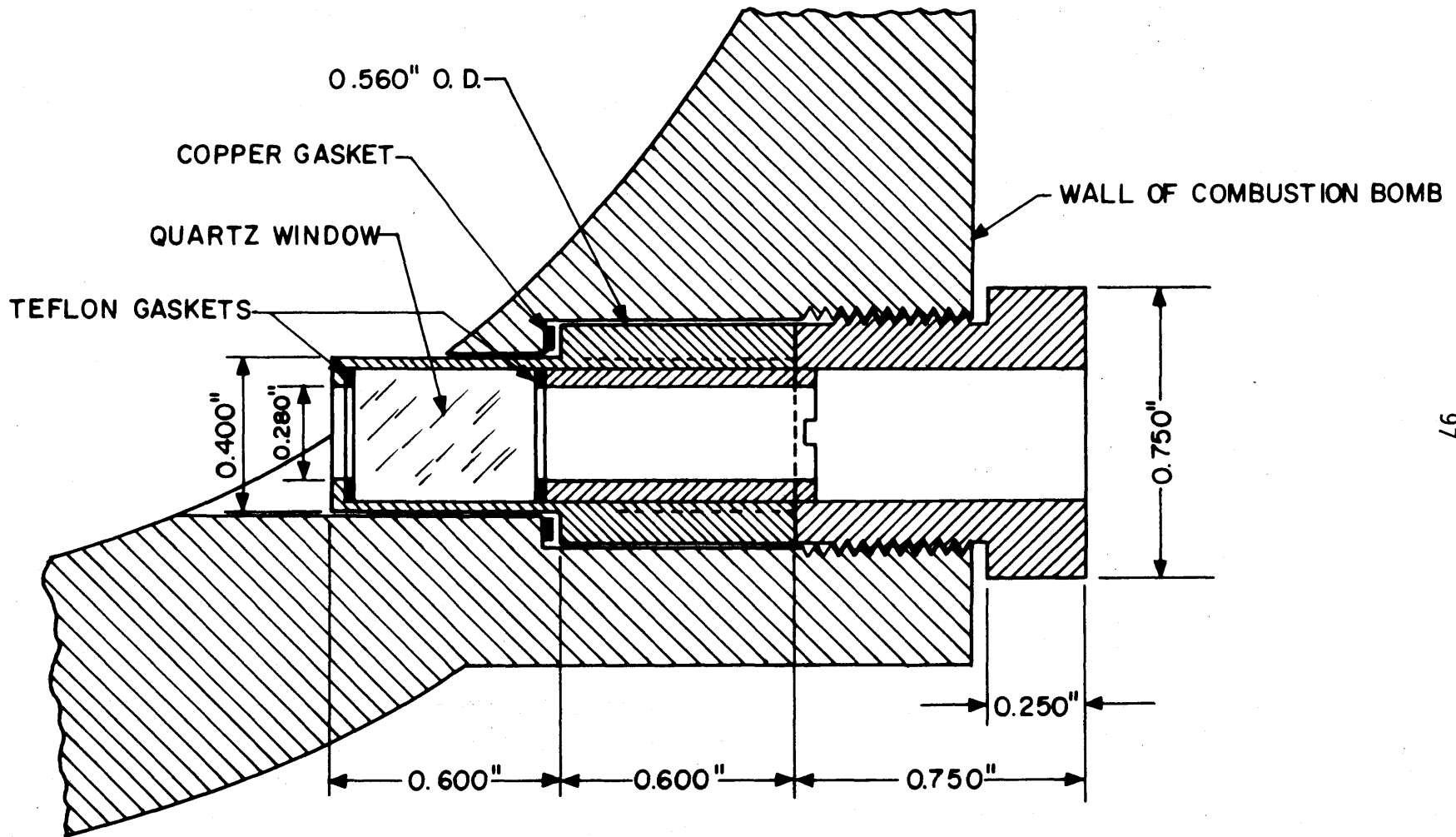
FIG. 11 Schematic Diagram of Window
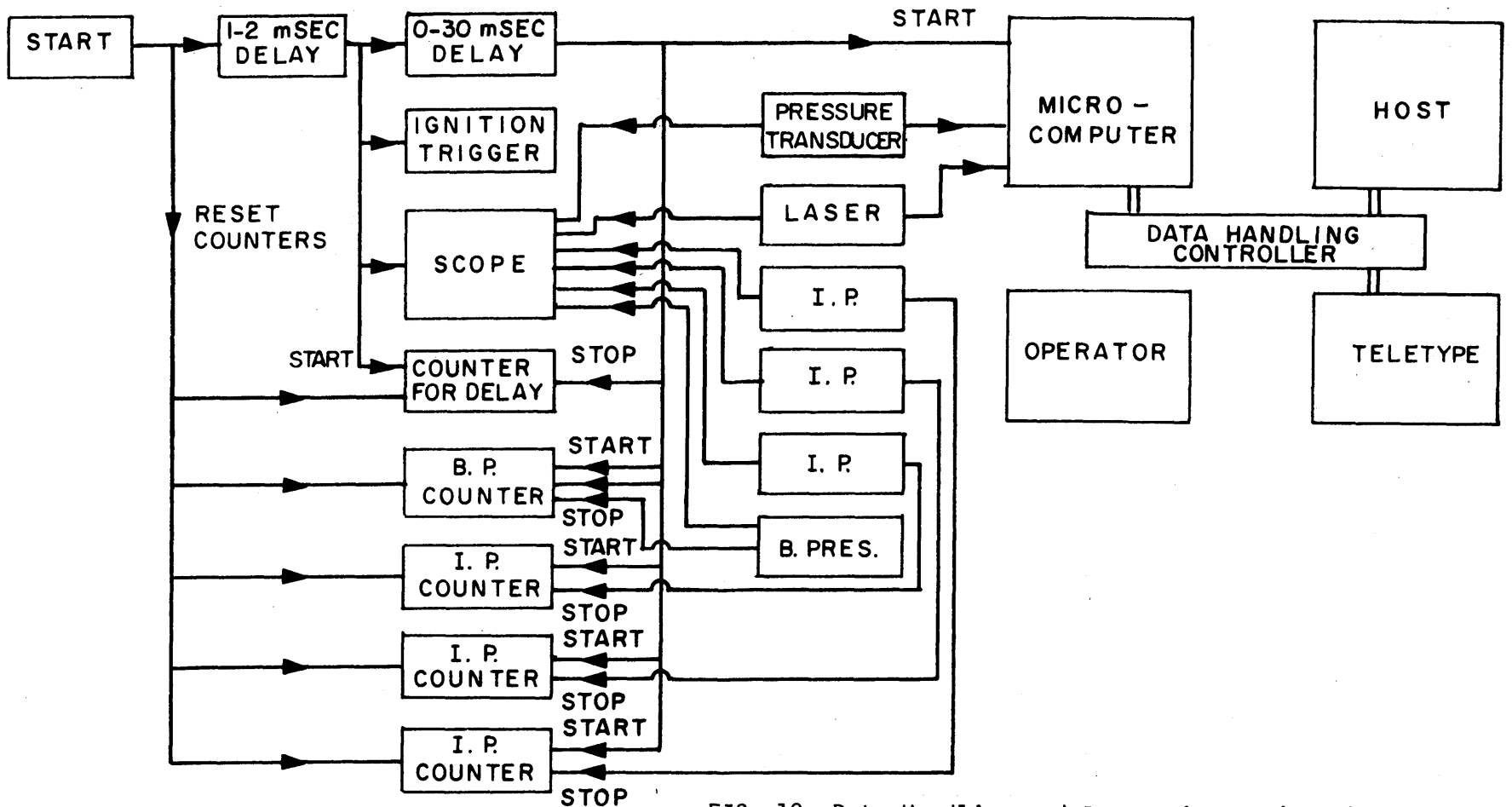
FIG. 12 Data Handling and Processing Equipments

Propane – Air Mixture

$$P_i = 1 \text{ ATM} \qquad T_i = 298 \text{ K} \qquad \phi = 1.0$$
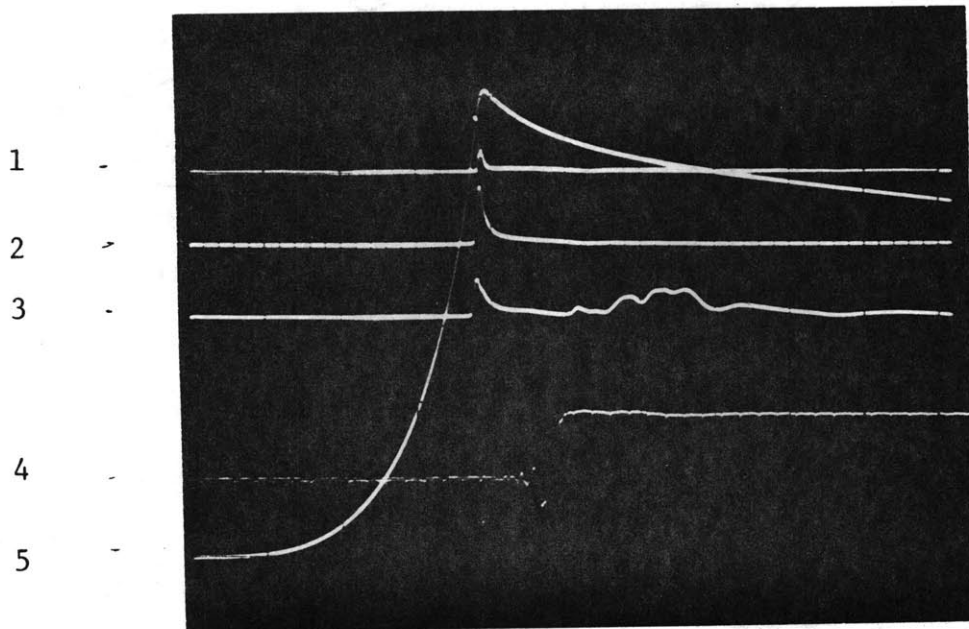
10 msec/div. Laser trace delayed 22 msec, sweep rate 1 msec/div.

Traces No. 1,2 and 3: Ionization Probe Signals

Trace No. 4: Laser Signal

Trace No. 5: Pressure Transducer Signal

FIG. 13
A TYPICAL OSCILLOGRAM FOR STOICHIOMETRIC PROPANE – AIR MIXTURE
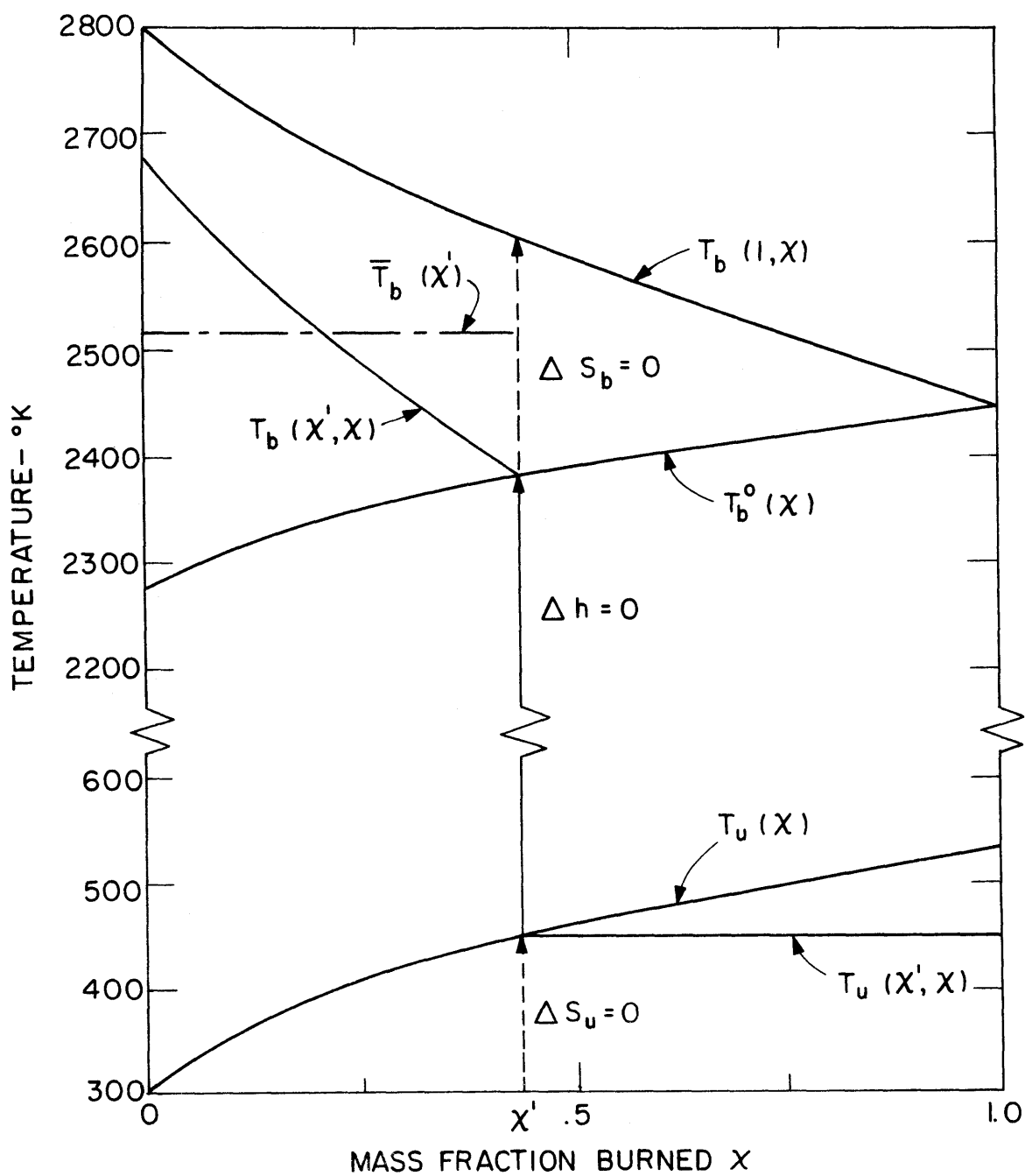
FIG. 14   The Relationship Between the Temperature Distributions
in the Fuel Air Mixtures as a Function of Mass Fraction
Burned
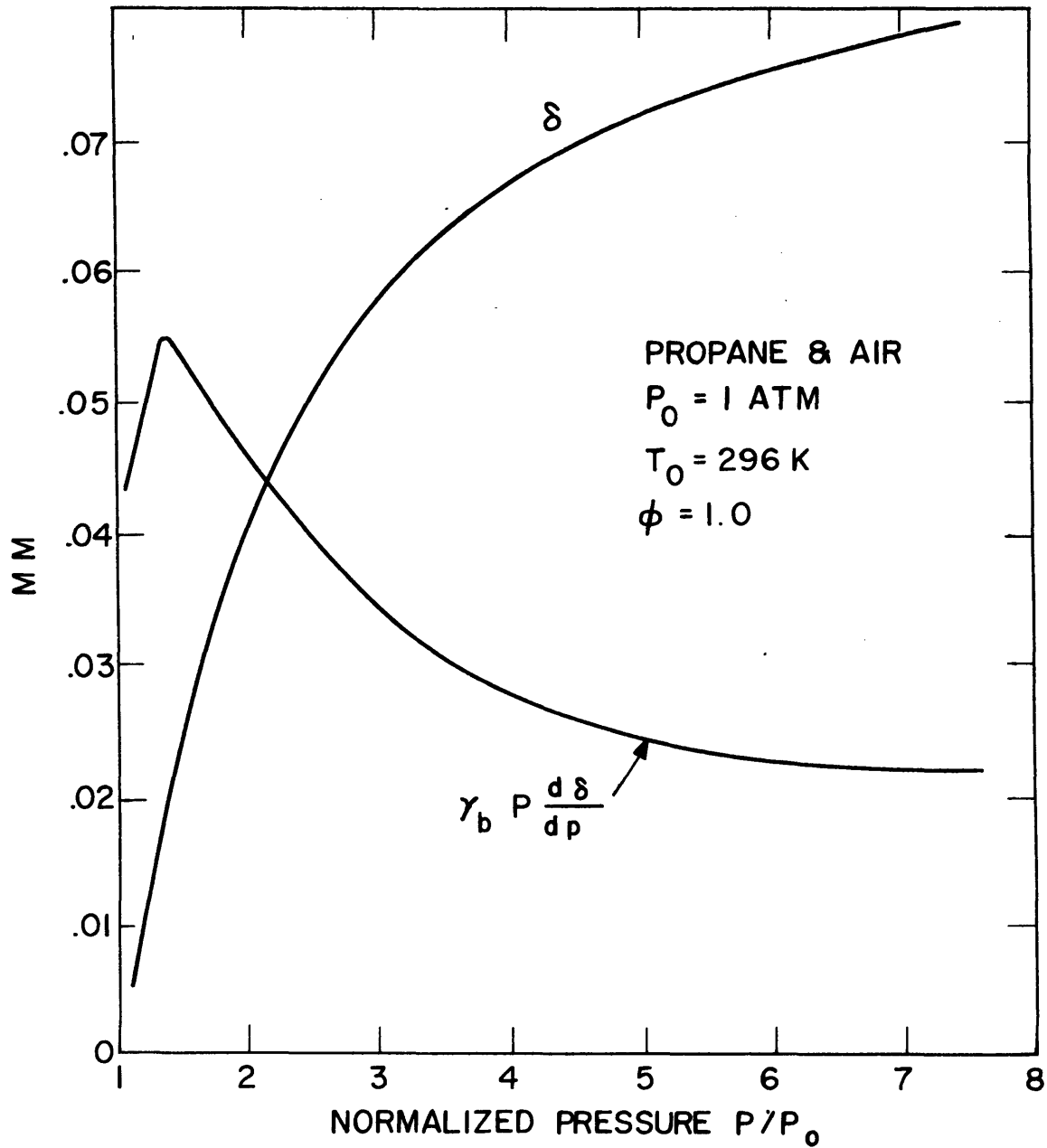
FIG. 15   Displacement Thickness (δ) and $\gamma_b P \frac{d\delta}{dp}$ as a Function of

Normalized Pressure for Stoichiometric Propane-Air Mixtures with
Initial Atmospheric Pressure and Initial Temperature of 298 K
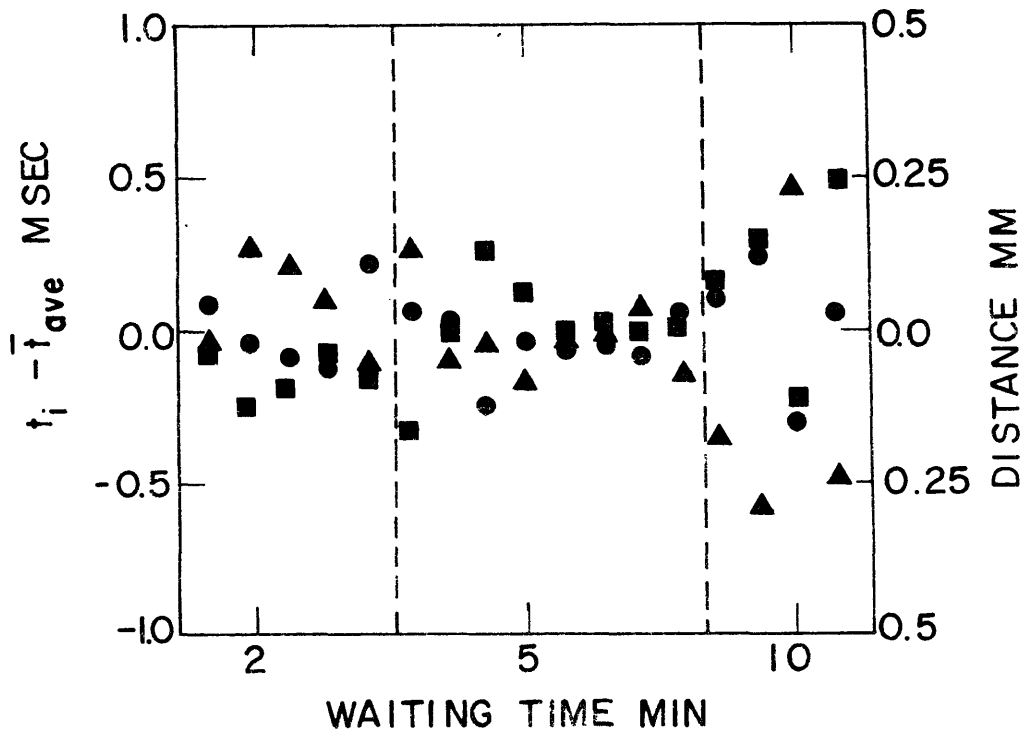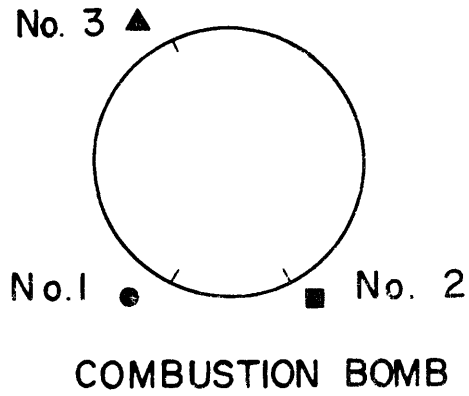
FIG. 16 Time Deviation of the Ionization Probe Pulses from the Mean Time $(t_i - \bar{t})$ as a Function of Waiting Time
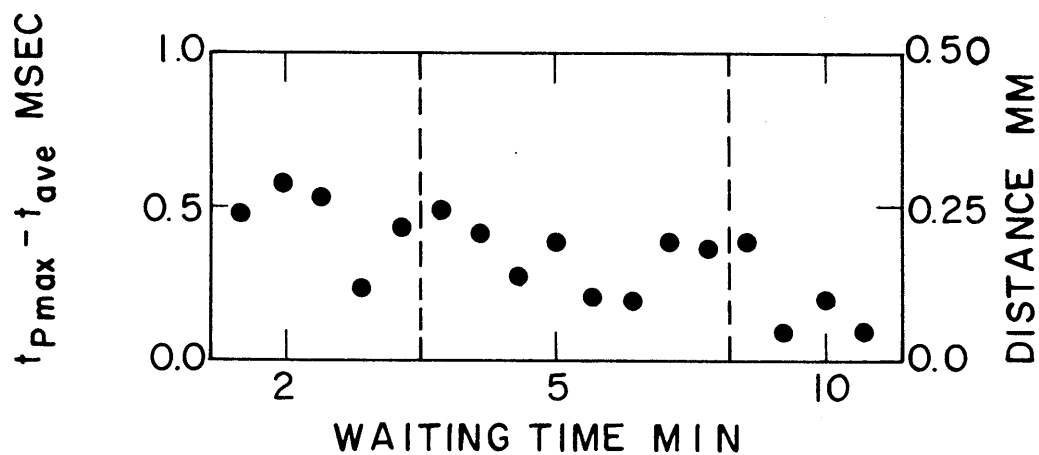
FIG. 17a   Difference of the Time When Peak Pressure Occurred
and the Mean Time of the Ionization Probe Pulses as
a Function of Waiting Time
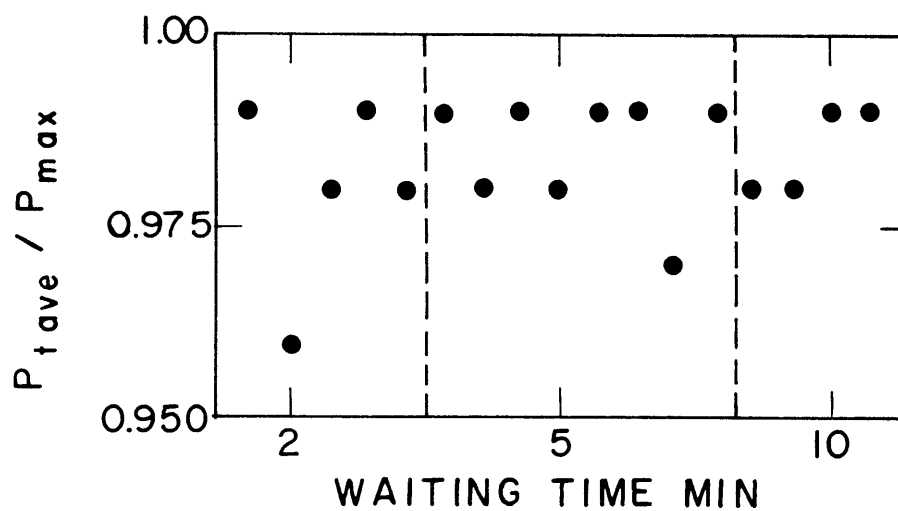
FIG. 17b   The Ratio of the Pressure Inside the Combustion Bomb
at the Average Arrival Time of the Flame for Three
Ionization Probes to the Maximum Pressure as a Function
of the Waiting Time

PRESSURE ATM

PROPANE & AIR
T_i = 298 K
P_i = 1 ATM
ϕ = 1.0
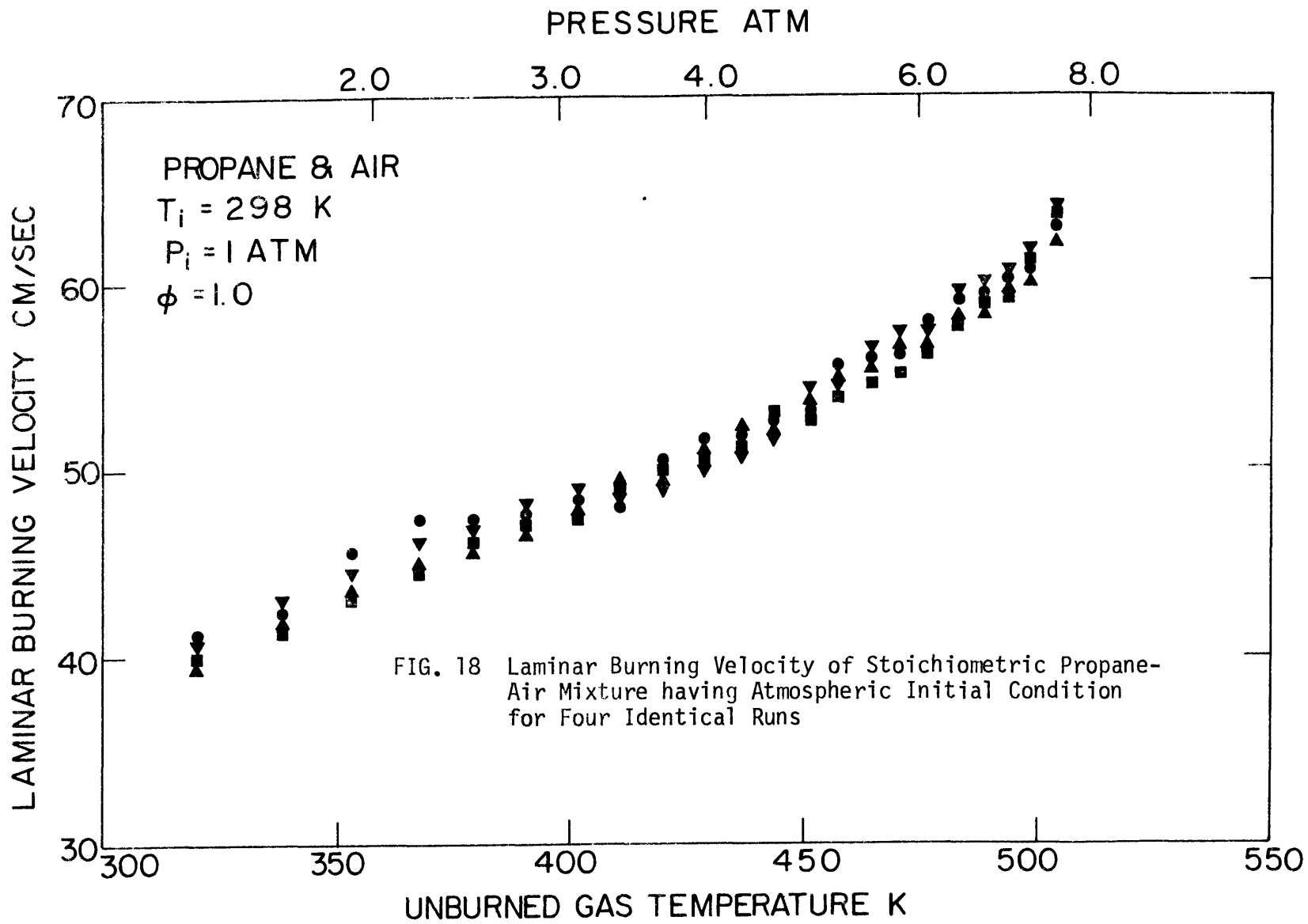
FIG. 18 Laminar Burning Velocity of Stoichiometric Propane-
Air Mixture having Atmospheric Initial Condition
for Four Identical Runs

LAMINAR BURNING VELOCITY CM/SEC

UNBURNED GAS TEMPERATURE K

104
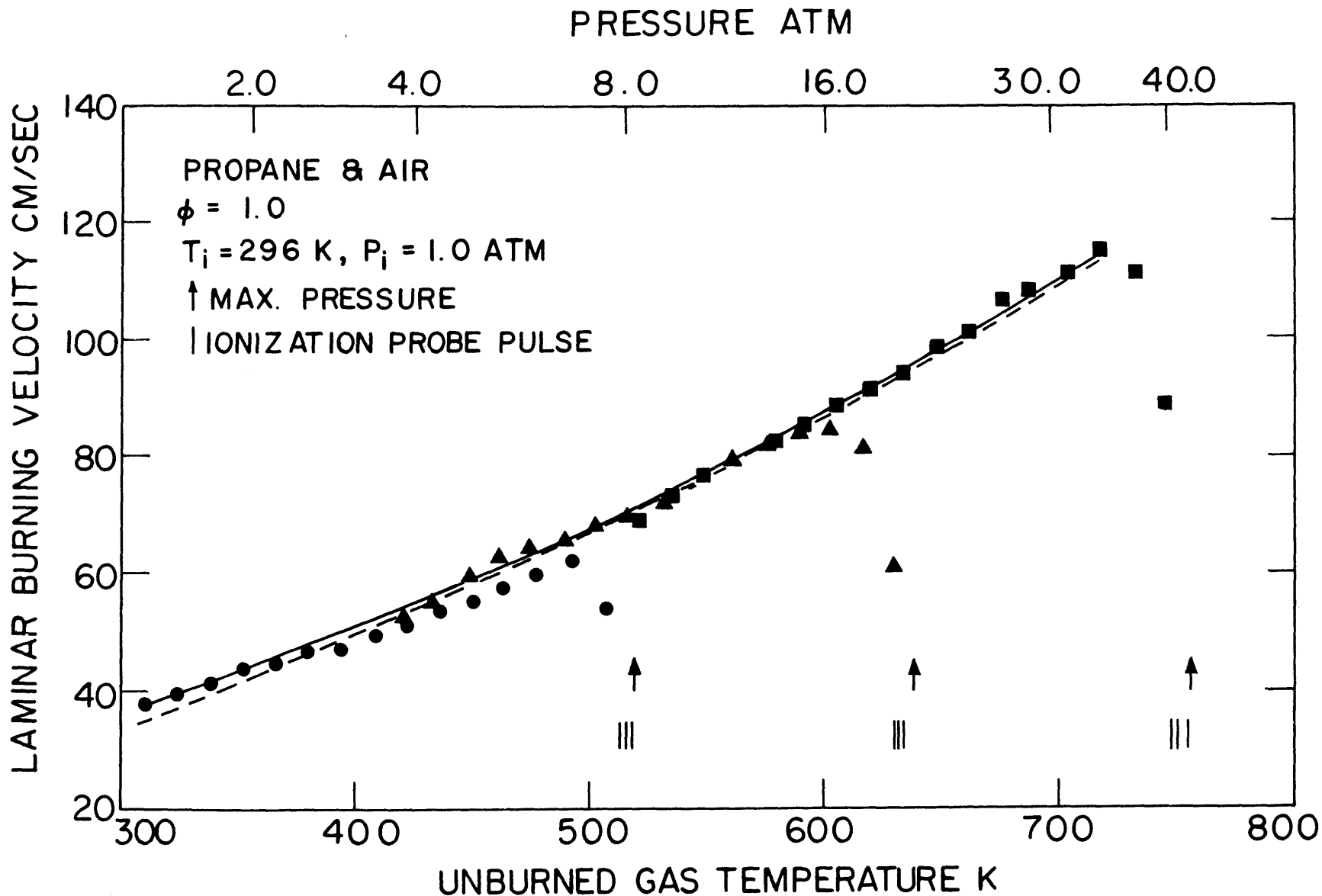
FIG. 19 Laminar Burning Velocity for Stoichiometric Propane-
Air Mixtures
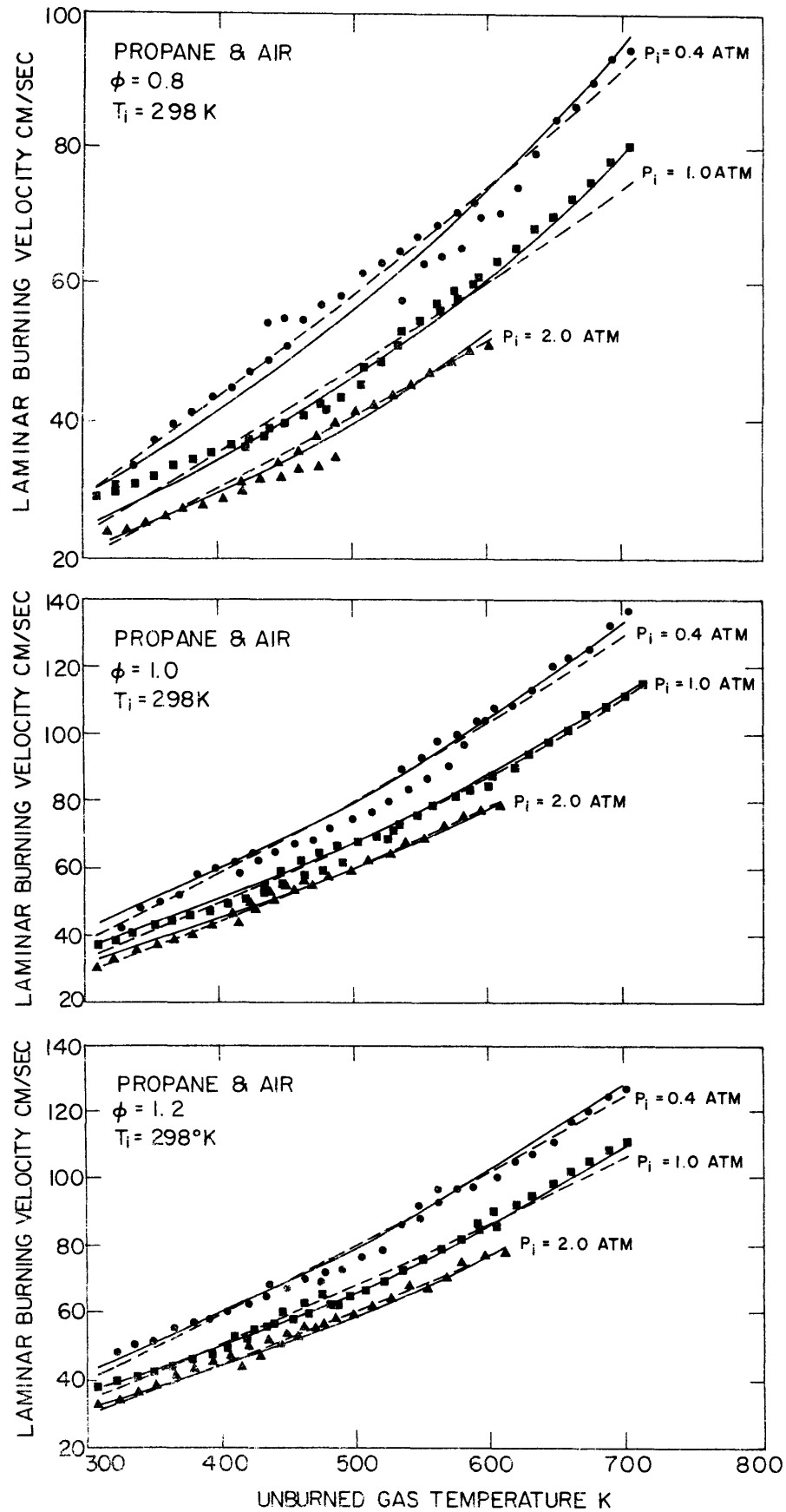
FIG. 20 Laminar Burning Velocity of Propane-Air Mixtures at Equivalence
Ratios of 0.8, 1.0, and 1.2
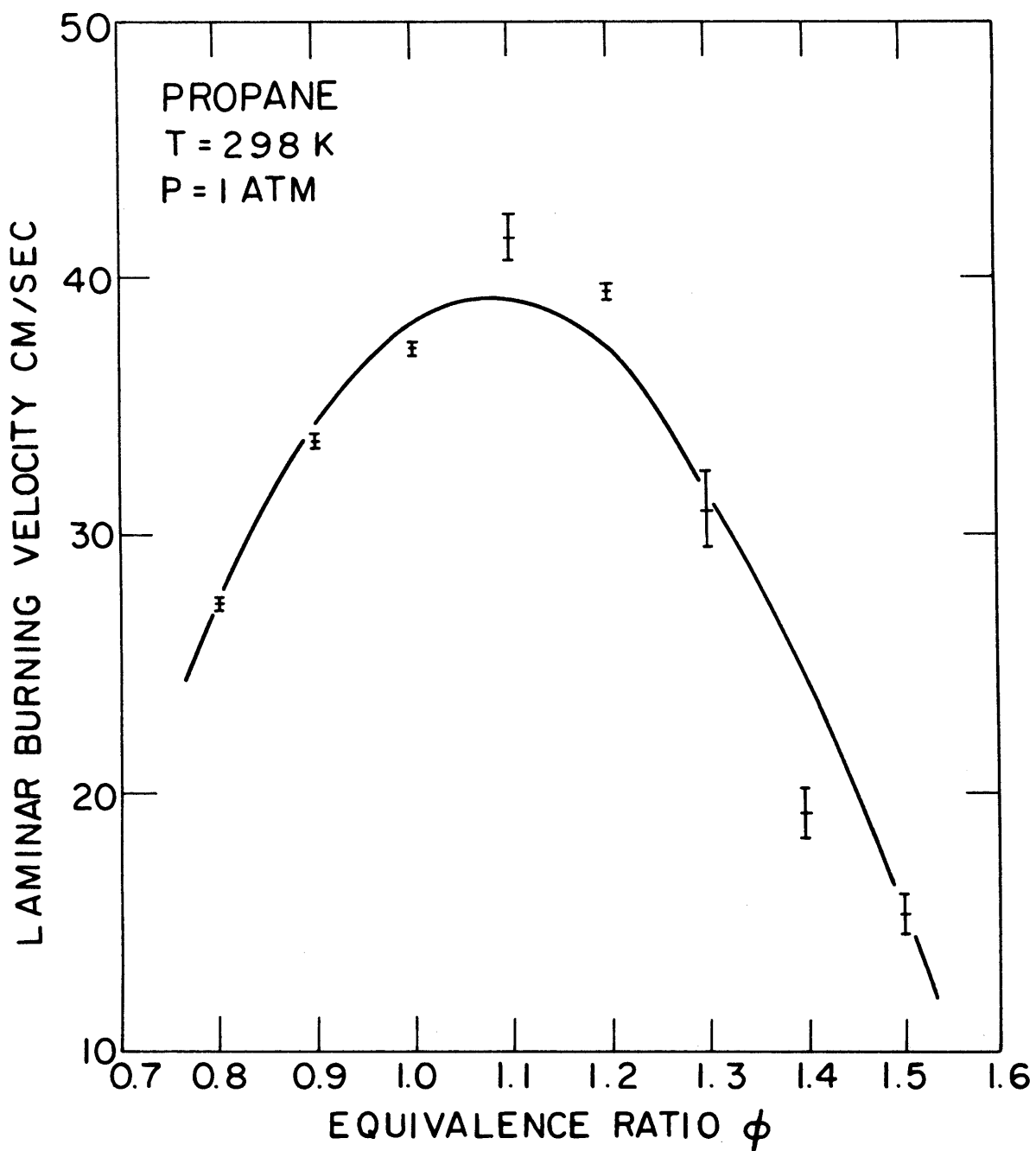
FIG. 21   Laminar Burning Velocity of Propane-Air Mixtures at
Atmospheric Condition as a Function of Equivalence Ratio
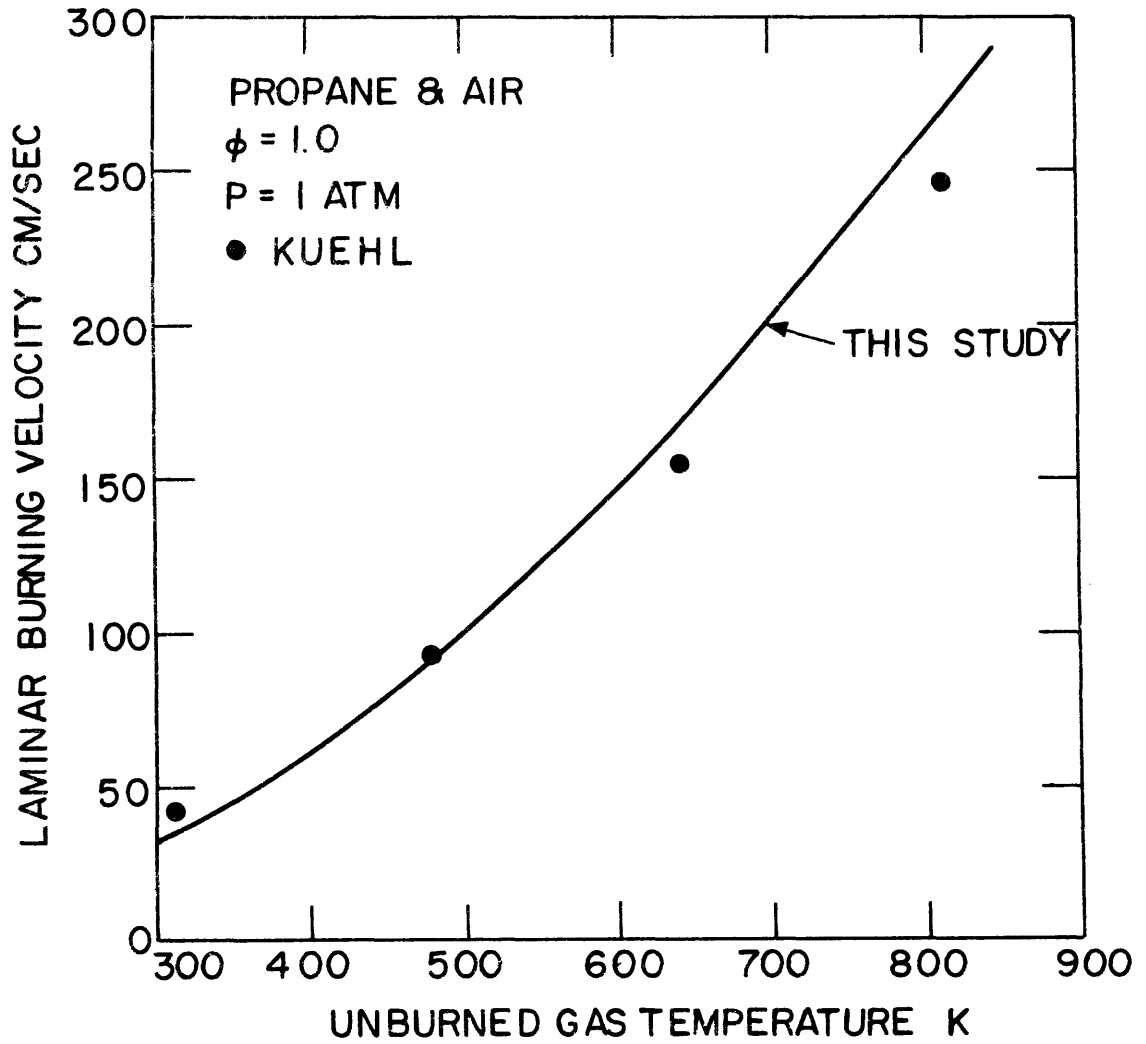
FIG. 22   Comparison of Measured Laminar Burning Velocity for
Propane-Air Mixtures with Those Reported by Kuehl [28]
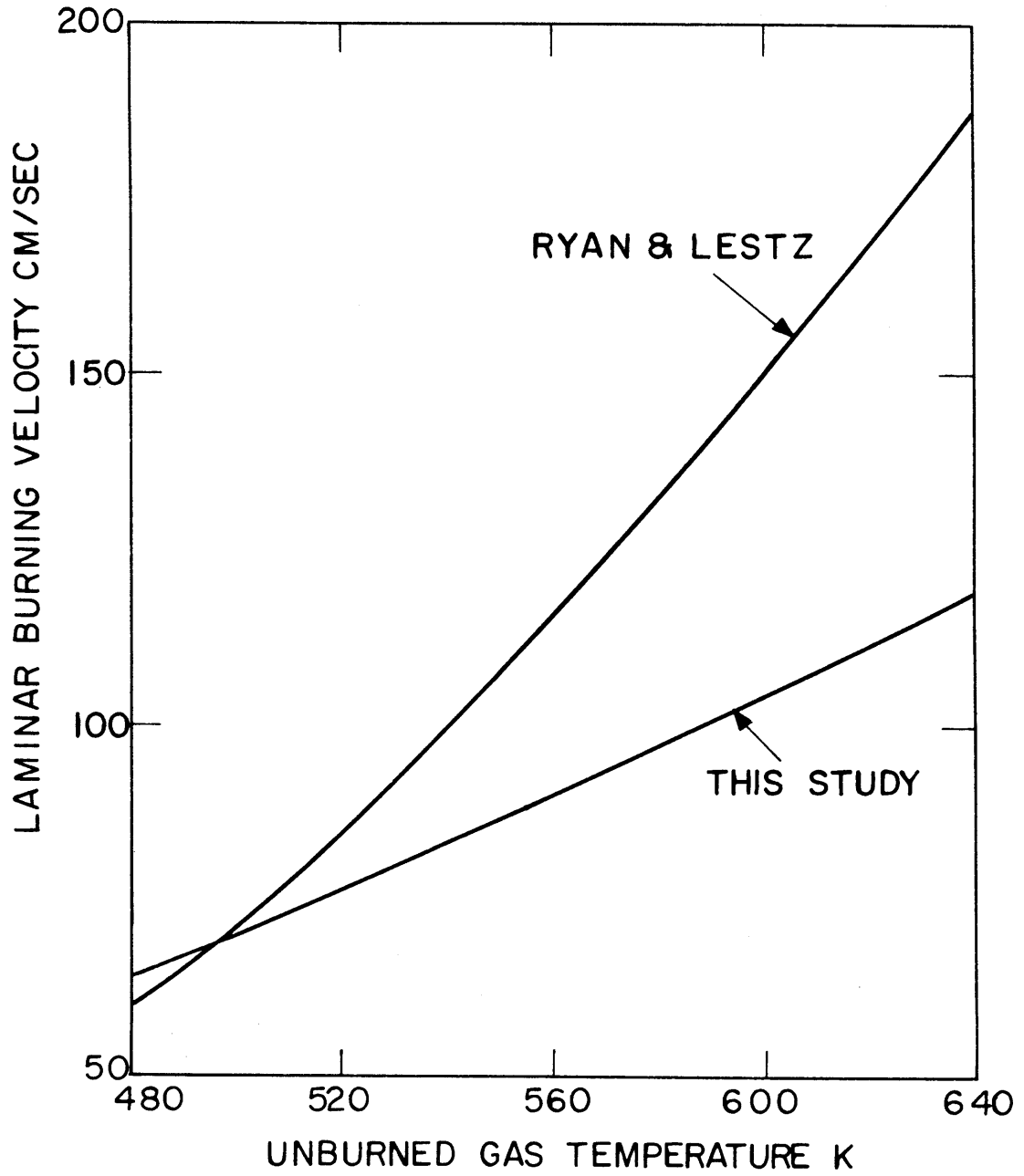
FIG. 23 Comparison of Measured Laminar Burning Velocity for
Propane-Air Mixtures with Those Reported by Ryan and
Lestz

FIG. 24 Laminar Burning Velocity of Isooctane-Air Mixtures at Equivalence Ratios of 0.8, 1.0, and 1.2
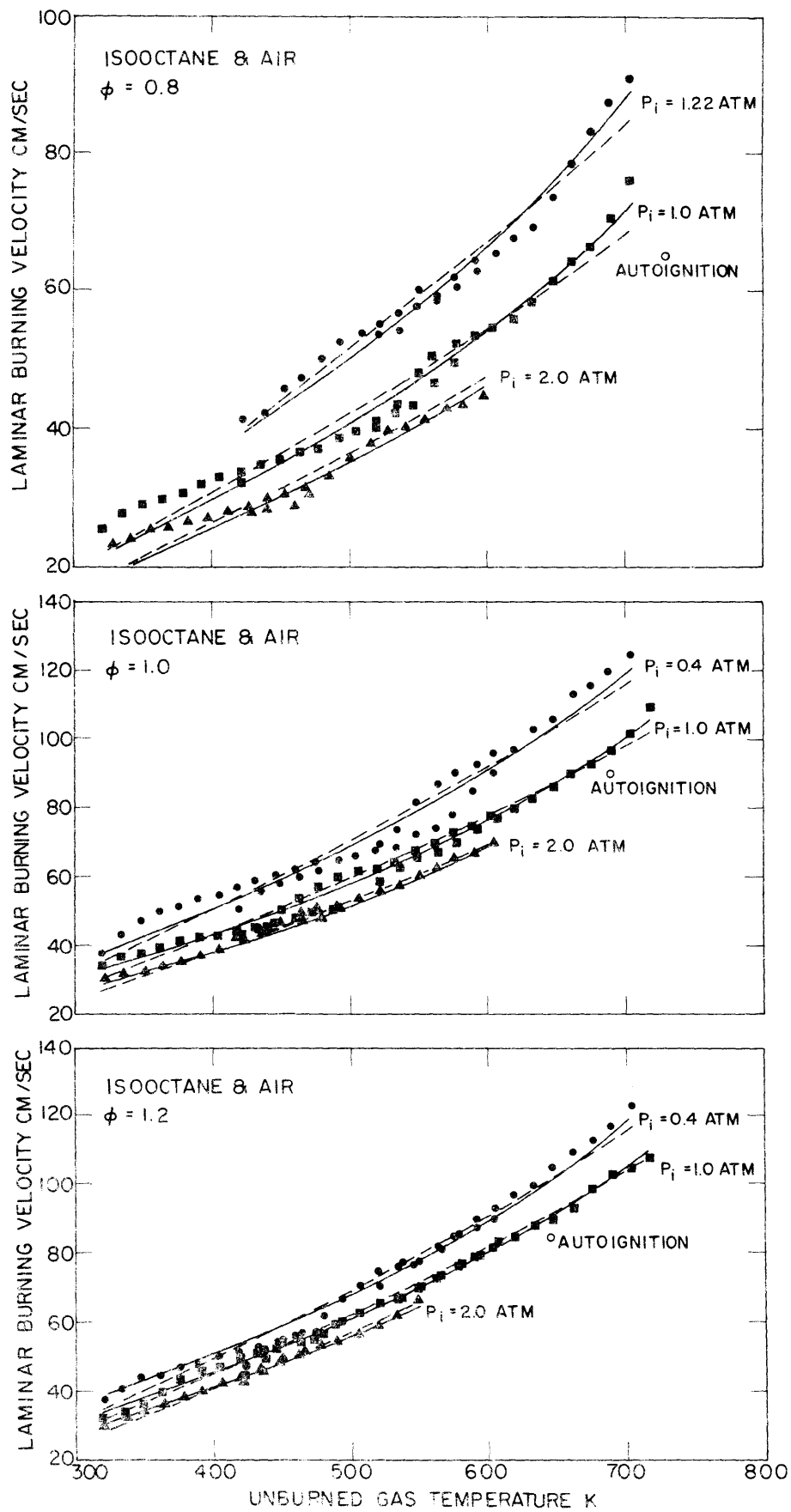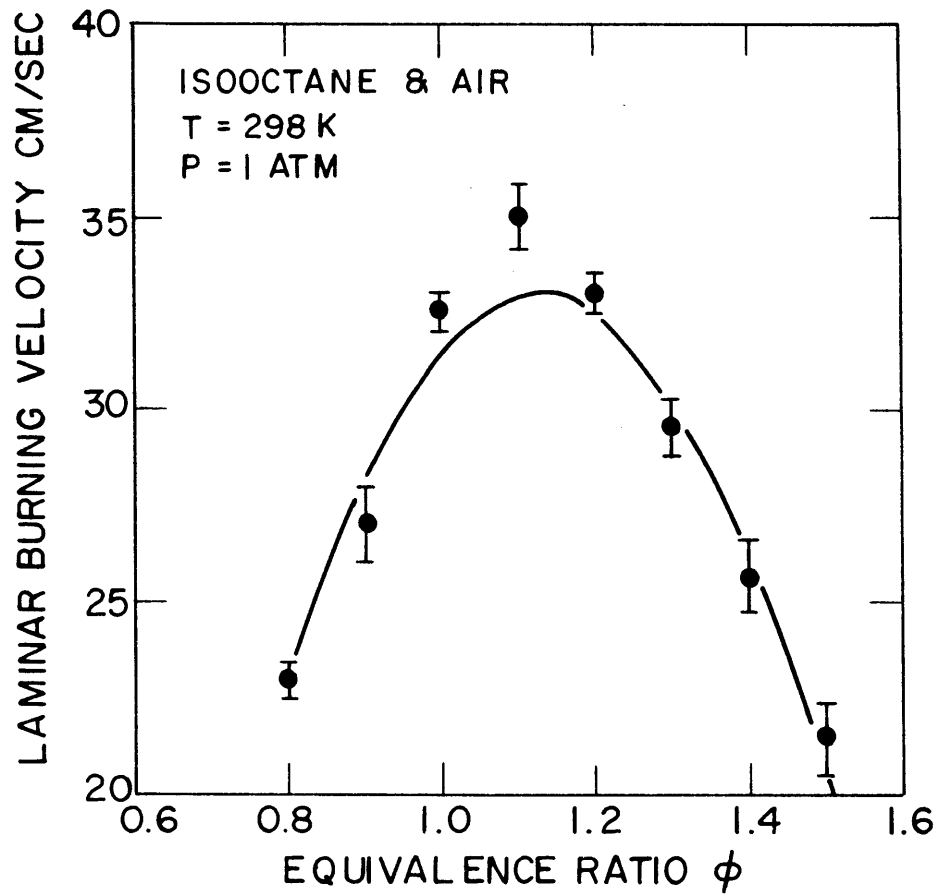
FIG. 25 Laminar Burning Velocity of Isooctane-Air
Mixtures at Atmospheric Condition as a
Function of Equivalence Ratio
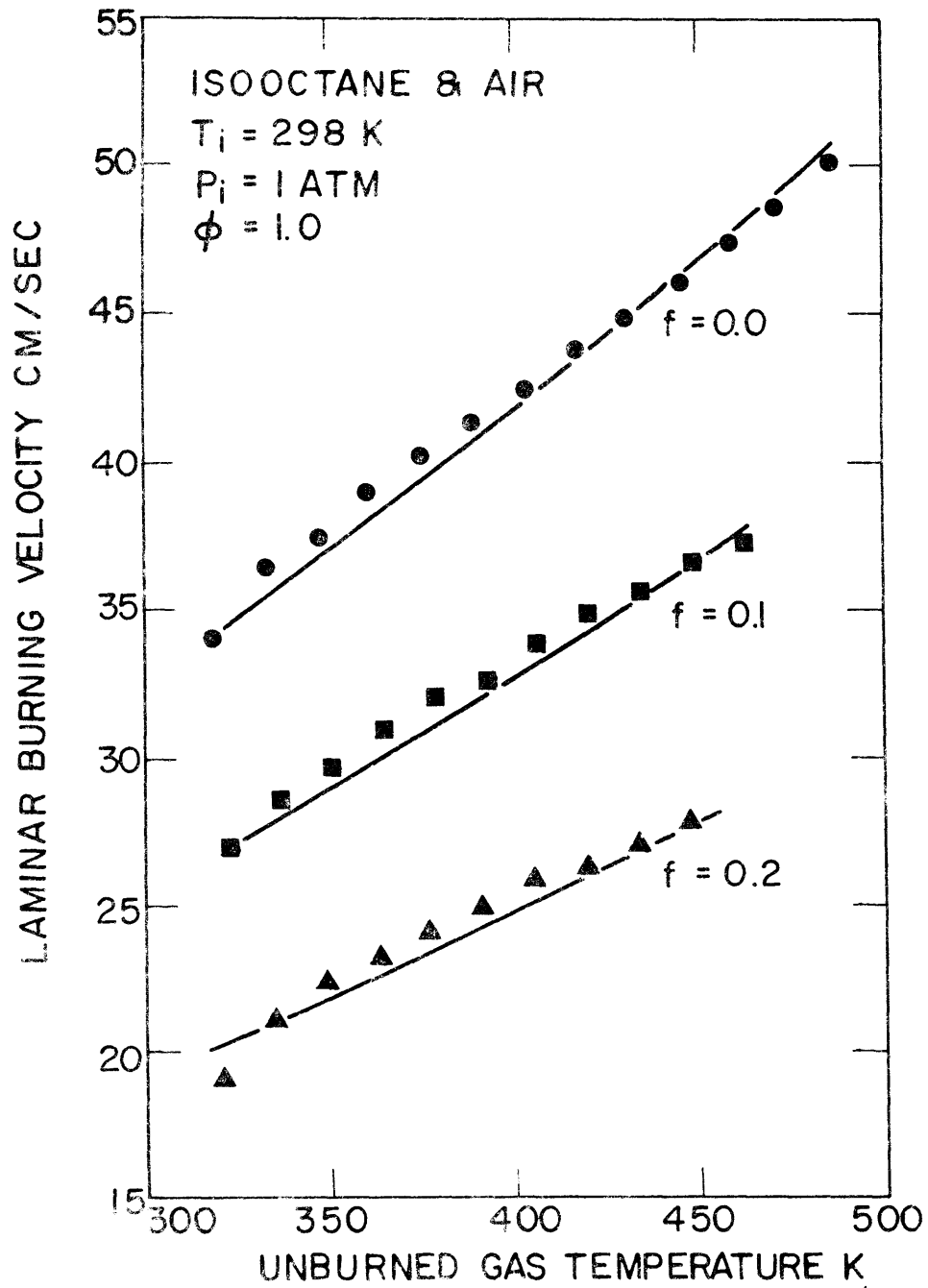
FIG. 26   Laminar Burning Velocity of Stoichiometric Isooctane-
Air Mixtures with Three Different Residual Fractions
of f=0, f=0.10, and f=0.20 as a Function of Unburned
Gas Temperature
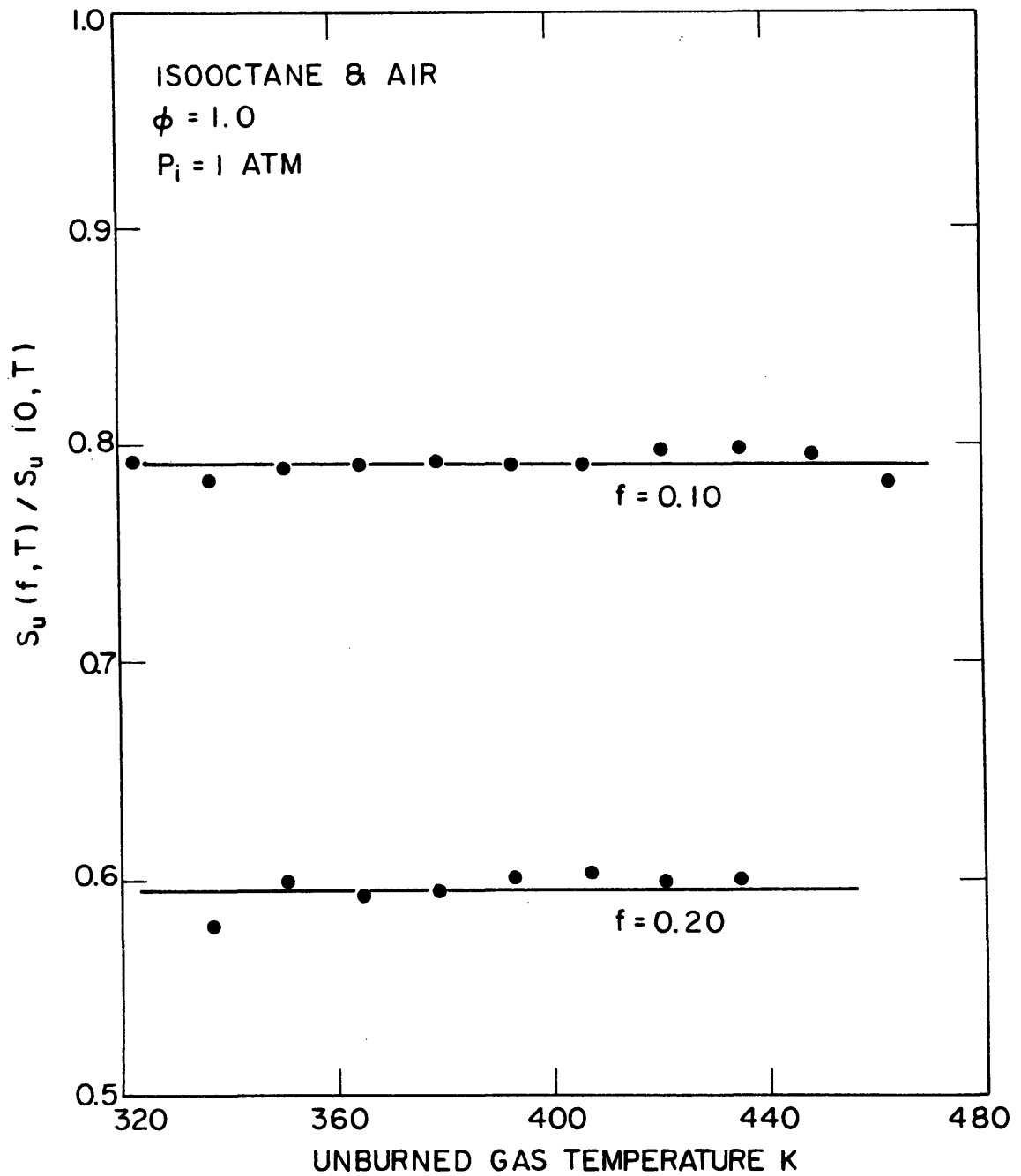
FIG. 27   Laminar Burning Velocity of Isooctane-Air Mixtures having Residual
          Fractions of f=0.10 and f=0.20 Normalized with Respect to the
          Burning Velocity with No Diluent as a Function of Unburned Gas
          Temperature

114
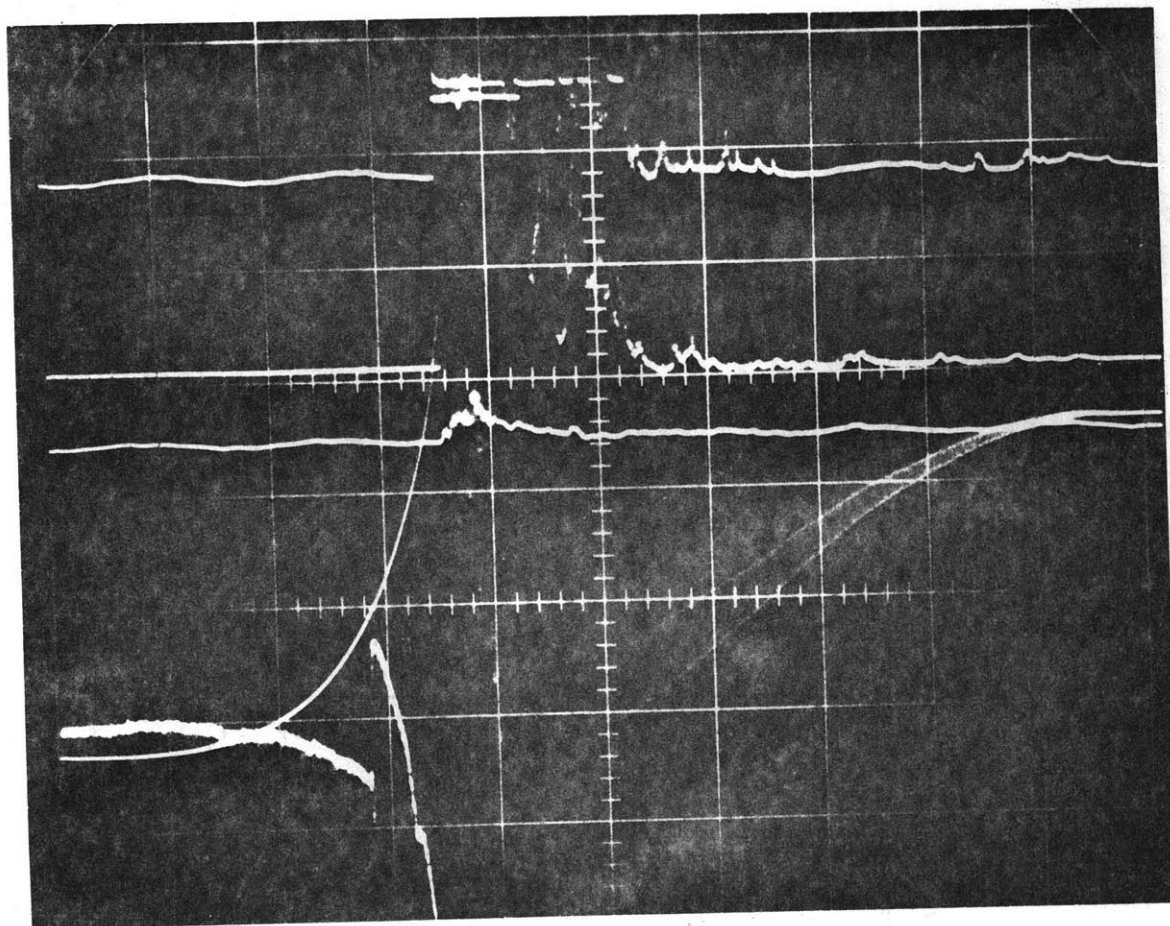
FIG. 28 Oscillogram for Stoichiometric Isooctane-Air Mixtures with Initial
Pressure of 15.1 atm and Initial Temperature of 500 K in which
Autoignition Occurred
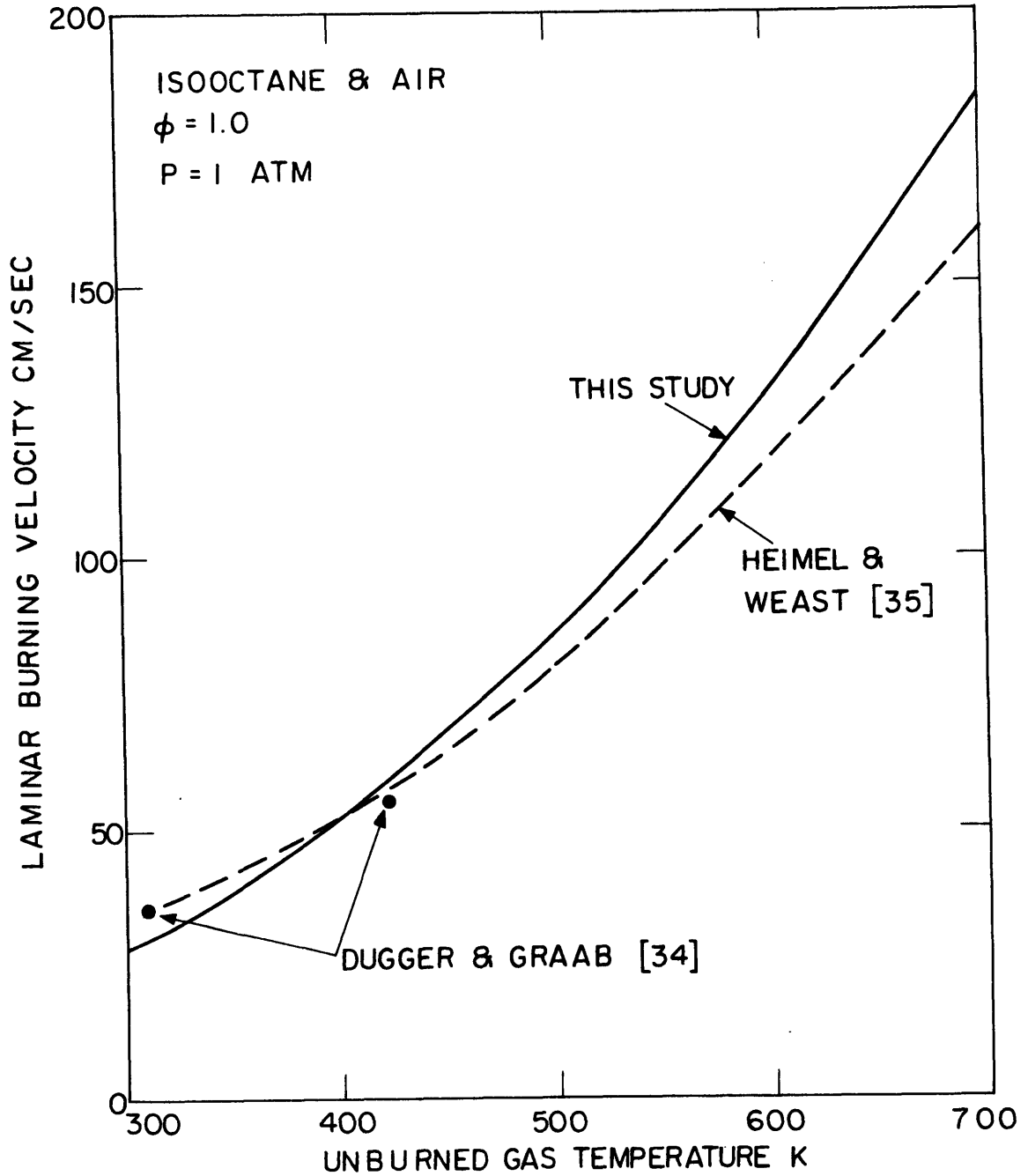
FIG. 29 Comparison of Measured Laminar Burning Velocity for Isooctane-
Air Mixtures with Those Reported by Heimel and Weast [35]
and Duggar and Graab [34]
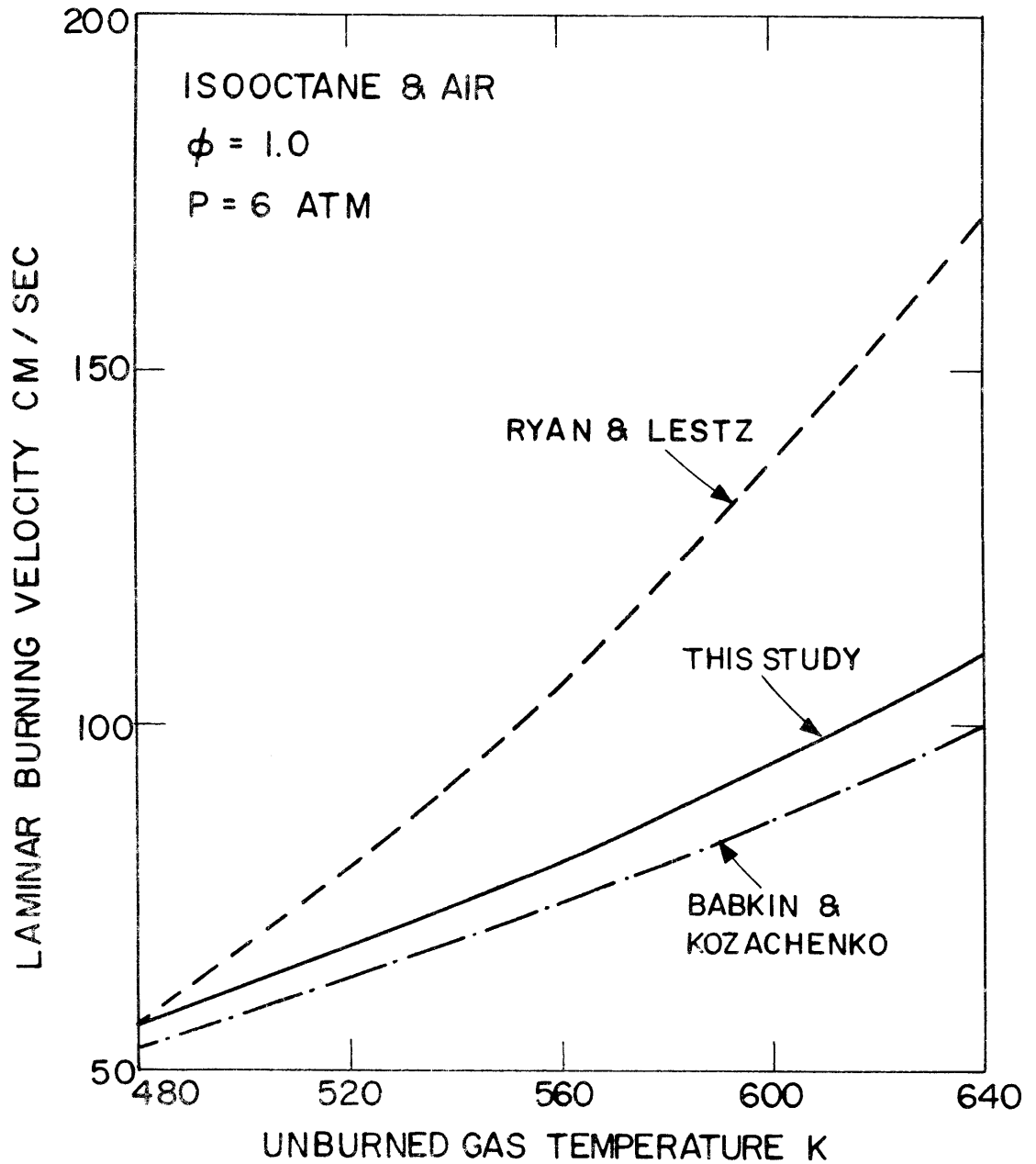
FIG. 30 Comparison of Measured Laminar Burning Velocity for Isooctane-
Air Mixtures with Those Reported by Ryan and Lestz [22] and
Babkin and Kozachenko [37]

FIG. 31   Laminar Burning Velocity of Methanol-Air Mixtures at Equivalence
Ratios of 0.8, 1.0, and 1.2
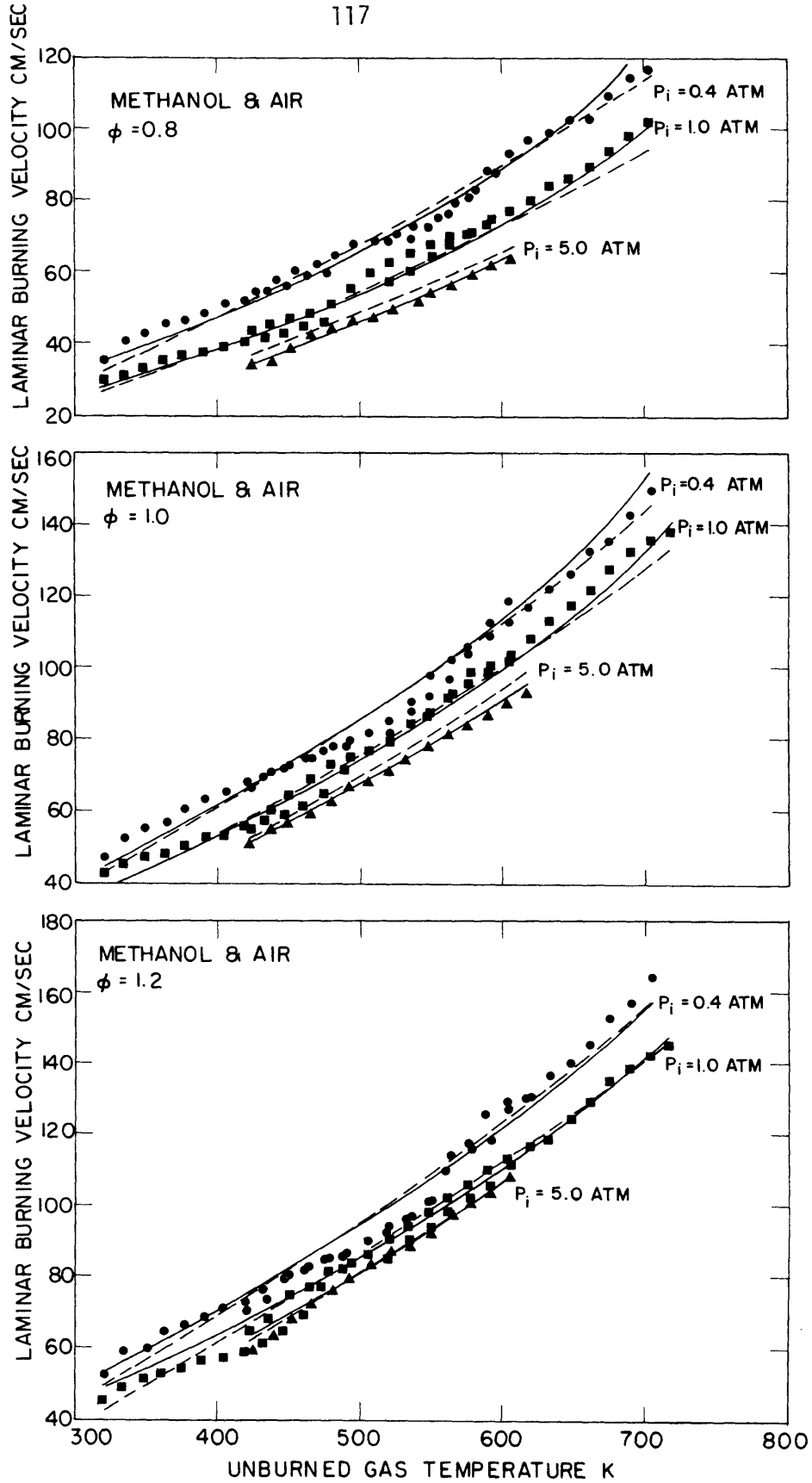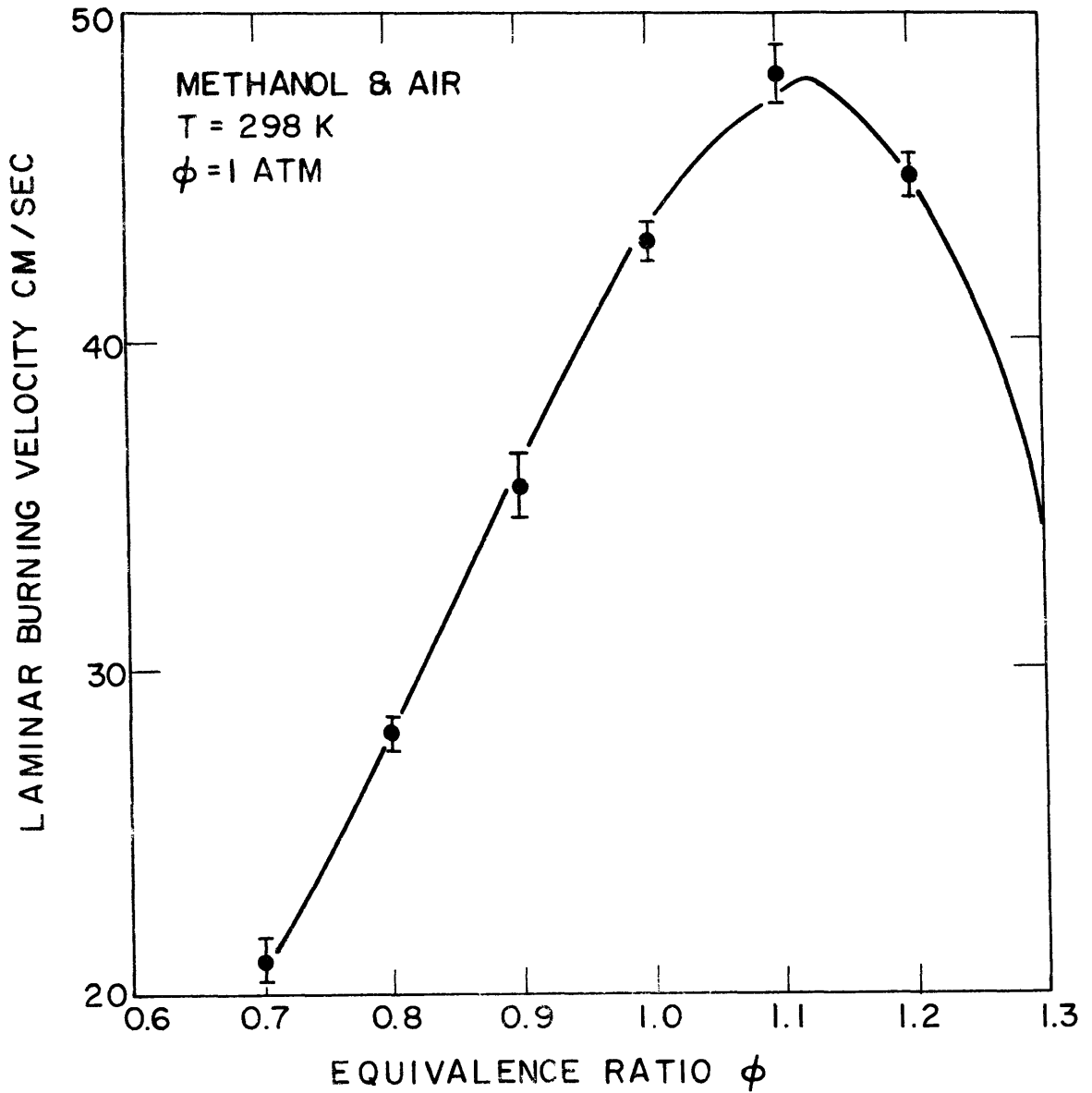
FIG. 32   Laminar Burning Velocity of Methanol-Air Mixtures at
Atmospheric Condition as a Function of Equivalence Ratio
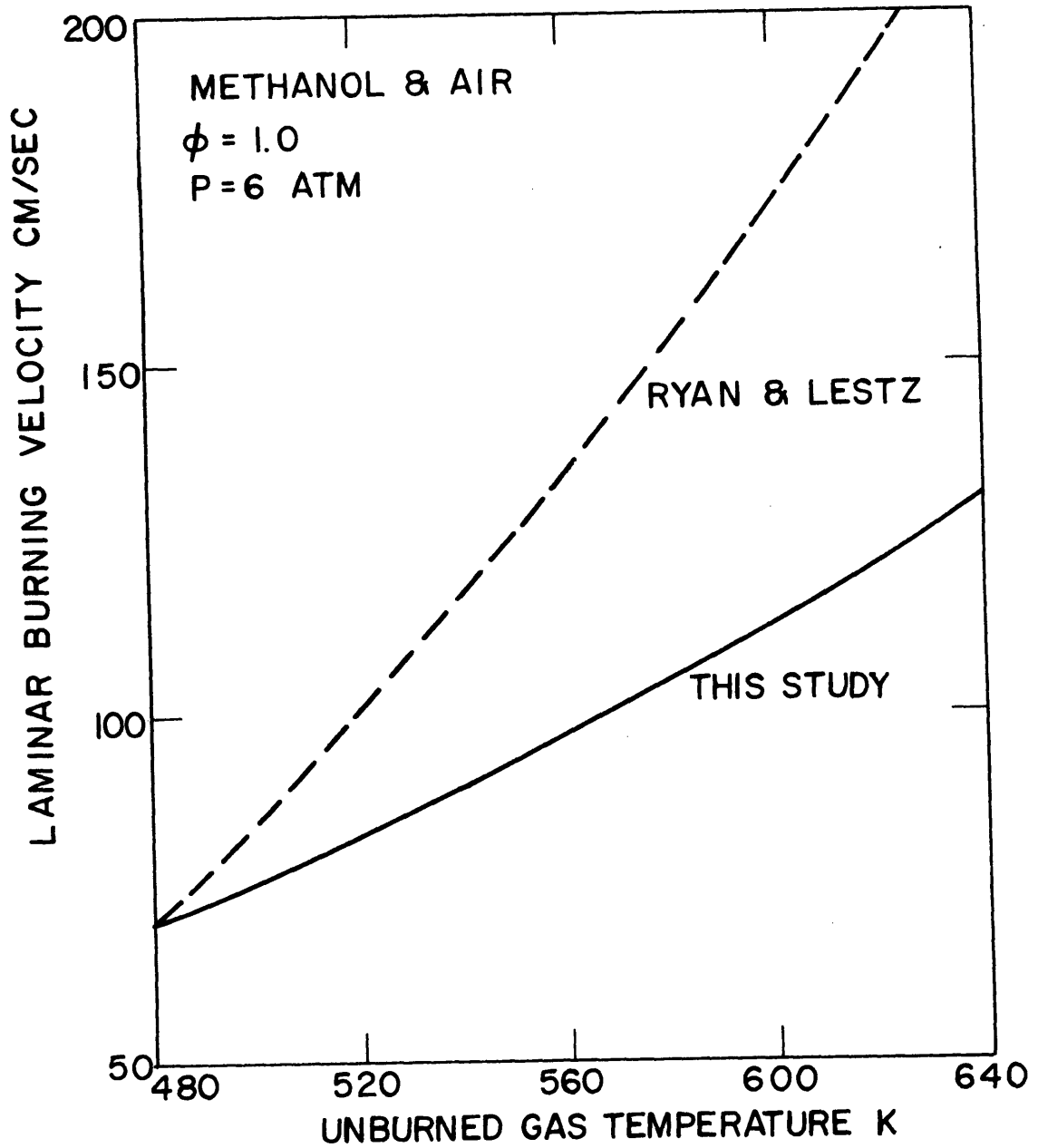
FIG. 33 Comparison of Measured Laminar Burning Velocity for
Methanol-Air Mixtures with Those Reported by Ryan
and Lestz [22]
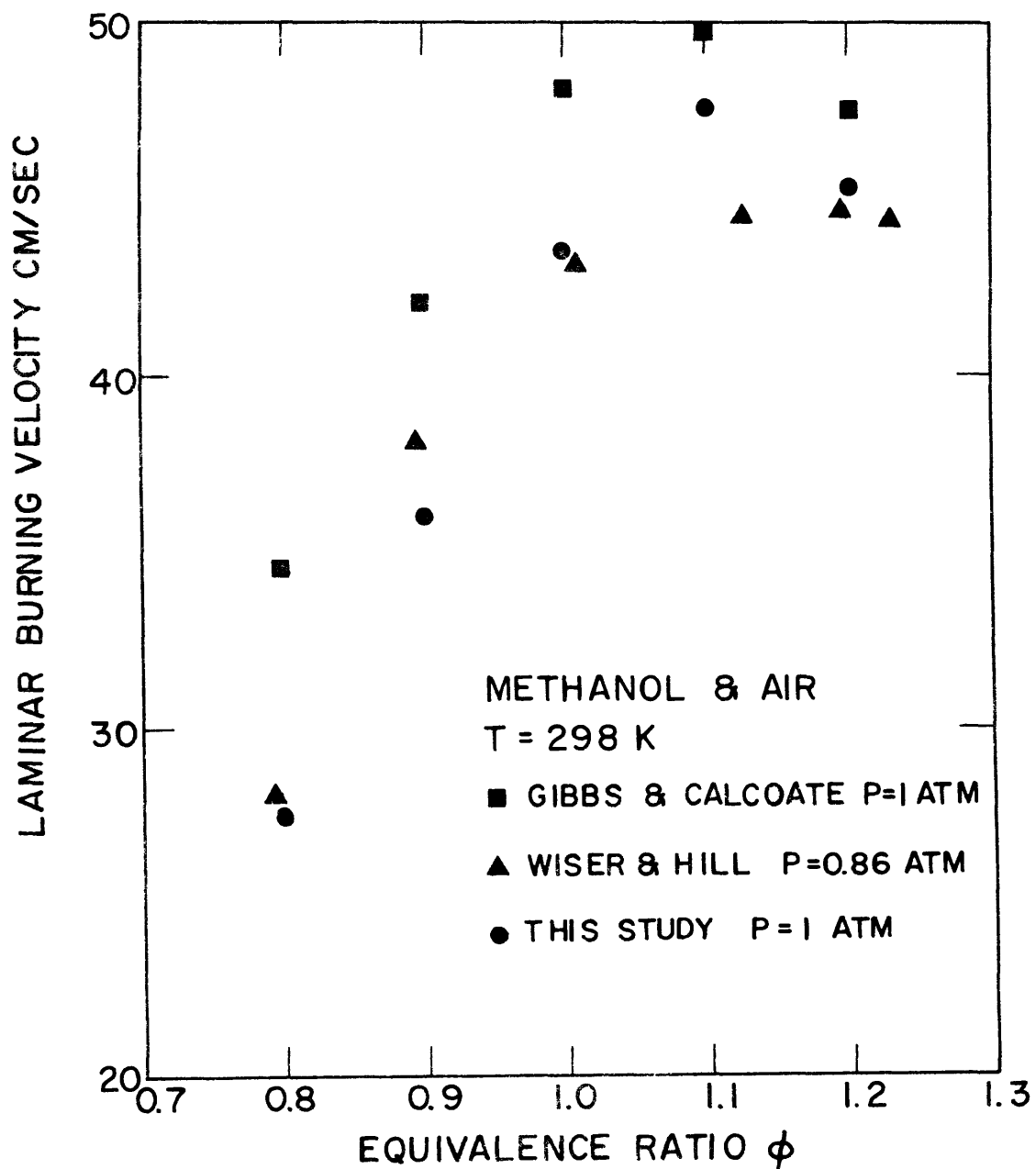
FIG. 34 Comparison of Measured Laminar Burning Velocity for Methanol-
Air Mixtures with Those Reported by Gibbs and Calcoate [38]
and Wiser and Hill [39]
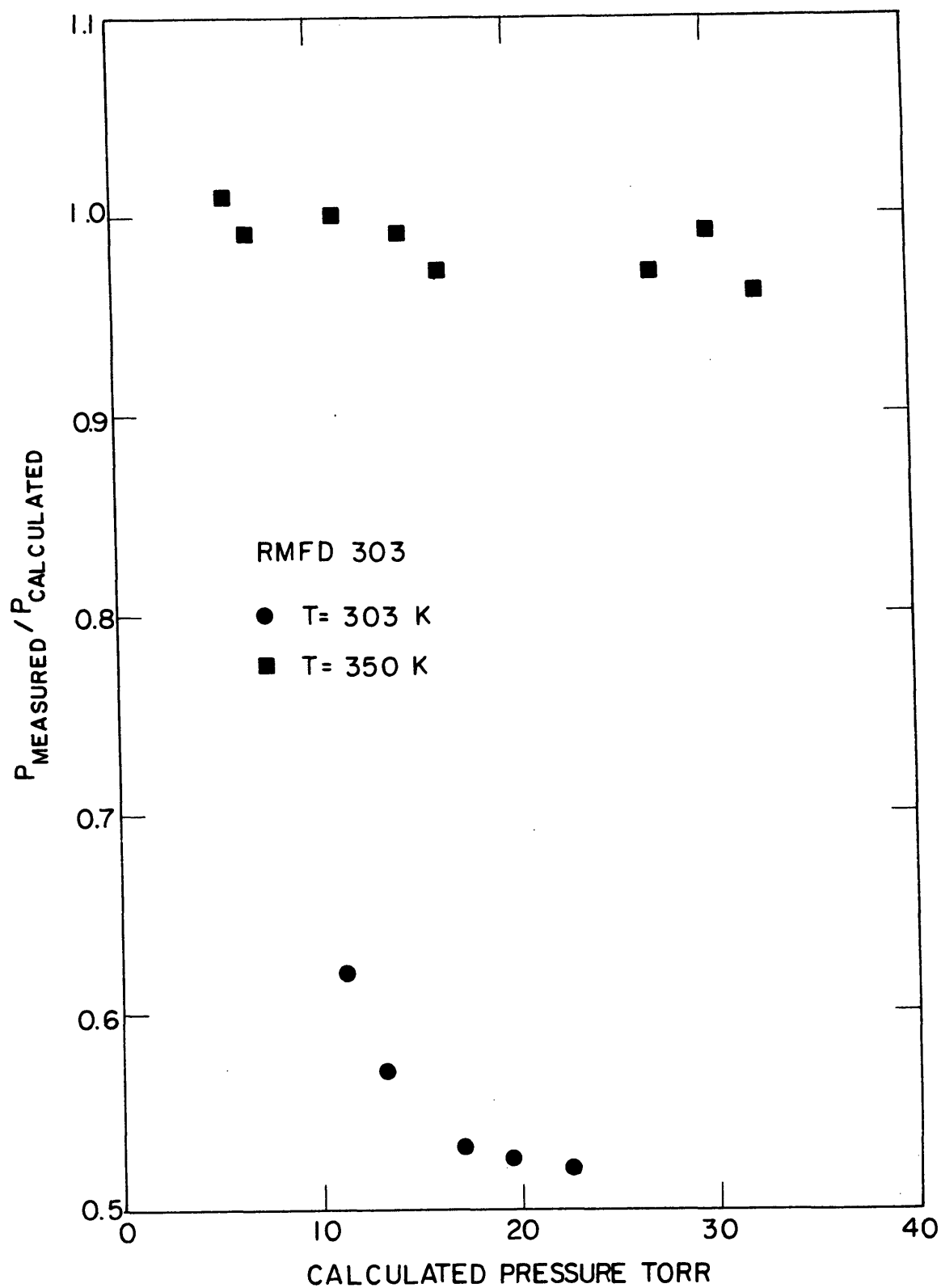
FIG. 35 Ratio of Measured Pressure to Calculated Pressure in the Manifold
for RMFD 303 (Indolene) as a Function of Calculated Pressure for
Two Temperatures of 300 K and 350 K

FIG. 36   Laminar Burning Velocity of RMFD 303 (Indolene)-Air Mixtures at Atmospheric Condition as a Function of Equivalence Ratio
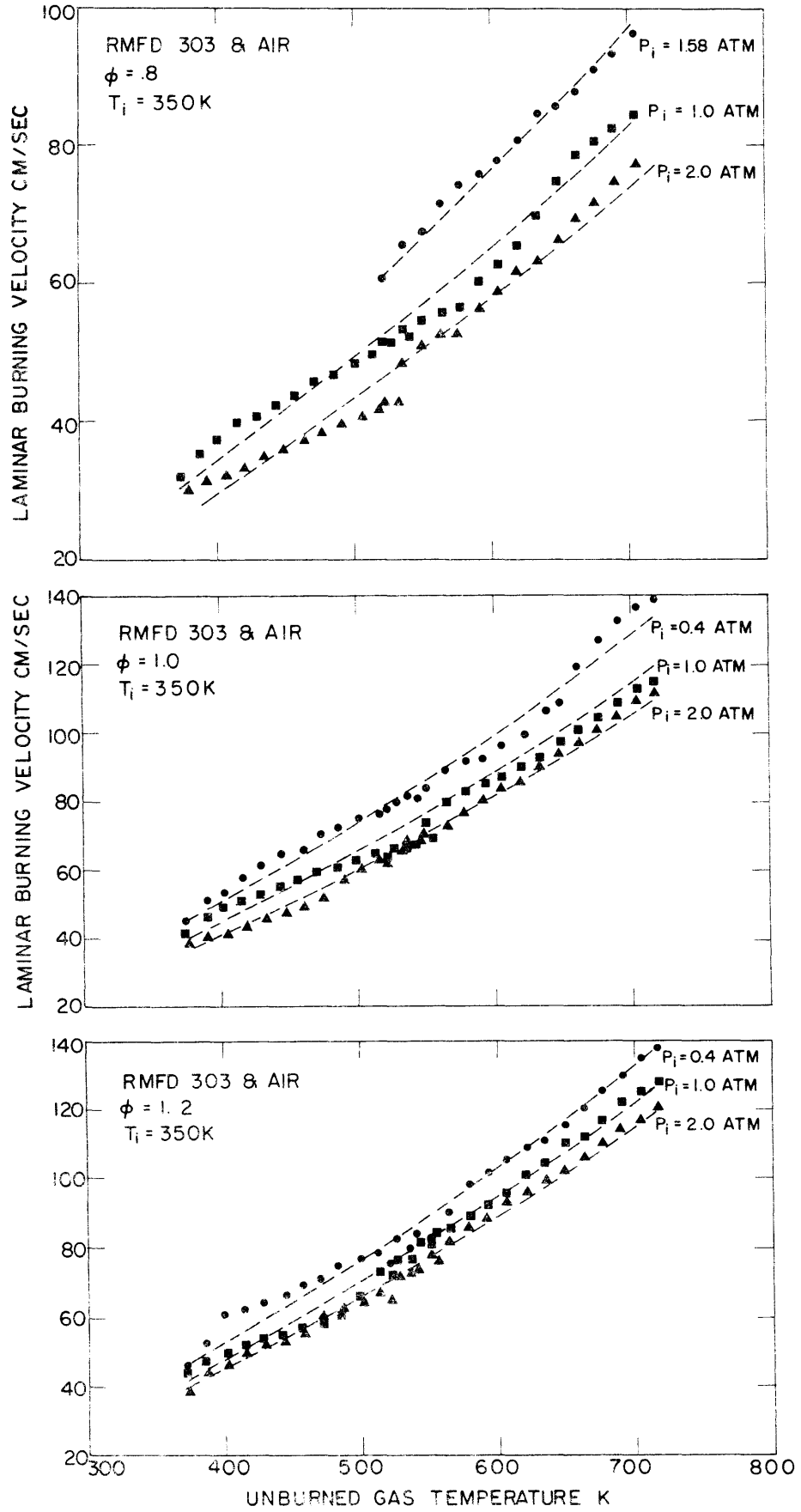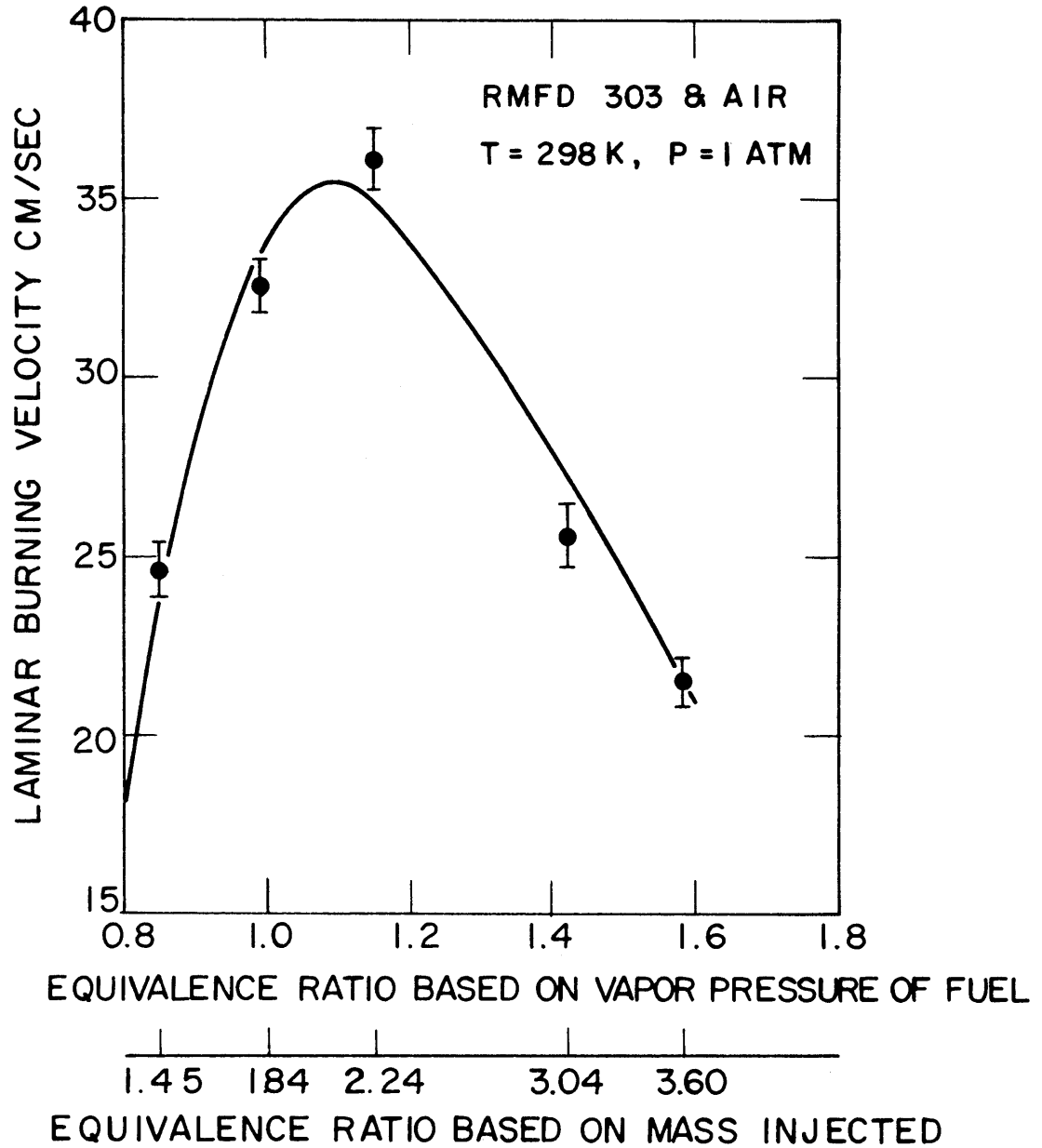
FIG. 37 Laminar Burning Velocity of RMFD 303 (Indolene)-Air
Mixtures at Equivalence Ratio of 0.8, 1.0, and 1.2
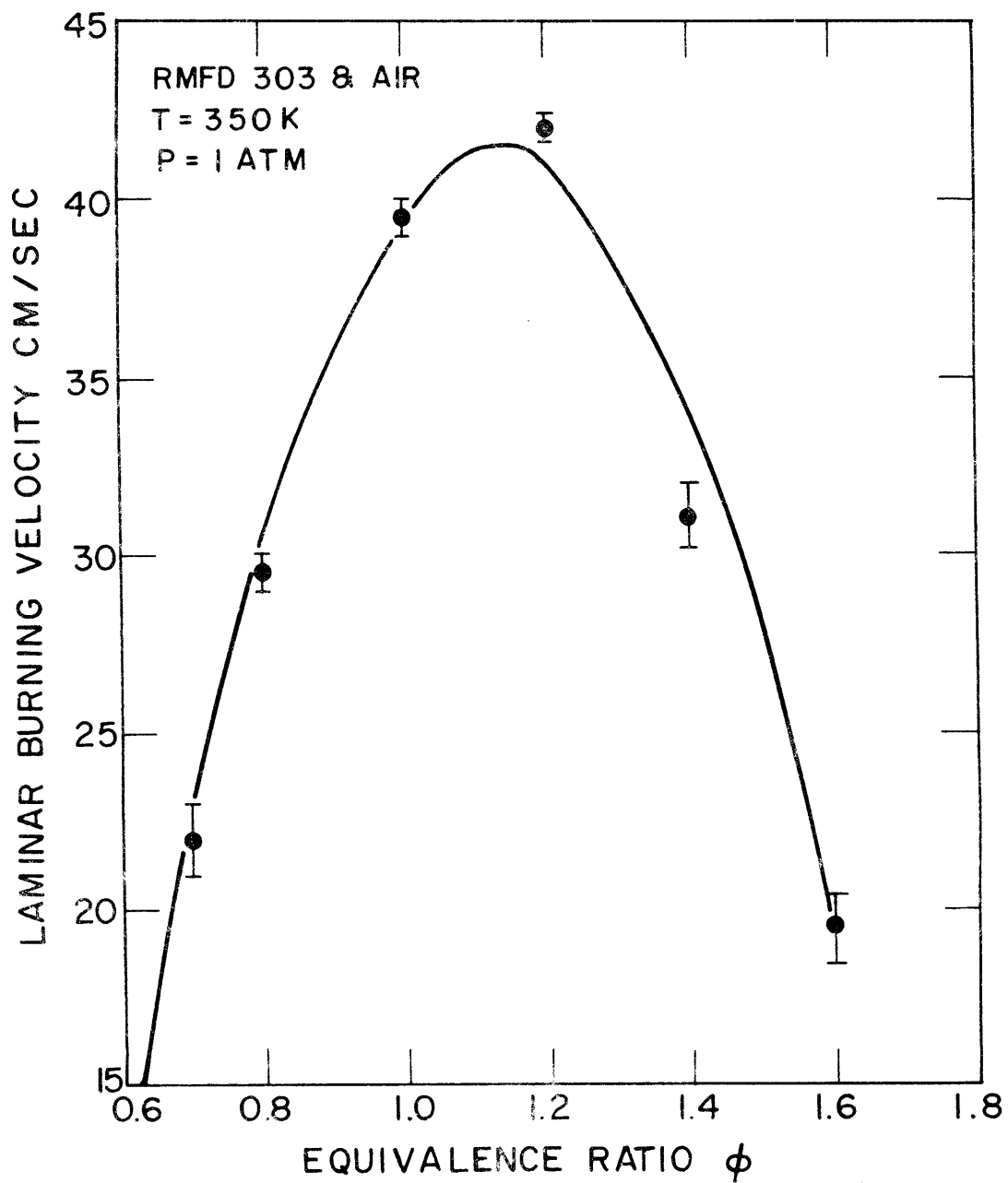
FIG. 38   Laminar Burning Velocity of RMFD 303 (Indolene)-
Air Mixtures at 1 atm Pressure and 350 K Temperature
as a Function of Equivalence Ratio

FIG. 39 Parameters S_{uo}, α, and β for Mixtures of Air with Indolene (RMFD 303), Isooctane, Methanol, and Propane as a Function of the Equivalence Ratio
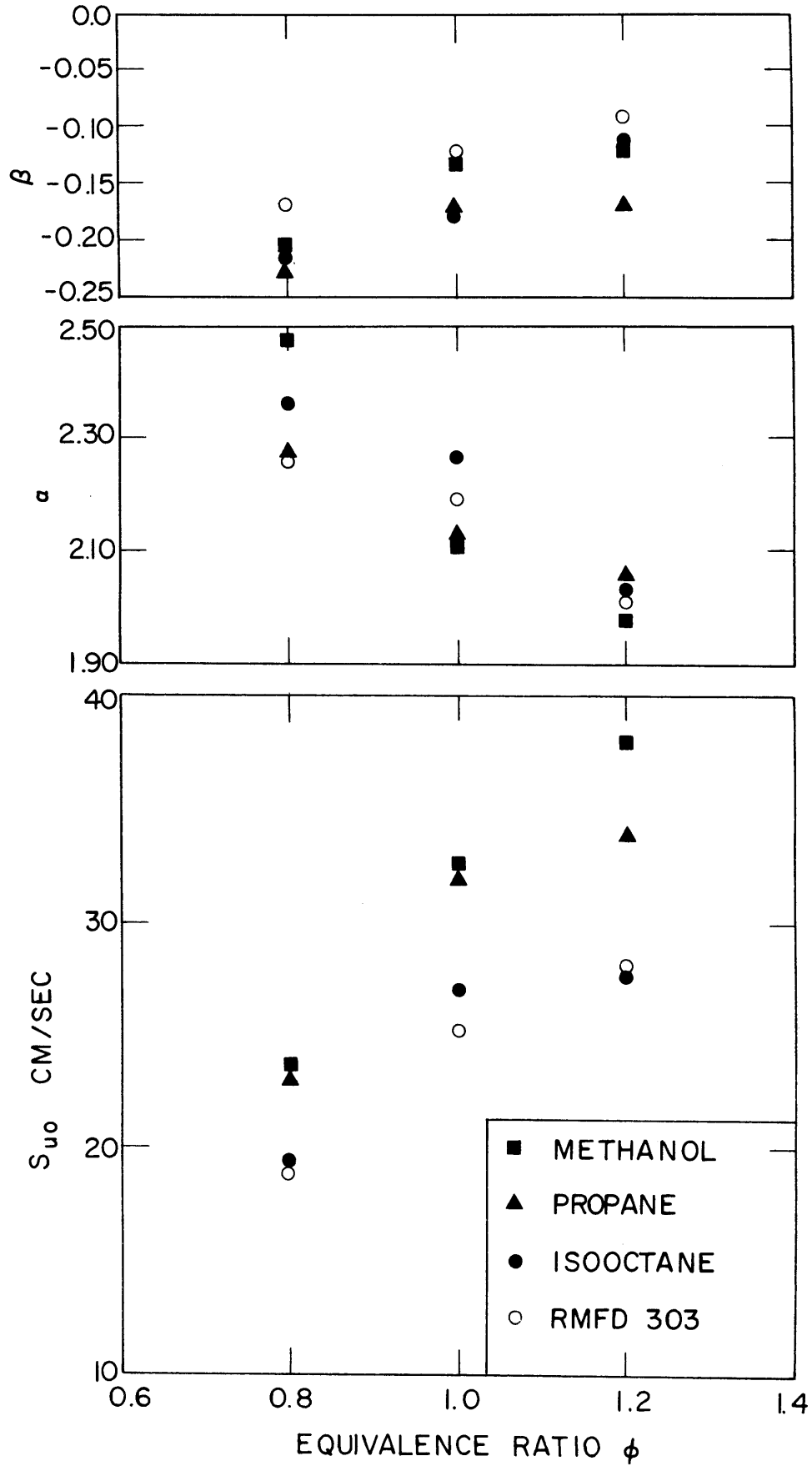
APPENDIX A

LIQUID FUEL INJECTION

Liquid fuel was injected with a syringe through a system into the manifold. In order to make a mixture partial pressure of fuel was calculated, then mass and volume of fuel were calculated at room temperature based on the assumption of perfect gas for fuel vapor.

It was observed that the measured pressures were different from the calculated pressure. Figure A-1 shows the ratio of measured pressure to calculated pressure as a function of calculated pressure for iso-octane, toluene, and benzene. The corresponding figure for RMFD 303 is shown in Chapter 6 of the text. It can be seen that even at very low pressure, much less than saturation pressure, the fuels do not evaporate completely. The volume of the bomb and manifold in these tests was 2300 cc including the combustion bomb, the plumbing lines, and the bourdon tube gauges. It was thought that some of the fuel was absorbed by the walls and in cracks. To check this idea tests were done with smaller total volume and with less area to volume ratio. In these tests the combustion bomb and the mercury manometer underneath the bomb (refer to Fig. 2) were used. The results for isooctane and RMFD 303 are shown in Fig. A.2. It can be seen that for isooctane the ratio of measured pressure to the calculated pressure is around 95% and as the area to volume ratio of the plumbing system is reduced, less fuel is absorbed by walls and in cracks. Although in the case of RMFD 303 the ratio of measured pressure to calculated pressure was increased from 55% (Fig. 35) to 70%, but this is

substantially less than the ratio for isooctane. The reason for this is that the saturation pressures for some constituents of RMFD 303 are very low and therefore the fuel does not evaporate completely at room temperature. For this reason the lowest initial temperature used for RMFD 303 was 350 K, so that the constituents of the fuel vapor would be the same as the liquid fuel.

128

FIG. A.1 Ratio of Measured Pressure to Calculated Pressure in the System for Isooctane, Toluene, and Benezene as a Function of Calculated Pressure at Room Temperature
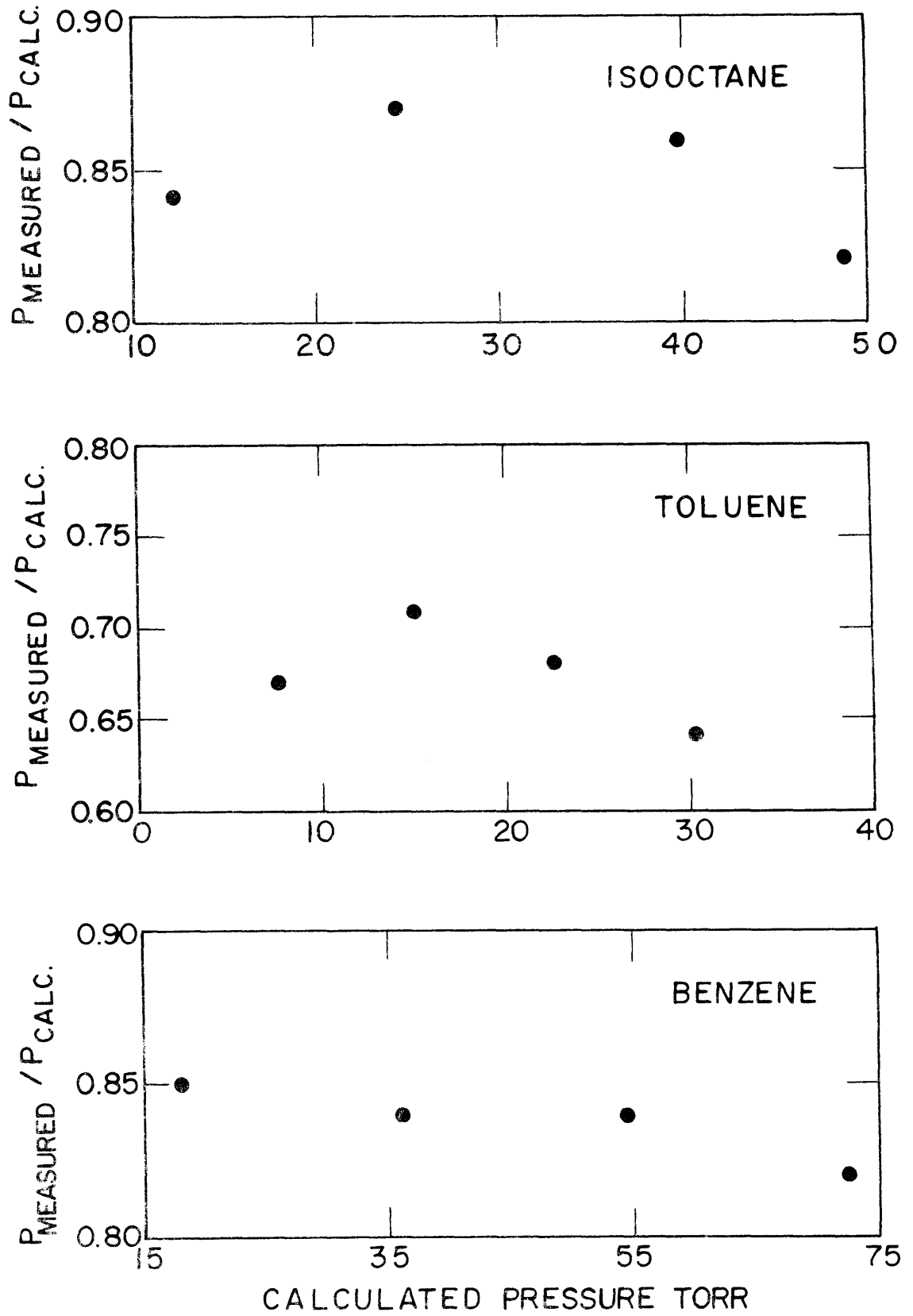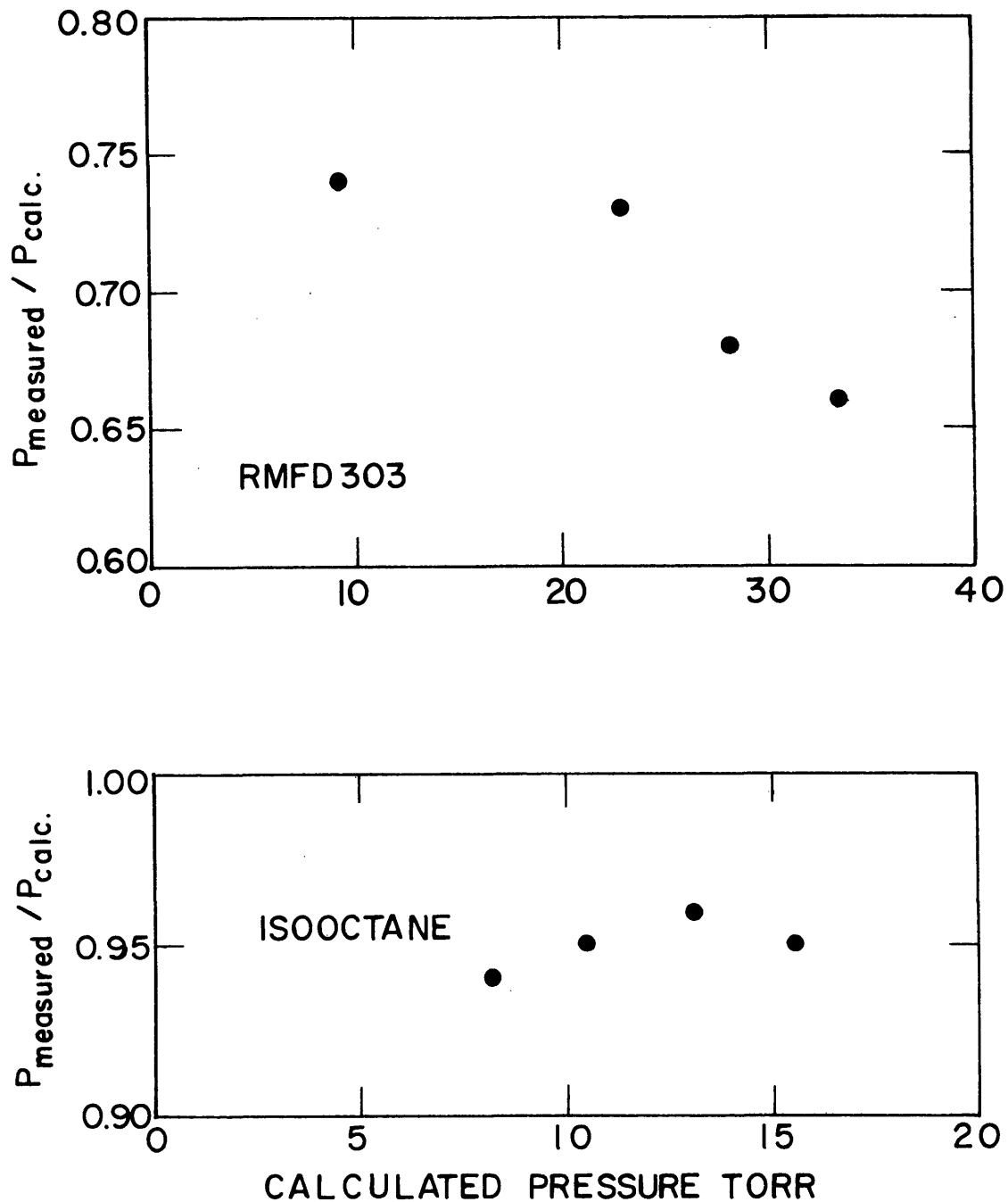
FIG. A.2 Ratio of Measured Pressure to Calculated Pressure in the
System Consisting of the Combustion Bomb and Mercury Manometer
Beneath the Oven for RMFD 303 and Isooctane as a Function of
Calculated Pressure at Room Temperature

APPENDIX B

CONSERVATION EQUATIONS

B.1 Conservation of Volume

The gas mixture within the combustion bomb consists of burned gases m_b and unburned gases $m_o - m_b$. The volume equation is as follows:

$$V_o = \int_o^{m_b} v_b dm + \int_{m_b}^{m_o} v_u dm \qquad (B-1)$$

The unburned gas itself consists of two parts. The first part is that portion of the unburned gas that is compressed isentropically. The second part is that portion of the unburned gas contained in the thermal boundary layer of the combustion bomb wall which conducts heat to the bomb wall. The volume of the unburned gas can be calculated as follows:

$$\int_{m_b}^{m_o} v_u dm = \frac{R}{p} \int_{m_b}^{m_o} (T-T_\infty) dm + \int_{m_b}^{m_o} v_{u\infty} dm \qquad (B-2)$$

where $v_{u\infty}$ and T_∞ are specific volumes and temperatures of the portion of the unburned gas that compresses isentropically, and T is the temperature of the unburned gas within the thermal boundary layer. Defining a mass coordinate η where

$$\eta \equiv \int_0^r \rho dr' \qquad (B-3)$$

where the wall is at zero coordinate.

Then

$$dm = A \, d\eta \qquad \text{(B-4)}$$

where A is the inside area of the combustion bomb.

The first term on the right hand side of Eq. (B-2) will be

$$\frac{R}{p} \int (T-T_\infty)dm = -\frac{R \, T_\infty}{p} A \int_0^\infty (1 - \frac{T}{T_\infty})d\eta \qquad \text{(B-5)}$$

using the definition of displacement thickness (Appendix C)

$$\delta = \frac{1}{\rho_\infty} \int_0^\infty (1 - \frac{T}{T_\infty})d\eta \qquad \text{(B-6)}$$

The equation (B-5) then becomes

$$\frac{R}{p} \int_{m_b}^{m_o} (T-T_\infty)dm = -\frac{R_\infty T_\infty}{p} A\delta = -A\delta \qquad \text{(B-7)}$$

and the conservation of volume will be

$$V_o + A\delta = \int_0^{m_b} v_b dm + \int_{m_b}^{m_o} v_u dm \qquad \text{(B-8)}$$

or dividing by m_o

$$\frac{V_o}{m_o} + A \frac{\delta}{m_o} = \int_0^x v_b dx' + \int_x^1 v_{u\infty} dx' \qquad \text{(B-9)}$$

B.2 Conservation of Energy

The energy equation for gases within the bomb is:

$$E_o - Q = \int_0^{m_b} e_b \, dm + \int_{m_b}^{m_o} e_u \, dm \qquad \text{(B-10)}$$

where E_o is total energy, and Q is heat transferred to the combustion bomb wall. Again the unburned gas consists of two parts

$$\int_{m_b}^{m_o} e_u \, dm = C_v \int_{m_b}^{m_o} (T-T_\infty) dm + \int_{m_b}^{m_o} e_{u\infty} \, dm \qquad \text{(B-11)}$$

where C_v is the specific heat of unburned gas at constant pressure. The first term on the right hand side of the equation can be simplified as the following:

$$C_v \int_{m_b}^{m_o} (T-T_\infty) dm = - A \, C_v T_\infty \int_0^\infty (1 - \frac{T}{T_\infty}) d\eta \qquad \text{(B-12)}$$

$$C_v \int_{m_b}^{m_o} (T-T_\infty) dm = - A \, C_v \, \rho_\infty \, T_\infty \, \delta \qquad \text{(B-13)}$$

One-dimensional heat conduction is used to calculate the heat transfer from the gass within the bomb to the bomb wall.

$$Q/A = \int k \frac{\partial T}{\partial r} \Big|_{R_B} d\tau \qquad \text{(B-14)}$$

where k is the thermal conductivity of the gas, and R_B is the radius of the combustion bomb. Substituting η for r :

$$Q/A = \int \rho k \left. \frac{\partial T}{\partial \eta} \right|_0 dt \qquad \text{(B-15)}$$

The following assumptions are made:

$$P_r = \frac{\mu C_p}{k} = 1 \qquad \text{(B-16)}$$

$$\mu \propto T \qquad \text{(B-17)}$$

and heat transfer becomes

$$Q/A = \int C_p \rho\mu \left. \frac{\partial T}{\partial \eta} \right|_0 dt \qquad \text{(B-18)}$$

Equation (C-10) of Appendix C is integrated to calculate the integrand of Eq. (B-18). It follows that:

$$- \rho\mu \left. \frac{\partial T}{\partial \eta} \right|_0 = \frac{\partial}{\partial t} \int_0^\infty (T-T_\infty)d\eta - \frac{\dot{T}_\infty}{T_\infty} \int_0^\infty (T-T_\infty)d\eta \qquad \text{(B-19)}$$

$$= - \frac{\partial}{\partial \tau} \rho_\infty T_\infty \delta + \frac{\dot{T}_\infty}{T_\infty} \rho_\infty T_\infty \delta \qquad \text{(B-20)}$$

Then

$$Q/A = C_p \rho_\infty T_\infty \delta - \int C_p \rho_\infty T_\infty \delta \, d \ln T_\infty \qquad \text{(B-21)}$$

using the isentropic relation between pressure and temperature

$$d \ln T_\infty = \frac{R}{C_p} d \ln p \qquad \text{(B-22)}$$

Then

$$Q/A = C_p \rho_\infty T_\infty \delta - \int \delta \, dp \qquad \text{(B-23)}$$

Substituting Eqs. (B-11), (B-13), and (B-23) into Eq. (B-10)

$$E_o - (C_p \rho_\infty T_\infty \delta A - A \int \delta dp) = \int e_b dm + \int e_{u\infty} dm - A C_v \rho_\infty T_\infty \delta \qquad \text{(B-24)}$$

$$E_o - A(\rho_\infty T_\infty \delta (C_p - C_v) - \int \delta \, dp) = \int e_b dm + \int e_{u\infty} dm \qquad \text{(B-25)}$$

$$E_o - A(p\delta - \int \delta \, dp) = \int e_b \, dm + \int e_{u\infty} dm \qquad \text{(B-26)}$$

or

$$E_o - A \int_0^\delta p \, d\delta' = \int_0^{m_b} e_b dm + \int_{m_b}^{m_o} e_{u\infty} dm \qquad \text{(B-27)}$$

and, by dividing by m_o

$$E_o/m_o - (A/m_o) \int_0^\infty p \, d\delta' = \int_0^x e_b dx' + \int_x^1 e_{u\infty} dx' \qquad \text{(B-28)}$$

APPENDIX C

DISPLACEMENT THICKNESS

C.1 Temperature Distribution Within the Thermal Boundary Layer

The continuity and energy equations within the thermal boundary

layer can be written as follows:

Continuity:

$$\frac{\partial \rho}{\partial t} + \frac{d}{dr} \rho u = 0 \tag{C-1}$$

Energy:

$$\rho \frac{D}{Dt} C_p T = \rho C_p \left(\frac{\partial T}{\partial t} + u \frac{\partial T}{\partial r} \right) = \frac{dp}{dx} \tag{C-2}$$

$$+ \frac{\partial}{\partial r} k \frac{\partial}{\partial r}$$

Equation (C-1) can be intergrated

$$\frac{\partial}{\partial t} \int_0^r \rho dr' + \rho u = 0 \tag{C-3}$$

Mass coordinate $\eta \equiv \int_0^r \rho dr'$ is used here, the equation (C-3)
becomes

$$\frac{\partial \eta}{\partial t} = - \rho u \tag{C-4}$$

Substituting the mass coordinate in Equation (C-2)

$$\rho \, \frac{D}{Dt} \, C_p T \;=\; \rho C_p \left(\frac{\partial T}{\partial t} + \rho u \, \frac{\partial T}{\partial \eta} \right) \;=\; \rho \, C_p \left(\frac{\partial T}{\partial t} - \frac{\partial \eta}{\partial t} \, \frac{\partial T}{\partial \eta} \right) \qquad (C\text{-}5)$$

and finally

$$\rho \, \frac{D}{Dt} \, C_p T \;=\; \rho C_p \left. \frac{\partial T}{\partial t} \right|_\eta \qquad (C\text{-}6)$$

Therefore the energy equation becomes

$$\rho \, C_p \left. \frac{\partial T}{\partial t} \right|_\eta \;=\; \frac{dp}{dt} + \rho \, \frac{\partial}{\partial \eta} \, \rho \, k \left. \frac{\partial T}{\partial \eta} \right|_t \qquad (C\text{-}7)$$

Using $Pr = 1$ and adding and subtracting $\dfrac{\partial T_\infty}{\partial t}$ to Eq. (C-7) then

$$\frac{\partial}{\partial \tau} (T - T_\infty) + \frac{\partial T_\infty}{\partial \tau} - \frac{RT}{C_p p} \, \frac{dp}{dt} \;=\; \rho \, \mu \, \frac{\partial^2 T}{\partial \eta^2} \qquad (C\text{-}8)$$

Using the isentropic relationship between pressure and T_∞

$$\frac{d \, \ell n \, T_\infty}{dt} \;=\; \frac{R}{C_p} \, \frac{d \, \ell n \, p}{dt} \qquad (C\text{-}9)$$

then

$$\frac{\partial}{\partial t} (T - T_\infty) + (T - T_\infty) \, \frac{\dot{T}_\infty}{T_\infty} \;=\; \rho \, \mu \, \frac{\partial^2 T}{\partial \eta^2} \qquad (C\text{-}10)$$

Multiplying Eq. (C-10) by $\dfrac{1}{T_\infty}$ and simplifying the equation results in

$$\frac{\partial}{\partial t} \left(\frac{T}{T_\infty} - 1 \right) \;=\; \rho \, \mu \, \frac{\partial^2}{\partial \eta^2} \left(\frac{T}{T_\infty} - 1 \right) \qquad (C\text{-}11)$$

Defining a new variable τ where

$$d\tau = \rho \mu \, dt \qquad \text{(C-12)}$$

and assuming that viscosity is proportional to temperature. Then

$$d\tau = \frac{P}{R} \left(\frac{\mu}{T} \right) dt = \frac{P}{R} \left(\frac{\mu_0}{T_0} \right) dt \qquad \text{(C-13)}$$

$$d\tau = \frac{P}{P_0} \left(\rho_0 \mu_0 \right) dt \qquad \text{(C-14)}$$

Defining another variable ϕ as

$$\phi = 1 - \frac{T}{T_\infty} \qquad \text{(C-15)}$$

and substituting Eqs. (C-12) and (C-15) into Eq. (C-11)

$$\frac{\partial \phi}{\partial \tau} = \frac{\partial^2 \phi}{\partial \eta^2} \qquad \text{(C-16)}$$

Equation (C-16) is one-dimensional heat conduction with the following boundary and initial conditions

$$\phi(0,\tau) = \phi_0(\tau) \qquad \text{(C-17)}$$

and

$$\phi(\eta,0) = 0 \quad . \qquad \text{(C-18)}$$

This problem is solved in Section C.3. The result is

$$\phi(\eta,\tau) = \frac{\eta}{2\sqrt{\pi}} \int_0^\tau \phi_0(s)(\tau-s)^{-3/2} e^{-\eta^2/4(\tau-s)} ds \tag{C-19}$$

where

$$ds = \rho_0\mu_0 \frac{p}{p_0} dt'' \tag{C-20}$$

and

$$\tau - s = \rho_0\mu_0 \int_{\tau'}^{t''} \frac{p''}{p_0} dt'' \tag{C-21}$$

Substituting temperature for ϕ

$$1 - \frac{T}{T_\infty} = \frac{1}{2\sqrt{\pi}} \rho_0\mu_0\eta \int_0^t (1 - \frac{T_0}{T_\infty}) \frac{p'}{p_0} (\tau - s)^{-3/2} e^{-\eta^2/4(\tau-s)} dt' \tag{C-22}$$

C.2 Displacement Thickness

Defining displacement thickness as the following

$$\delta = \frac{1}{\rho_\infty} \int_0^\infty (\rho - \rho_\infty)dr \tag{C-23}$$

and using mass coordinate instead of distance

$$\delta = \frac{1}{\rho_\infty} \int_0^\infty (1 - \frac{\rho_\infty}{\rho})d\eta = \frac{1}{\rho_\infty} \int_0^\infty (1 - \frac{T}{T_\infty})d\eta \tag{C-24}$$

139

Substituting Eq. (C-22) into Eq. (C-24)

$$\delta = \frac{1}{\rho_\infty} \int_0^\infty \int_0^t (1 - \frac{T_0}{T_\infty'}) \frac{1}{2\sqrt{\pi}} e^{-\eta^2/4(\tau-s)} (\tau-s)^{-3/2} \eta \, ds d\eta \quad (C-15)$$

or

$$\delta = \frac{1}{\rho_\infty} \int_0^\tau (1 - \frac{T_0}{T_\infty'})(\tau-s)^{-1/2} (\frac{1}{\sqrt{\pi}} \int_0^\infty e^{-\eta^2/4(\tau-s)} \frac{d\eta^2}{4(\tau-s)})ds \quad (C-26)$$

and

$$\delta = \frac{1}{\sqrt{\pi} \, \rho_\infty} \int_0^\tau (1 - \frac{T_0}{T_\infty'})(\tau-s)^{-1/2} \, ds \quad (C-27)$$

Using Eqn.(C-20) into Eq. (C-27)

$$\delta(t) = \frac{\rho_0 \mu_0}{\rho_\infty \sqrt{\pi}} \int_0^t \frac{p'}{p_0} (1 - \frac{T_0}{T_\infty'})(\tau-s)^{-1/2} \, dt' \quad (C-28)$$

Using Eq. (C-21) into Eq. (C-28) and simplifying it

$$\delta(t) = (\frac{\mu_0}{\pi \, \rho_0})^{1/2} \int_0^t (\frac{p'}{p})^{\frac{1}{\gamma_u}} ((\frac{p'}{p_0})^{\gamma_u-1/\gamma_u} - 1) \quad (C-29)$$

$$(\int_{t'}^t (\frac{p''}{p_0} \, dt'')^{-1/2} \, dt'$$

C.3 Solution to Heat Conduction Equation with Variable

Boundary Condition

The problem is a standard textbook problem which can be found

on page 527 of reference [41]

Statement of problem:

$$\frac{\partial^2 T}{\partial x^2} = \frac{1}{\alpha^2} \frac{\partial T}{\partial t} \qquad 0 < x < \infty \tag{C-30}$$

B.C. $\quad T(0,t) = F(t)$ $\hspace{5cm}$ (C-31)

I.C. $\quad T(x,0) = 0$ $\hspace{5cm}$ (C-32)

Solution:

Let $A(x,t)$ solve the problem with $F(\tau) = 1$, then

$$T(x,t) = \begin{cases} 0 & \tau < \tau_1 \\ \\ A(x,t-\tau) & \tau > \tau_1 \end{cases} \tag{C-33}$$

solves the problem with $F(\tau) = \begin{cases} 0 & \tau < \tau_1 \\ \\ 1 & \tau > \tau_1 \end{cases}$ $\hspace{2cm}$ (C-34)

Defining $A(x,t-\tau)$ to be zero for $\tau < \tau_1$. Then using Duhamel's

principle [41]

$$T(x,t) = F(0)A(x,t)+[F(\tau_1)-F(0)] A(x,t-\tau_1)+[F(\tau_2)-F(\tau_1)]A(x,t-\tau_2) +$$

$$\ldots + [F(\tau_n)-F(\tau_{n-1})] A(x,t-\tau_n) \tag{C-35}$$

Solves the problem when the temperatute at x=0 is given by:

$$0 \qquad \qquad \tau < 0$$

$$F(0) \qquad \qquad 0 < \tau < \tau_1$$

$$F(\tau_1) \qquad \qquad \tau_1 < \tau < \tau_2$$

. .
. .
. .
. .

$$F(\tau_i) \qquad \qquad \tau_i < \tau < \tau_{i+1}$$

. .
. .
. .
. .
. .

$$F(\tau_n) \qquad \qquad \tau_n < \tau$$

The above solution approximates the solution to the present problem.

In the limit, as n → ∞ and $\tau_{i+1} - \tau_i \to 0$ for all i , this approximation converges to the exact solution. In reference [41] it is shown that the limit of approximation is:

$$T(x,t) = A(x,0)\ F(t) + \int_0^t F(\tau)\ \frac{\partial A(x,t,\tau)}{\partial \tau}\ d\tau \qquad \qquad (C\text{-}36)$$

but T(x,0) = 0 and A(x,0) = 0 , therefore

$$T(x,t) = \int_0^t F(\tau)\ \frac{\partial A(x,t-\tau)}{\partial \tau}\ d\tau \qquad \qquad (C\text{-}37)$$

To find $A(x,t)$ consider a solution of the form

$$A(x,t) = T_1(x,t) - T_2(x,t) \qquad\qquad \text{(C-38)}$$

where $T_1(x,t)$ solves the problem with boundary and initial conditions of

$$T(0,\tau) = 1$$

$$\qquad\qquad \text{(C-39)}$$

$$T(x,0) = 1$$

and $T_2(x,t)$ solves the problem with boundary and initial conditions of

$$T(0,\tau) = 0$$

$$\qquad\qquad \text{(C-40)}$$

$$T(x,0) = 1$$

then

$$A(0,t) = 1$$

$$\qquad\qquad \text{(C-41)}$$

and

$$A(x,0) = 0$$

It is obvious that $T(x,t) = 1$ is the solution for $T_1(x,t)$ and

$$T(x,t) = \text{erf} \left(\frac{x}{2\alpha\sqrt{t}} \right) \qquad\qquad \text{(C-42)}$$

is the solution for $T_2(x,t)$ (Section 9.14 of Reference [41]).

Then

$$A(x,t) = 1 - \frac{2}{\sqrt{\pi}} \int_0^{\frac{x}{2\alpha\sqrt{t}}} e^{-u^2} du \qquad \text{(C-43)}$$

Substituting Eq. (C-43) into Eq. (C-37)

$$T(x,t) = \int_0^t F(\tau) \frac{\partial}{\partial t} \left(1 - \frac{2}{\sqrt{\pi}} \int_0^{\frac{x}{2\alpha\sqrt{t-\tau}}} e^{-u^2} du\right) d\tau \qquad \text{(C-44)}$$

$$T(x,t) = \int_0^t F(\tau) \left(- \frac{2}{\sqrt{\pi}} e^{\frac{-x^2}{4\alpha^2(t-\tau)}}\right) \frac{\partial}{\partial t} \left(\frac{x}{2\alpha\sqrt{t-\tau}}\right) d\tau \qquad \text{(C-45)}$$

$$T(x,t) = \frac{-2}{\sqrt{\pi}} \left(\frac{x}{2\alpha}\right) \int_0^\tau F(\tau) e^{\frac{-x^2}{4(t-\tau)}} \frac{\partial}{\partial t} (t-\tau)^{-1/2} d\tau \qquad \text{(C-46)}$$

and finally

$$T(x,t) = \frac{x}{2\alpha\sqrt{\pi}} \int_0^\tau F(\tau) e^{\frac{-x^2}{4\alpha^2(t-\tau)}} (t-\tau)^{-3/2} d\tau \qquad \text{(C-47)}$$

APPENDIX D

THE FRACTURE ERROR IN X INTRODUCED BY

USING AVERAGE BURNED GAS TEMPERATURE TO CALCULATE

BURNED GAS PROPERTIES

The volume and mass conservation equations are:

$$V/M + A \, \delta/M = \int_0^x v_b \, dx' + \int_x^1 v_b dx' \qquad \text{(D-1)}$$

$$E/M - (A/M) \int_0^\delta p d\delta' = \int_0^x e_b dx + \int_x^1 e_u dx' \qquad \text{(D-2)}$$

$v_b(T_b, p)$ and $\rho_b(T_b, p)$ can be expanded in a Taylor series about the mean gas temperature

$$\bar{T}_b = \frac{1}{x} \int_0^x T_b(x', x) dx' \qquad \text{(D-3)}$$

which are

$$e_b(T_b, p) = e_b(\bar{T}_b) + \left(\frac{\partial e_b}{\partial T} \right)_{\bar{T}_b} (T_b - \bar{T}_b)$$

$$+ \frac{1}{2} \left(\left(\frac{\partial^2 e_b}{\partial T^2} \right) \right)_{p \, \bar{T}_b} (T_b - \bar{T}_b)^2 + \dots \qquad \text{(D-4)}$$

$$v_b(T_b, p) = v_b(\bar{T}_b) + \left(\frac{\partial v_b}{\partial T} \right)_{\bar{T}_b} (T_b - \bar{T}_b) + \left(\left(\frac{\partial^2 v_b}{\partial T^2} \right) \right)_{p \, \bar{T}_b} (T_b - \bar{T}_b)^2 + \dots$$

$$\text{(D-5)}$$

Neglecting terms of order $(T_b - \overline{T}_b)^3$ and higher and substituting Eqs. (D-4) and (D-5) into Eqs. (D-1) and (D-2) will result in

$$V/M + A \, \delta/M = x \, v_b(p,\overline{T}_b) + (1-x) \, v_u + \frac{1}{2} \left(\left(\frac{\partial^2 v_b}{\partial T^2} \right) \right)_{p \, \overline{T}_b} \int_0^x (T_b - \overline{T}_b)^2 dx' \tag{D-6}$$

$$E/M - (A/M) \int_0^\delta p d\delta' = x \, e_b(p,\overline{T}_b) + (1-x)e_u +$$

$$+ \frac{1}{2} \left(\left(\frac{\partial^2 e_b}{\partial T^2} \right) \right)_{p \, \overline{T}_b} \int_0^x (T_b - \overline{T}_b)^2 dx' \tag{D-7}$$

The burned gas temperature can be approximated as the following

$$T_b(x',x) = \overline{T}_b + \Delta T \left(\frac{1}{2} - \frac{x'}{x} \right) \tag{D-8}$$

where $T_b(x',x)$ is the temperature of the element burned at mass fraction burned x' when the mass fraction burned is x, and ΔT is the spread in burned gas temperature which is about 500°K.

Assuming that molecular weight does not change within the burned gas, and, substituting Eq. (D-8) into Eqs. (D-6) and (D-7) will result in:

$$V/M + A \, \delta/M = x \, v_b(p,\overline{T}_b) + (1-x)v_u \tag{D-9}$$

$$E/M - (A/M) \int_0^\delta p d\delta' = x \, e_b(p,\overline{T}_b) + (1-x) \, e_u + (x/24) \left(\frac{\partial C_{vb}}{\partial T} \right)(\Delta T)^2 \tag{D-10}$$

The following procedure is used to calculate the fractional error in x:

$$f_1 = V/M + A \delta/M - v_u - x(v_b(\overline{T}_b) - v_u) \tag{D-11}$$

$$f_2 = E/M - (A/M) \int_0^\delta pd\delta' - x(e_b(\overline{T}_b) - e_u) \tag{D-12}$$

$$df_1 = (v_b - v_u)dx - x \left. \frac{\partial v_b}{\partial \overline{T}_b} \right|_p dT_b = 0 \tag{D-13}$$

$$df_2 = (e_b - e_u)dx - x \left. \frac{\partial e_b}{\partial T} \right|_p dT_b = x \Delta e_b \tag{D-14}$$

where $\Delta e_b = \frac{1}{24} \left(\frac{\partial C_{vb}}{\partial T} \right)(\Delta T)^2$. Solving for $\frac{dx}{x}$ in Eqs. (D-13) and (D-14) results in:

$$\frac{dx}{x} = \frac{x \Delta e_b \left(\frac{\partial v_b}{\partial T_b} \right)_p}{(e_b - e_u)\left(\frac{\partial v_b}{\partial T} \right)_p - (v_b - v_u)\left(\frac{\partial e_b}{\partial T} \right)_p} \tag{D-15}$$

Using the following relations:

$$\left(\frac{\partial v_b}{\partial T_b} \right)_p = \frac{R_b}{p} \tag{D-16}$$

$$e_b(\overline{T}_b) - e_u = h_b(\overline{T}_b) - h_u + R_b T_b - R_u T_u \tag{D-17}$$

$$h_b(\overline{T}_b) - h_u = C_p(\overline{T}_b - T_b^\circ) = C_p \Delta T \tag{D-18}$$

Equation (D-15) becomes:

$$\frac{dx}{x} = \frac{(\Delta T^2) \left(\frac{\partial C_{vb}}{\partial T} \right)_p}{24(\overline{T}_b - T_u)\left(C_p \frac{\Delta T}{T_b - T_u} - C_v + R\right)} \tag{D-19}$$

Considering $C_p \frac{\Delta T}{T_b - T_u}$ and R are much smaller than C_v Eq. (D-19) will be

$$\frac{dx}{x} \approx \frac{(\Delta T)^2}{24(\overline{T}_b - T_b)C_{vb}} \left(\frac{\partial C_{vb}}{\partial T} \right)_P \tag{D-20}$$

and $\frac{dx}{x}$ for the cases investigated is not more than 0.002. Therefore average burned gas temperature has been used to calculate the thermo-dynamic properties of burned gases.

APPENDIX E

FUEL THERMODYNAMIC PROPERTIES

In the thermodynamic analysis of the combustion process in the combustion bomb, specific enthalpy and specific heat values for different species are required. Specific enthalpy h and specific heat at constant pressure c_p can be expressed by the following relationships:

$$c_{pi} = a_{i1} + a_{i2}t + a_{i3}t^2 + a_{i4}t^3 + a_{i5}/t^2 \tag{E-1}$$

$$h_i = a_{i1}t + a_{i2}t^2/2 + a_{i3}t^3/3 + a_{i4}t^4/4 \tag{E-2}$$

$$- a_{i5}/t + a_{i6} + a_{i8}$$

where

a_{ij} = fitted values, J-1 to 5

a_{i6} = constant for using 298K as datum

a_{i8} = constant for using 0 K as datum

C_{pi} = specific heat at constant pressure (cal/gm.mole.K)

h_i = specific enthalpy (cal/gm.mole)

t = temperatue in K/1000

The coefficients a_{ij} are obtained by curve fitting JANAF [22] table data to the above functional form. The fitted constants for CO_2, H_2O, CO, H_2, O_2, N_2, C_8H_{18}, C_3H_8, and CH_3OH are given in Appendix A of LoRouso [23].

For multi-component fuels such as RMFD 303,thermodynamic properties are defined by summing mole-weighted contributions from its components. Hence specific heat and specific enthalpy for a fuel of average molecular weight $\overline{M}_f$ are:

$$C_p = \frac{1}{\overline{M}_f} \sum_{k=1}^{n} y_K \left(\sum_{J=1}^{4} (a_{KJ}\, t^{J-1}) + \frac{a_{k5}}{t^2} \right) \qquad (E-3)$$

and,

$$h = \frac{1}{\overline{M}_f} \sum_{k=1}^{n} y_K \left(\sum_{J=1}^{4} \left(\frac{a_{kJ}\, t^{J}}{J} \right) - \frac{a_{k5}}{t} \right.$$

$$\left. + a_{k6} + a_{k8} \right) \qquad (E-4)$$

where

y_K = mode fraction of component K in the fuel

$\overline{M}_f$ = average molecular weight gm/gm.mole

a_{KJ} = same as a_{iJ} in Eqs. (E-1) and (E-2)

Table E-1 shows the coefficient a_{IJ} for different fuels. For more information references [23] and [36] should be consulted.

TABLE E-1

COEFFICIENTS FOR DETERMINING THERMODYNAMIC PROPERTIES OF VARIOUS FUELS
300 K < T < 1000 K

NAME	FORMULA	a_{i1}	a_{i2}	a_{i3}	a_{i4}	a_{i5}	a_{i6}	a_{i8}
Propane	C_3H_8	- 1.4867	+ 74.339	- 39.0649	+ 8.05426	+ .0121948	-27.3111	+ 8.8500
Methane	CH_4	- .291491	+ 26.3271	- 10.6096	+ 1.56557	+0.165726	-18.3313	+ 4.3000
Isooctane	C_8H_{18}	-17.9283	+242.674	-172.904	+51.362	+0.418388	-56.1743	+20.225
Methanol	CH_3OH	- 2.70585	+ 44.1677	- 27.5009	+ 7.21927	+0.20299	-48.3211	+ 5.37100
RMFD 302	$C_{8.056}H_{15.121}$	-23.70726	+258.678	-204.2074	+71.1899	+0.576267	-41.81371	+17.798
RMFD 303	$C_{7.8}H_{13.214}$	-22.5012	+227.9934	-177.258	+56.0483	+0.484497	-29.7816	+15.235
Toluene	C_7H_8	-19.5613	+176.392	-135.306	+41.5136	+0.237377	+11.8563	+ 9.856
Benezene	C_6H_6	-15.3997	+142.517	-111.628	+34.5597	+0.126649	+19.4247	+ 7.581
n-Heptane	C_7H_{16}	-15.1162	+210.313	-147.158	+42.8266	+0.357146	-47.2987	+17.945
Ethyl-Benzene	C_8H_{10}	-18.7091	+198.583	-151.776	+46.4746	+0.217607	+ 6.44725	+12.132
Undecene	$C_{11}H_{22}$	-29.2788	+348.87	-276.331	+89.7694	+0.846336	-36.3036	+25.034
Nonene	C_9H_{18}	-25.5929	+290.542	-233.238	+76.7157	+0.726636	-25.7007	+20.479

150

APPENDIX F

CONSTANT ENTHALPY COMBUSTION IN THE BOMB

To show the combustion process in the combustion bomb is isenthalpic the conservation equations of (B-9) and (B-18) are used:

$$\frac{v_0}{m_0} + \frac{A\delta}{m_0} = \int_0^X v_b(s_b,p)dx' + (1-x)\ v_u\ (s_u,p) \tag{F-1}$$

$$\frac{F_0}{m_0} - \frac{A}{m_0} \int_0^\delta p\ d\delta' = \int_0^X e_b(s_b,p)dx' + (1-x)\ e_u(s_u,p) \tag{F-2}$$

Equation (F-1) is multiplied by p and added to Eq. (F-2)

$$e_0 + pv_0 + \frac{A}{m_0}\ (p\delta - \int_0^\delta pd\delta') = \int_0^X h_b(s_b,p)dx' + (1-x)\ h_u(s_u,p) \tag{F-3}$$

or

$$h_0 + \frac{A}{m_0} \int_0^p \delta\ dp' = \int_0^X h_b(s_b,p)dx' + (1-x)\ h_u(s_u,p) \tag{F-4}$$

Differentiating Eq. (D-4) with respect to p and using $de = dv = 0$ will result in:

$$v_0 + \frac{A\delta}{m_0} = (h_b(s_b,p) - h_u(s_u,p))\ \frac{dx}{dp} + \int_0^X \left(\frac{\partial h_b}{\partial p}\right)\bigg|_{s_b} dx'$$

$$(1-x)\ \left(\frac{\partial h_u}{\partial p}\right)\bigg|_{s_u} \tag{F-5}$$

Equation (F-1) can be used in Eq. (F-5)

$$h_b(s_b,p) - h_u(s_u,p) \ \frac{dx}{dp} + \int_0^x \left(\frac{\partial h_b}{\partial p} \right)\bigg|_{s_b} dx' +$$

$$+ \ (1-x)\left(\frac{\partial h_u}{\partial p} \right)\bigg|_{s_u} = \int_0^x v_b(s_b,p)dx' \qquad\qquad (F\text{-}6)$$

$$+ \ (1-x) \ v_u(s_u,p)$$

and consequently:

$$h_b(s_b,p) = h_u(s_u,p) \qquad\qquad (F\text{-}7)$$

That is the combustion process is isenthalpic.

APPENDIX G

dx/dp CALCULATION

The conservation equations are written as follows:

$$v_0 + \frac{A\delta}{m_0} = \int_0^X v_b(s_b,p)dx' + (1-x) \, v_u(s_u,p) \tag{G-1}$$

$$e_0 - \frac{A}{m_0} \int_0^\delta pd\delta' = \int_0^X e_b(s_b,p)dx' + (1-x) \, e_u(s_u,p) \tag{G-2}$$

Equation (G-1) is differentiated with respect to p

$$\frac{A}{m_0} \frac{d\delta}{dp} = (v_b(s_b,p) - v_u(s_u,p) \frac{dx}{dp} + \int_0^X \left(\frac{\partial v_b}{\partial p} \right)\Big|_{s_b} dx'$$

$$+ (1-x) \left(\frac{\partial v_u}{\partial p} \right)\Big|_{s_u} \tag{G-3}$$

for semi-perfect gas

$$pv = RT \tag{G-4}$$

and

$$\frac{dp}{p} + \frac{dv}{v} = \frac{dR}{R} + \frac{dT}{T} \tag{G-5}$$

Using the first law of Thermodynamics

$$de = C_v dT = Tds - pdv \tag{G-6}$$

Substituting Eq. (G-4) in Eq. (E-6)

$$ds = C_v \frac{dT}{T} + R \frac{dv}{v}$$
(G-7)

Substituting Eq. (E-5) into Eq. (G-7)

$$ds = (C_v + R) \frac{dv}{v} + C_v \frac{dp}{p} - C_v \frac{dR}{R}$$
(G-8)

Then

$$0 = \gamma \left(\frac{\partial v}{\partial p} \right) + \frac{v}{p} - \frac{v}{R} \left(\frac{\partial R}{\partial p} \right)_s$$
(G-9)

or

$$\left(\frac{\partial v}{\partial p} \right)_s = - \frac{1}{\gamma} \frac{v}{p} \left(1 - \left(\frac{\partial \ln R}{\partial \ln p} \right)_s \right)$$
(G-10)

Substituting Eq. (G-10) into Eq. (G-3)

$$(v_b - v_u) \frac{dx}{dp} = \frac{A}{m_0} \frac{d\delta}{dp} + \frac{1}{p} \int_0^X \frac{v_b}{\gamma_b} \left(1 - \left(\frac{\partial \ln R_b}{\partial \ln p} \right)_s \right) dx'$$

$$+ (1-x) \frac{v_u}{p\gamma_u} \left(1 - \left(\frac{\partial \ln R_u}{\partial p} \right)_{s_u} \right)$$
(G-11)

for slowly varying γ and R

$$(v_b - v_u) \frac{dx}{dp} = \frac{A}{m_0} \frac{d\delta}{dp} + \frac{1}{p\gamma_b} \int_0^x v_b(s_b, p)dx'$$

$$+ (1-x) \frac{v_u}{p\gamma_u} \tag{G-12}$$

Substituting Eq. (G-1) into Eq. (G-12)

$$\gamma_b p(v_b - v_u) \frac{dx}{dp} = \gamma_b p \frac{A}{m_0} \frac{d\delta}{dp} + v_0 + \frac{A\delta}{m_0}$$

$$+ (1-x) v_u \left(\frac{\gamma_b}{\gamma_u} - 1 \right) \tag{G-13}$$

rearranging the terms in Eq. (G-13)

$$\frac{dx}{dp} = \frac{v_0}{\gamma_b(R_b T_b - R_u T_u)} \left(1 - (1-x) \frac{v_u}{v_0} \left(1 - \frac{\gamma_b}{\gamma_u}\right)\right.$$

$$\left. + \frac{A}{v_0} \left(\gamma_b p \frac{d\delta}{dp} + \delta\right)\right) \tag{G-14}$$

APPENDIX H

RESIDUAL GASES SIMULATION

The combustion products of fuel-air mixtures primarily consist of nitrogen, carbon dioxide, and water vapor. Residual gases are used in combustors to reduce peak temperature, and consequently to reduce the formation of nitric oxides. The residual gases are simulated by a mixture of nitrogen and carbon dioxide. The specific heat of the mixture should be as close as possible to the specific heat of the combustion products. Figure H.1 shows the specific heats for the combustion products of stoichiometric iso-octane-air mixtures, and for different mixtures of the nitrogen-carbon dioxide mixture as a function of temperature. It can be seen that the specific heat of combustion products is lower than the specific heat of a mixture composed of 20% carbon dioxide (volume percent) and 80% nitrogen, and that it is higher than the specific heat of a mixture composed of 15% carbon dioxide and 85% nitrogen. It should be noticed that Figure H.1 does not include dissociation of molecules, which increases specific heat, but as dissociation occurs in mixtures of carbon dioxide and nitrogen as well as combustion products the relationship between specific heats for different mixtures in Fig. H.1 will not change a lot. For this study a mixture of 15% carbon dioxide and 85% nitrogen with a molecular weight of 30.4 was used.

The figure plots C_p (cal/gm mole K) versus temperature (K) for several gas mixtures:

- 0.25 CO_2 + 0.75 N_2
- 0.2 CO_2 + 0.8 N_2
- RESIDUAL GASES
- 0.15 CO_2 + 0.85 N_2
- 0.1 CO_2 + 0.9 N_2

x-axis: TEMPERATURE K (300, 700, 1100, 1500, 1900, 2300, 2700)

y-axis: C_p (cal /gm mole K) (7, 8, 9, 10, 11)
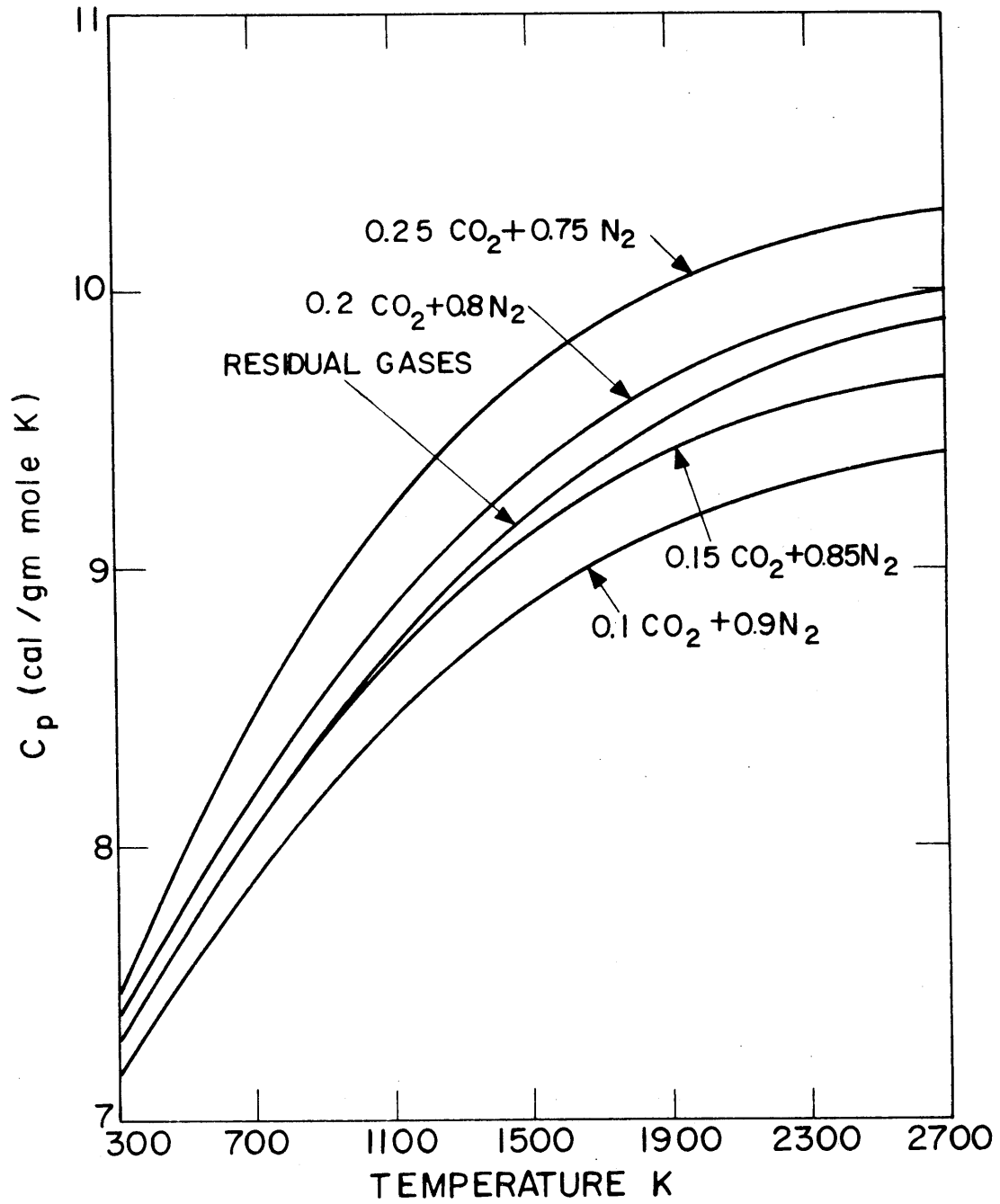
APPENDIX I

COMPUTER PROGRAMS

This appendix contains some of the computer programs used in this study. The main program,called "FLAME", calculated the laminar burning velocity of a fuel-air-residual mixture given the initial conditions of the mixture and the pressure-time history of the combustion process. The pressure-time history was read from a raw data file and the results were saved in a reduced data file. There are 12 subroutines and subprograms used in the "FLAME" program. These are UPROP, CLDPRD, HPROD, TRANSP, PPDTCL, TRAP, TSUBU, TEMP, IDATE, TIME, SUFIT, HGASJO.

Subprograms UPROP, CLDPRD, HPROD, TSUBU, and TEMP calculated the unburned and burned gas properties and are described by Andre By [40]. Programs IDATE and TIME were used to register the date and time of the experiment and are standard subroutines in the PDP 11/60 computer. Program TRAP, another standard subroutine, was used for numerical integration using the trapezoidal rule. Program HGASJO was used to solve simultaneous linear algebraic equation. For each run program SUFIT fitted the calculated burning velocity in the form $S_u = S_{uo}(\frac{T}{T_{uo}})^\epsilon$. The values of ϵ from three measurements along an isentrope were compared to check the validity of the data.

Program TRANSP was used to calculate the transport properties of the fuel-air-residual mixture. Program PPDTCL was used to calculate the pressure for a constant increment of unburned gas temperature, and

to calculate time rate of change of pressure of the combustion process.

The program FLAME and subprograms TRANSP and PPDTCL are listed at the end of the appendix. The comments within the programs should help to make the programs easily understood. A typical output of the program is shown in Fig. I-1.

```
C**********************************************************************
C
C      PROGRAM FLAME
C
C      PURPOSE:
C        TO CALCULATE LAMINAR BURNING VELOCITY OF FUEL-AIR MIXTURE FROM
C        A PRESSURE TIME TRACE OF THE COMBUSTION PROCESS
C
C      INPUTS:
C        NAME OF THE RAW DATA FILE
C
C        INPUTS FROM RAW DATA FILE
C        FNAM   -NAME OF FUEL
C        PNOT   -INITIAL PRESSURE (ATM)
C        TNOT   -INITIAL TEMPERATURE (K)
C        PHI    -EQUIVALENCE RATIO
C        RESFRK -RESIDUAL FRACTION
C        FN     -THE FIRST FOR CHARACTERS OF CHEMICAL FORMULA OF FUEL
C        PSPMVT -CALIBRATION CONSTANT OF CHARGE AMPLIFIER (PSIA/MVOLT)
C        TDELY  -DELAYTIME OF A/D CONVERTOR (MSEC)
C        TOTIM  -TOTAL TIME OF A/D CONVERTOR (MSEC)
C        TIP    -THREE IONIZATION PROBES TIME (MSEC)
C        TBP    -TIME OF BALANCING OF BALANCED-PRESSURE INDICATOR (MSEC)
C        PBP    -BALANCING PRESSURE(PSIA)
C        NPN    -256 POINTS OF PRESSURE DATA
C        NLAS   -256 POINTS OF LASER DATA
C
C        NAME OF REDUCED DATA FILE
C        OPTION-OPTION TO BE USED TO CALIBRATE PRESSURE DATA
C
C      RESULTS:
C        ?RHONOT-DENSITY OF INITIAL GAS MIXTURE (GM/CC)
C        PMAXK  -MAXIMUM PRESSURE OF KISTLER PRESSURE TRANSDUCER (ATM)
C        XFINLK -MAX. MASS FRACTION BURNED USING KISTLER TRANSDUCER
C        PINF   -INFLECTION POINT OF PRESSURE SIGNAL (ATM)
C        TIMIN  -TIME AT WHICH INFLECTION POINT OF PRESSURE SIGNAL OCCURS
C        EXPNT  -EXPONENT OF PRESSURE CURVE FIT (SOUBROUTINE PPDTCL)
C        CHMASS -MASS OF GAS MIXTURE (GM)
C        TH     -VECTOR OF TIME (MSEC)
C        PR     -VECTOR OF PRESSURE (ATM)
C        X      -VECTOR OF CUMULATIVE MASS FRACTION BURNED
C        XDOT   -VECTOR OF RATE OF MASS FRACTION BURNED
C        FRN    -VECTOR OF NORMALIZED FLAME RADIUS W.R.T. BOMB RADIUS
C        QOUT   -VECTOR OF CUMULATIVE HEAT TRANSFER TO COMBUSTION BOMB
C                 WALL (CAL/GM)
C        SU     -VECTOR OF LAMINAR BURNING VELOCITY (CM/SEC)
C        DELTA  -VECTOR OF DISPLACEMENT THICKNESS (CM)
C        TU     -VECTOR OF UNBURNED GAS MIXTURE TEMPERATURE (K)
C        TBAV   -VECTOR OF AVERAGE BURNED GAS TEMPERATURE (K)
C        TBNO   -VECTOR OF ADIABATIC FLAME TEMPERATURE (K)
C        RHOU   -VECTOR OF UNBURNED GAS MIXTURE DENSITY (KG/M3)
C        RHOB   -VECTOR OF BURNED GAS MIXTURE DENSITY (KG/M3)
C        EUAV   -VECTOR OF SPECIFIC ENERGY OF UNBURNED MIXTURE (CAL/GM)
C        EBAV   -VECTOR OF SPECIFIC ENERGY OF BURNED MIXTURE (CAL/GM)
C        GAMMAU -VECTOR OF SPECIFIC HEAT RATIO OF UNBURNED MIXTURE
```

```
C          IONP   -THREE PRES. AT THE TIMES OF I.P. PUSES (ATM)
C          IONRA  -THREE FLAME RADIUS AT THE TIMES OF I.P. PULSES(CM)
C          DFW    -THREEDISTANCES FROM WALL AT THE TIMES OF I.P. PULSES (MM)
C          XION   -THREE MASS FRACTION BURNED AT THE TIMES OF I.P. PULSES
C          TUI    -THREE UNBURNED GAS TEMP. AT THE TIMES OF I.P. PULSES
C          THMAX  -TIME AT WHICH MAXIMUM PRESSURE OCCURS (MSEC)
C          PMAX   -MAXIMUM PRESSURE (ATM)
C          TMAX   -MAX. UNBURNED GAS TEMPERATURE (K)
C          RMSIPR-RMS OF FLAME RADII WHEN IONIZATION PULSES OCCUR (MM)
C          PBP    -BALANCING PRESSURE (ATM)
C          PTBP   -KISTLER PRESSURE AT THE TIME OF EQUILIBRIUM (ATM)
C          PTBPA -KISTLER PRESSURE INCLUDING CORRECTION (ATM)
C          PTE    -PERCENTAGE DIFFERENCE OF B.P.I. & KISTLER GAUGE
C          FRPR   -RADIUS OF FLAME FRONT WHEN IT CROSSES THE LASER BEAM (CM)
C          RADER -VALUE OF (6.464-FRPR)/6.464   (6.464 CM IS THE DISTANCE
C                  FROM CENTER OF THE BOMB TO THE LASER BEAM
C
C
C       SUBROUTINES AND SUBPROGRAM REQUIRED:
C          UPROP  CLDPRD  HPROD   TRANSP  PPDTCL  TRAP  TSUBU  TEMP
C          IDATE  TIME   SUFIT  HGASJO
C
C       REMARKS:
C          IN CASE OF PROBLEM CONTACT MOHAMAD METGHALCHI AT 253-6647
C
C***************************************************************************
        DIMENSION PR(30),TH(30),X(30),XDOT(30),FNAM(20),RHOU(30),FR(30),
     &FA(30),SU(30),EUAVA(30),DELTAA(30),DDLTDP(30),TBAVA(30),TBNOA(30),
     &RHOBA(30),EBAVA(30),DISPLA(100),PNEXT(2),TN(256),PN(256),NPN(256)
     & ,PCTDLT(100),ID(258,2),NLAS(256),XMOLE(7),FRN(30),NLAS1(256)
        DIMENSION ITIM(4), A1(24),AFUEL(5),AENTH(6,5),EMOL(4,5),PTDELT(30)
        DIMENSION TIP(3),PIP(3),RIP(3),TU(256),SUC(30),TUN(30),PDOT(30)
        DIMENSION DISPLT(260),TNEXT(2),RAW(4),TMFA(2),REDUC(4)
     &,QOUT(30),GAM(260),SIGMAA(5),EPORKA(5)
        BYTE NRAW(15),NREDUC(15)
        COMMON/FUEL/AF(6),ENW,CX,HY,OZ,QLOWER
        COMMON/CHARGE/PHI,DEL,PSI,RESFRK,CHMASS,TREF,CFUEL
        COMMON/A/A
        COMMON XINT(260),DELTDP(260)
        EQUIVALENCE (RAW(1),NRAW(1)),(AANONE,NRAW(5)),(REDUC(1),NREDUC(1))
        DATA COMBV,NDD/1853.3333,256/
        DATA NREAD,NRITE/5,5/
        DATA PSCALE/2.42173E-2/
        DATA TBNO/2000./,BAREA/724.0201/
        DATA IDG/0/,TINC/14./,NDP/2/
        DATA AFUEL/4HCH4 ,4HC3H8,4HC8H1,4HCH3O,4HC7.8/
        DATA AENTH/-.291491,26.3271,-10.6096,1.56557,0.165726,-14.0313,
     &           -1.4867,74.339,-39.0649,8.05426,.0121948,-18.4611,
     &           -17.9283,242.674,-172.904,51.362,.418388,-35.9493,
     &           -2.70585,44.1677,-27.5009,7.21927,.20999,-42.9501,
     &           -22.501,227.993,-177.258,56.048,.484498,-14.547/
        DATA EMOL/0.0,1.0,4.0,0.0,
     &          0.0,3.0,8.0,0.0,
     &          0.0,8.0,18.0,0.0,
     &          0.0,1.0,4.0,1.0,
```

```
      &           0.0,7.8,13.214,0.0/
       DATA SIGMAA/3.796,5.061,7.451,3.584,6.6/
       DATA EPORKA/144,254,320,507,360/
       DATA RAW/4HDM1:,4H      ,4H .R,4HAW /,REDUC/4HDM1:,4H      ,4H .R,
      & 4HED  /,IPR/2HPR/,ILA/2HLA/
       DATA LRAW/2/,LREDUC/1/,NVERS/1/
       DATA ERLIM/.001/,MAXITS/100/,RALAS/6.464/
C
C INPUT SECTION
C MAJORITY OF DATA READ FROM DISK FILE
C C DISK FILE NAMES
       WRITE(5,6000)
6000   FORMAT(' INPUT:RAW DATA FILE NAME')
       READ(5,6001) (NRAW(I),I=5,10)
6001   FORMAT(6A1)
       WRITE(5,6002)
6002   FORMAT(' INPUT:REDUCED DATA FILE NAME (6CHAR)("NONE" MEANS'
      & ,' NO REDUCED DATA STORED)')
       NRAW(15)=0
       NREDUC(15)=0
       READ(5,6001)(NREDUC(I),I=5,10)
C
C READ RAW DATA -
       OPEN (UNIT=LRAW,NAME=NRAW,TYPE='OLD',READONLY)
       READ(LRAW,6003) I1,I2,I3,ITIM,IVRS
6003   FORMAT(8X,I2,1X,I2,1X,I2,8X,4A2,12X,I2)
       READ(LRAW,6004) FNAM
6004   FORMAT(3X,20A4)
       READ(LRAW,6005) PNOT,TNOT,PHI,RESFRK,FN,PSPMVT
      & ,TDELY,TOTIM,TIP,TBP,PBP
6005   FORMAT(4(1X,E10.3),1X,A4/6(1X,E10.3))
C READ MICRO DATA
       DO 5000 I=1,2
       ICHAN=I
       READ(LRAW,6006,END=7000) (ID(J,I),J=1,258)
6006   FORMAT(16(16(1X,I4),/),1X,A2,3X,I4)
5000   CONTINUE
7000   CONTINUE
C END OF INPUT
       CLOSE (UNIT=LRAW)
       WRITE(NRITE,2210)
 2210 FORMAT(5X,'INPUT:OPTION TO BE USED 1(KISTLER),2(MATCH X(MAX.)),3(
      &BAL. PRES.)')
       READ(NREAD,*)OPTION
       IF(OPTION-2)2241,2242,2243
 2241 WRITE(NRITE,2212)
 2212 FORMAT(5X,'KISTLER SIGNAL IS USED FOR PRESSURE')
       GO TO 2231
 2243 WRITE(NRITE,2213)
 2213 FORMAT(5X,'BAL. PRES. IS USED TO CALIBRATE KISTLER SIGNAL')
       GO TO 2231
 2242 CONTINUE
       WRITE(NRITE,2214)
 2214 FORMAT(5X,'FORCING X(MAX) TO BE A DESIRED VALUE IS USED TO CALIBRAT
      &E THE KISTLER SIGNAL')
```

```
0060              WRITE(NRITE,2230)
0061        2230 FORMAT(5X,'INPUT: MAX. MASS FRACTION BURNED DESIRED')
0062              READ(5,*)XF
0063        2231 CONTINUE
           C IDENTIFY CHANNEL WITH PRESSURE DATA AND CHANNEL WITH
           C LASER DATA
0064              NPR=0
0065              NLA=0
0066              DO 5001 I=1,ICHAN
0067              IF( ID(257,I) .EQ. IPR) NPR=I
0068              IF(ID(257,I) .EQ. ILA) NLA=I
0069        5001 CONTINUE
0070              IF(NPR) 7001,7001,7002
0071        7002  DO 5002 I=1,256
0072        5002   NPN(I)=ID(I,NPR)
0073              IF(NLA)7003,7003,7004
0074        7004 DO 5003 I=1,256
0075        5003 NLAS(I)=ID(I,NLA)
0076              GO TO 7005
0077        7001  WRITE(NRITE,6008)
0078        6008  FORMAT(' NO PRESSURE DATA PGM QUITS')
0079              STOP
0080        7003  WRITE(NRITE,6009)
0081        6009  FORMAT(' NO LASER DATA PGM CONTINUES')
0082        7005  CONTINUE
           C ACTUAL PROGRAM CONTINUES
0083              DELT=TOTIM/NDD
           C      FIND THE ENTHALPY COEFFICIENTS AND FUEL CHARACTERISTICS
           C
0084              DO 61 I=1,5
0085              NF=I
0086              IF(FN.EQ.AFUEL(I)) GO TO 62
0087          61  CONTINUE
0088          62  DO 63 I=1,6
0089          63  AF(I)=AENTH(I,NF)
0090              ENW=EMOL(1,NF)
0091              CX=EMOL(2,NF)
0092              HY=EMOL(3,NF)
0093              OZ=EMOL(4,NF)
0094              SIGMA=SIGMAA(NF)
0095              EPOVRK=EPORKA(NF)
           C
           C      READ IONIZATION PROBS TIMES
           C
0096              DO 92 I=1,3
0097          92  TIP(I)=TIP(I)+TDELY
           C OUTPUT SECTION
0098              IF(IDG .EQ. 0) GO TO 7771
0099              WRITE(NRITE,100) (FNAM(I),I=1,20)
0100         100  FORMAT(20A4)
0101              WRITE(NRITE,200) ( AF(I),I=1,6)
0102              WRITE(NRITE,300) ENW,CX,HY,OZ
0103              WRITE(NRITE,400)PNOT,TNOT,PHI,RESFRK
0104              WRITE(NRITE,101)TOTIM,PSPMVT,DELP,TDELY
0105              WRITE(NRITE,98) (TIP(I),I=1,3)
```

```
      WRITE(NRITE,6698)
  98  FORMAT(5X,3F10.0)
6698   FORMAT(//'    RAW DATA'/)
      WRITE(NRITE,6669) NPN
6669  FORMAT(16(1X,I4))
 506  FORMAT(5X,'WAITING FOR PRES. DATA ')
7771  PTRESH=2.0*PNOT
      DO 102 I=1,NDD
      PN(I)=(NPN(I))*2.44*PSPMVT/14.7+PNOT
      TN(I)=(I-1)*DELT+TDELY
      IF(I.EQ.1) GO TO 102
      IF(PN(I).GT.PTRESH.AND.PN(I).LT.PN(I-1)) GO TO 104
 102  CONTINUE
 104  NOUT=I-1
      THMAX=TN(NOUT)
C
C     FIND THE TIME WHEN FLAME FRONT CROSSES LASER BEAM
C
      IF(NLA)8800,8800,8801
8801  NLAS1(1)=0
      DO 8802 I=2,NDD
8802  NLAS1(I)=NLAS(I)-NLAS(I-1)
      DO 8803 I=2,NDD
      IF(NLAS1(I-1).GT.75.AND.NLAS1(I-1).GT.NLAS1(I)) GO TO 8804
8803  CONTINUE
8804  I=I-1
      TFLA=(TN(I)+TN(I-1))/2.
8800  CONTINUE
C
C     CALL UPROP TO CALCULATE INITIAL MASS,INTERNAL ENEGY , AND INITIAL DENSITY
C
      CALL UPROP(PNOT,TNOT,PHI,DEL,PSI,RESFRK,ENTHLP,CSUBP,CSUBT,RHONOT,
     &          DRHODT,DRHODP,CHI,XMOLE)
      WRITE(NRITE,7310)RHONOT
7310  FORMAT(5X,'RHONOT=',F10.6)
      ENOT=ENTHLP*1000.-PNOT*PSCALE/RHONOT
      VNOT=1./RHONOT
      CHMASS=RHONOT*COMBV
C
      WRITE(NRITE,5537)PN(NOUT)
C     CALIBRATE PRASSURE DATA EITHER BY MATCHING THE BP OR THE FINAL
C      MASS FRACTION BURNED
C
      PBP=PBP/14.7
2222  CONTINUE
      DO 180 I=1,NOUT
      IF(TBP-TN(I))181,182,180
 182  PTBP=PN(I)
      GO TO 183
 181  DPTBP=(TBP-TN(I-1))*(PN(I)-PN(I-1))/DELT
      PTBP=DPTBP+PN(I-1)
      GO TO 183
 180  CONTINUE
 183  CONTINUE
      DPDTBA=(PN(I)-PN(I-1))/(TN(I)-TN(I-1))
```

```
FORTRAN IV-PLUS V02-51          15:45:27    20-SEP-79              PAGE 6
FLAME.FTN          /TR:BLOCKS/WR

0150          DELTAT=3.3668*(7.83*.005*.001/(DPDTBA))**(.333333)
0151          TBPA=TBP-DELTAT
0152          PTBPA=PN(I-1)+(TBPA-TN(I-1))*DPDTBA
0153          FACT=(PBP-PNOT)/(PTBPA-PNOT)
0154          PTE=(PTBPA-PBP)*100./PBP
0155          IF(OPTION .NE. 3)GO TO 2221
0156          DO 184 I=1,NOUT
0157     184  PN(I)=PNOT+FACT*(PN(I)-PNOT)
0158    2221  CONTINUE
        C
        C     CALIBRATE PRES. SIGNAL BY MATCHING THE FINAL MASS FRACTION
        C     BURNED TO A DESIRED VALUE
        C
        C
0159          DATA SFIN,TBFIN/0.95,2500./
0160          TUFIN=TSUBU(PN(NOUT),PNOT,TNOT,ERLIM)
        C     FIND PRESSURES CORRESPONDING TO IONIZATION PROBES
0161          CALL UPROP(PN(NOUT),TUFIN,PHI,DEL,PSI,RESFRK,ENTHLP,CSUBP,CSUBT,
             &      RHOUFI,DRHODT,DRHODP,CHI,XMOLE)
0162          VUFIN=1./RHOUFI
0163          EUFIN=ENTHLP*1000.-PSCALE*PN(NOUT)/RHOUFI
0164          J=0
0165    2223  J=J+1
0166          IF(IDG.NE.0)
             &WRITE(NRITE,2224)J
0167    2224  FORMAT(5X,'NO. OF ITERATION IS',I3)
0168          CALL HPROD(PN(NOUT),TBFIN,CHI,DEL,PSI,H,CP,CT,RHO,DRHODT,DRHODP)
0169          VBFIN=1./RHO
0170          EBFIN=H*1000.-PSCALE*PN(NOUT)/RHO
0171          F1=ENOT-EBFIN*SFIN-(1.-SFIN)*EUFIN
0172          F2=VNOT-VBFIN*SFIN-(1.-SFIN)*VUFIN
0173          DF1DS=EUFIN-EBFIN
0174          DF2DS=VUFIN-VBFIN
0175          DF1DTB=(-CP-PN(NOUT)*PSCALE*DRHODT/(RHO*RHO))*SFIN
0176          DF2DTB=SFIN*DRHODT/(RHO*RHO)
0177          D1=DF1DS*DF2DTB-DF1DTB*DF2DS
0178          D2=F2*DF1DTB-F1*DF2DTB
0179          D3=F1*DF2DS-F2*DF1DS
0180          DELS=D2/D1
0181          DELTBV=D3/D1
0182          SRATIO=DELS/SFIN
0183          TRATIO=DELTBV/TBFIN
0184          IF(J-MAXITS)2225,2226,2226
0185    2225  IF(ABS(SRATIO).LT.ERLIM .AND. ABS(TRATIO).LT.ERLIM) GO TO 2226
0186          SFIN=SFIN+DELS
0187          TBFIN=TBFIN+DELTBV
0188          GO TO 2223
0189    2226  WRITE(NRITE,2227)SFIN
0190    2227  FORMAT(5X,'MASS FRACTION BURNED AT MAX. PRES. =',F8.3)
0191          IF(OPTION.NE.2)GO TO 2220
0192    5537  FORMAT(5X,'MAX. PRES. OF THE KISTLER TRANSDUCER=',F6.2,' ATM')
0193          WRITE(NRITE,5587)TN(NOUT)
0194    5587  FORMAT(5X,'TIME AT WHICH MAX. PRES. OCCURS=',F7.2,'MSEC')
0195          DO 2228 I=1,260
0196    2228  PN(I)=PNOT+(XF/SFIN)*(PN(I)-PNOT)
```

```
 2220 CONTINUE
C
      DO 5594 I=1,3
      DO 96 J=1,NOUT
      IF(TIP(I)-TN(J))95,94,93
 93   IF(J.EQ.NOUT)PIP(I)=PN(NOUT)
      GO TO 96
 94   PIP(I)=PN(J)
      GO TO 97
 95   DPIP=(TIP(I)-TN(J-1))*(PN(J)-PN(J-1))/DELT
      PIP(I)=PN(J-1)+DPIP
      GO TO 97
 96   CONTINUE
 97    CONTINUE
      IF(IDG.NE.0)
     &WRITE(NRITE,5593)I,PIP(I)
 5593 FORMAT(3X,I1,'TH I.P. ','P=',F7.3,'ATM')
 5594 CONTINUE
C
C     CALCULATE UNBURNED GAS TEMPERATURE
C
      DO 70 I=1,NOUT
      P=PN(I)
      TEMPU=TSUBU(P,PNOT,TNOT,ERLIM)
 70   TU(I)=TEMPU
      PMAX=PN(NOUT)
      TMAX=TU(NOUT)
      DO 7301 I=1,7
 7301 XMOLE(I)=0.0
      CALL UPROP(PNOT,TNOT,PHI,DEL,PSI,RESFRK,ENTHLP,CSUBP,CSUBT,RHONOT,
     &      DRHODT,DRHODP,CHI,XMOLE)
C
C     CALL TRANSP TO CALCULATE INITIAL VISCOSITY OF THE MIXTURE
C
      CALL TRANSP(SIGMA,EPOVRK,XMOLE,TNOT,PNOT,VISC,THCOND,DIFFUS)
      DSFCTR=SQRT(VISC/(3141.593*RHONOT))
C
C     DSFCTR HAS THE DIMENSION OF CM/(MSEC)**.5
C     CALL XXDTCL TO CALCULATE P AND PDOT ARRAY OF CONSTANT INCREMENT OF
C     UNBURNED GAS TEMPERATURE.ALSO TO FIND INFLECTION POINT FOR PRESSURE
C     CURVE(POINT WITH MAX. PDOT) , AND THE EXPONENT N FOR FITING THE
C     PRESSURE DATA TO THE FOLLOWING RELATION:
C         P=PNOT+(PINF-PNOT)*(TIME/TIMIN)**N
C
      CALL XXDTCL(PN,TN,TH,TU,TINC,NOUT,NDP,PR,PDOT,TUN,NNPTS
     &       ,PINF,TIMIN,EXPNT)
      WRITE(NRITE,7311)PINF,TIMIN,EXPNT
 7311 FORMAT(5X,'PINF=',F6.3,' TIMIN=',F8.3,' EXPNT=',F6.3)
C
C     CALL UPROP TO CALCULATE THE ARRAY OF UNBURNED SPECIFIC HEAT
C
      DO 7302 I=1,NOUT
      P=PN(I)
      TEMPU=TU(I)
      CALL UPROP(P,TEMPU,PHI,DEL,PSI,RESFRK,ENTHLP,CSUBP,CSUBT,RHO,
```

```
                &      DRHODT,DRHODP,CHI,XMOLE)
0231              R=PSCALE*P/(TEMPU*RHO)
0232              GAM(I)=CSUBP/(CSUBP-R)
0233       7302 CONTINUE
0234              DO 5453 I=1,260
0235              XINT(I)=0.0
0236       5453 DELTDP(I)=0.0
           C
           C
           C      THIS SEGMENT CALCULATES THE DISPLACEMENT THICKNESS BY PERFORMING
           C        INTEGRATION
           C
0237              DISPLT(1)=0.0
0238              DO 7304 I=2,NOUT
0239              J=I-1
0240              DO 7305 K=1,J
0241              DFCTR2=((PN(K)/PN(I))**(1./GAM(K)))*((PN(K)/PNOT)**((GAM(K)-1)/
                 &GAM(K)))-1.)
0242              DFCTR3=1./SQRT((TN(I)-TN(K))+(PINF-PNOT)*(TN(I)**(EXPNT+1.)-TN(K)
                 &**(EXPNT+1.))/((EXPNT+1.)*PNOT*(TIMIN**EXPNT)))
0243              XINT(K)=DFCTR2*DFCTR3
0244       7305 CONTINUE
0245              CALL TRAP(J,DELT,XINT,VALUE)
0246              EXTRA=2*((PN(I)/PNOT)**((GAM(I)-1)/GAM(I))-1.)*(SQRT(DELT*PNOT/
                 &PN(I)))
0247              DISPLT(I)=DSFCTR*(VALUE+EXTRA)
0248       7304 CONTINUE
0249              DO 7331 I=1,NOUT
0250       7331 XINT(I)=0.0
0251              DELTDP(1)=0.0
0252              DO 7332 I=2,NOUT
0253              J=I-1
0254              DO 7333 K=1,J
0255              DFCTR4=((PN(K)/PNOT)**(1./GAM(K)-2.))*TN(K)**(EXPNT-1.)
0256              DFCTR5=1./SQRT(TN(I)-TN(K)+(PINF-PNOT)*(TN(I)**(EXPNT+1.)-TN(K)**
                 &(EXPNT+1.))/((EXPNT+1.)*PNOT*TIMIN**EXPNT))
0257              XINT(K)=DFCTR4*DFCTR5
0258       7333 CONTINUE
0259              CALL TRAP(J,DELT,XINT,VALUE)
0260              EXTRA=2*(PN(I)/PNOT)**(1./GAM(I)-2.5)*TN(I)**(EXPNT-1.)*
                 &SQRT(DELT)
0261              DFCTR6=((GAM(I)-1.)/GAM(I))*DSFCTR*(TN(I)**(1.-EXPNT))*((PN(I)/
                 &PNOT)**((2.*GAM(I)-1.)/GAM(I)))/PN(I)
0262              DELTDP(I)=DFCTR6*(VALUE+EXTRA)-DISPLT(I)/(GAM(I)*PN(I))
0263       7332 CONTINUE
0264              DO 7337 I=1,3
0265              P=PIP(I)
0266              IF(IDG.NE.0)
                 &WRITE(NRITE,2256)I,P
0267       2256 FORMAT(5X,I1,'TH IONIZATION PROBE',3X,'P=',F8.3)
0268              TEMPU=TSUBU(P,PNOT,TNOT,ERLIM)
0269              J=NNPTS+I
0270              PR(J)=PIP(I)
0271              TUN(J)=TEMPU
0272       7337 TH(J)=TIP(I)
0273              NDPTS=NNPTS+3
```

```
          C
          C       CALCULATE D(DELTA)/DP FOR CONSTANT INCREMENT OF UNBURNED GAS
          C       TEMPERATURE
          C
0274              DO 7338 I=1,NDPTS
0275              DO 7339 J=1,NOUT
0276              IF(PR(I)-PN(J)) 7340,7341,7342
0277         7342 GO TO 7339
0278         7341 DELTAA(I)=DISPLT(J)
0279              DDLTDP(I)=DELTDP(J)
0280              GO TO 7338
0281         7340 DELTAA(I)=DISPLT(J-1)+(DISPLT(J)-DISPLT(J-1))*(PR(I)-PN(J-1))/
                 &(PN(J)-PN(J-1))
0282              DDLTDP(I)=DELTDP(J-1)+(DELTDP(J)-DELTDP(J-1))*(PR(I)-PN(J-1))/
                 &(PN(J)-PN(J-1))
0283              GO TO 7338
0284         7339 CONTINUE
0285         7338 CONTINUE
          C
          C       CALCULATE THE INTEGRAL OF P W.R.T. DELTA.DELTA IS DIVIDED TO
          C       100 POINTS WITH 99 CONSTANT INCREMENT IN BETWEEN
          C
0286              DELINC=(DISPLT(NOUT)-DISPLT(1))/99.
0287              DISPLA(1)=DISPLT(1)
0288              PCTDLT(1)=PN(1)
0289              DO 7343 I=2,100
0290              DISPLA(I)=DISPLA(I-1)+DELINC
0291              DO 7344 J=1,NOUT
0292              IF(DISPLA(I)-DISPLT(J)) 7345,7346,7347
0293         7347 GO TO 7344
0294         7346 PCTDLT(I)=PN(J)
0295              GO TO 7343
0296         7345 PCTDLT(I)=PN(J-1)+(PN(J)-PN(J-1))*(DISPLA(I)-DISPLT(J-1))/
                 &(DISPLT(J)-DISPLT(J-1))
0297              GO TO 7343
0298         7344 CONTINUE
0299         7343 CONTINUE
0300              DO 7348 I=1,NOUT
0301         7348 XINT(I)=0.0
0302              DO 7349 I=1,100
0303              CALL TRAP(I,DELINC,PCTDLT,VALUE)
0304         7349 XINT(I)=0.0242173*VALUE
          C
          C       0.0242173 IS CONVERSION FACTOR FROM ATM-CM TO CAL/CM**2
          C       XINT IS THE VALUE OF INTEGRAL OF P*D(DELTA)
          C
          C       CONVERT XINT TO ARRAY HAVING CONSTANT TU INCREMENT
          C
0305              DO 7350 I=1,NDPTS
0306              DO 7351 J=1,100
0307              IF(PR(I)-PCTDLT(J))7352,7353,7354
0308         7354 GO TO 7351
0309         7353 PTDELT(I)=XINT(J)
0310              GO TO 7350
0311         7352 PTDELT(I)=XINT(J-1)+(XINT(J)-XINT(J-1))*(PR(I)-PCTDLT(J-1))/
```

```
              &(PCTDLT(J)-PCTDLT(J-1))
0312              GO TO 7350
0313         7351 CONTINUE
0314         7350 CONTINUE
0315              IF(IDG .EQ. 0) GO TO 7370
0316              WRITE(NRITE,7371)
0317         7371 FORMAT(6X,'TIME',5X,'PRESS',6X,'PDOT',5X,'DELTA',1X,'D(DELTA)/DP'
              &,4X,'P*D(DELTA)')
0318              DO 7372 I=1,NDPTS
0319         7372 WRITE(NRITE,7373)TH(I),PR(I),PDOT(I),DELTAA(I),DDLTDP(I),PTDELT(I)
0320         7373 FORMAT(2F10.3,4F10.6)
0321         7370 CONTINUE
0322              DO 7355 I=1,NOUT
0323         7355 GAM(I)=0.0
      C
      C
      C          ERLIM IS MAXIMUM ALLOWABLE RELATIVE ERROR
      C          MAXITS IS MAXIMUM NUMBER OF ITERATION
      C
      C
      C          CALCULATE THE ARRAY OF UNBURNED MIXTURE DENSITY,TEMPERATURE,
      C          SPECIFIC ENERGY,GAS CONSTANT,SPECIFIC HEAT RATIO,AND ADIABATIC
      C          FLAME TEMPERATURE
      C
0324              DO 1 I=1,NDPTS
0325              P=PR(I)
0326              TEMPU=TUN(I)
0327              CALL UPROP(P,TEMPU,PHI,DEL,PSI,RESFRK,ENTHLP,CSUBP,CSUBT,RHO,
              &DRHODT,DRHODP,CHI,XMOLE)
0328              R=PSCALE*P/(TUN(I)*RHO)
      C
      C          CALCULATE SPECIFIC HEAT RATIO
      C
0329              GAM(I)=CSUBP/(CSUBP-R)
0330              RHOU(I)=RHO
      C
      C          CALCULATE ADIABATIC FLAME TEMPERATURE BY CALLING SUBROUTINE TEMP
      C          AND SETTING THE ENTHALPY OF UNBURNED GAS EQUAL TO ENTHALPY OF
      C          BURNED PRODUCT
      C
0331              CALL TEMP(P,TBNO,PHI,DEL,PSI,ENTHLP,TBNO,ERMAX,MAXITS,IER)
0332              TBNOA(I)=TBNO
0333         1    EUAVA(I)=ENTHLP*1000.-PSCALE*P/RHOU(I)
      C
      C          SOLVE FOR MASS FRACTION BURNED AND TEMPERATURE OF BURNED MIXTURE
      C          USING MASS AND ENERGY CONSERVATION EQUATION AND USING NEWTON-
      C          RAPHSON ITERATION METHOD
      C
0334              DATA S,TBAV/0.005,2000.0/
0335              DO 5 I=1,NDPTS
0336              IF(IDG .NE. 0)
              *WRITE(NRITE,508) I
0337          508 FORMAT(5X,'THE',I5,'TH DATA,POINT')
0338              P=PR(I)
0339              IF(P.EQ.PNOT) GO TO 40
0340              VUAV=1.0/RHOU(I)
```

```
|41            EUAV=EUAVA(I)
|42            J=0
|43      2     J=J+1
|44            IF(IDG .NE. 0)
              *WRITE(NRITE,509) J
|45    509     FORMAT(5X,'NO. OF ITERATION IS',I5)
       C
       C       USING SUBROUTINE HPROD TO CALCULATE DENSITY AND INTERNAL
       C       ENERGY OF BURNED MIXTURE
       C
|46            CALL HPROD(P,TBAV,CHI,DEL,PSI,H,CP,CT,RHO,DRHODT,DRHODP)
|47            VBAV=1.0/RHO
|48            EBAV=H*1000.-PSCALE*P/RHO
|49            F1=ENOT-EBAV*S-(1.0-S)*EUAV-BAREA*PTDELT(I)/CHMASS
|50            F2=VNOT-VBAV*S-(1.0-S)*VUAV+BAREA*DELTAA(I)/CHMASS
|51            DF1DS=EUAV-EBAV
|52            DF2DS=VUAV-VBAV
|53            DF1DTB=(-CP-P*PSCALE*DRHODT/(RHO*RHO))*S
|54            DF2DTB=S*DRHODT/(RHO*RHO)
|55            D1=DF1DS*DF2DTB-DF1DTB*DF2DS
|56            D2=F2*DF1DTB-F1*DF2DTB
|57            D3=F1*DF2DS-F2*DF1DS
|58            DELS=D2/D1
|59            DELTBV=D3/D1
|60            SRATIO=DELS/S
|61            TRATIO=DELTBV/TBAV
|62            IF(J-MAXITS)3,4,4
|63      3     IF(ABS(SRATIO).LT.ERLIM.AND.ABS(TRATIO).LT.ERLIM)GO TO 4
|64            S=S+DELS
|65            TBAV=TBAV+DELTBV
|66            GO TO 2
|67     40     X(I)=0.
|68            TBAVA(I)=0.
|69            RHOBA(I)=0.
|70            EBAVA(I)=0.
|71            XDOT(I)=0.0
|72            GO TO 5
|73      4     X(I)=S
|74            RHOBA(I)=1./VBAV
|75            EBAVA(I)=H*1000.-PSCALE*P/RHOBA(I)
|76            TBAVA(I)=TBAV
|77            RB=PSCALE*PR(I)/(TBAVA(I)*RHOBA(I))
|78            GAMB=CP/(CP-RB)
|79            RU=PSCALE*PR(I)/(TUN(I)*RHOU(I))
|80            CPU=RU*GAM(I)/(GAM(I)-1.)
|81            QOUT(I)=(BAREA/CHMASS)*(CPU*RHOU(I)*TUN(I)*DELTAA(I)-PSCALE*
              &DELTAA(I)*PR(I)+PTDELT(I))
|82            DXDP=(VNOT-(1.-X(I))*(1.-GAMB/GAM(I))/RHOU(I)+BAREA*DELTAA(I)*
              &(GAMB*PR(I)*DDLTDP(I)/DELTAA(I)+1.)/CHMASS)/(GAMB*(RB*TBNOA(I)-
              &RU*TUN(I)))*PSCALE
|83            XDOT(I)=DXDP*PDOT(I)
|84            IF(IDG .EQ. 0)GO TO 7383
|85            WRITE(NRITE,7381)
|86   7381     FORMAT(6X,'GAMB',5X,'GAMU',8X,'P',2X,'D(DELTA)/DP',5X,'DELTA',6X,'
              &DXDP',6X,'PDOT',6X,'XDOT')
```

```
87              WRITE(NRITE,7382)GAMB,GAM(I),PR(I),DDLTDP(I),DELTAA(I),DXDP,PDOT(I
                &),XDOT(I)
88       7382  FORMAT(3F10.3,5F10.5)
89       7383  CONTINUE
90       5     CONTINUE
         C
         C     CALCULATE FLAME RADIUS AND FLAME AREA
         C
91             DO 6 I=1,NDPTS
92             IF(X(I).EQ.0.) GO TO 45
93             FR(I)=(3.0*X(I)*CHMASS/(4.0*3.141593*RHOBA(I)))**(1.0/3.0)
94             FA(I)=4.0*3.141593*(FR(I)**2.0)
95             GO TO 6
96       45    FR(I)=0.
97             FA(I)=0.
98       6     CONTINUE
         C
         C     FIND THE TIME WHEN FLAME FRONT CROSSES LASER BEAM USING PRESSURE
         C     DATA
         C
99             IF(NLA)8815,8815,8814
00       8814  CONTINUE
01             DO 8810 I=1,NDPTS
02             IF(TFLA-TH(I))8811,8812,8810
03       8812  FRPR=FR(I)
04             GO TO 8813
05       8811  FRPR=FR(I-1)+(FR(I)-FR(I-1))*(TFLA-TH(I-1))/(TH(I)-TH(I-1))
06             GO TO 8813
07       8810  CONTINUE
08       8813  CONTINUE
09             RADER=100.0*(RALAS-FRPR)/RALAS
10       8815  CONTINUE
         C
         C     CALCULATE BURNING VELOCITY
         C
11             DO 33 I=1,NNPTS
12             IF(IDG .EQ. 0) GO TO 7772
13             WRITE(NRITE,151)
14       151   FORMAT(5X,'I',5X,'CHMASS',5X,'XDOT',5X,'RHOU',5X,'FA')
15             WRITE(NRITE,152)I,CHMASS,XDOT(I),RHOU(I),FA(I)
16       152   FORMAT(I6,4F9.4)
17       7772  CONTINUE
18             IF(FA(I).EQ.0.) GO TO 37
19             SU(I)=1000.*CHMASS*XDOT(I)/(RHOU(I)*FA(I))
20             GO TO 33
21       37    SU(I)=0.
22       33    CONTINUE
         C
         C     PRINT GIVEN DATA AND RESULTS
         C
23       7006  WRITE(NRITE,600) (FNAM(I),I=1,20)
24             WRITE(NRITE,700)
25             WRITE(NRITE,200) (AF(I),I=1,6)
26             WRITE(NRITE,900)COMBV
27             WRITE(NRITE,910) PNOT
```

```
!8              WRITE(NRITE,920) TNOT
!9              WRITE(NRITE,930) PHI
!0              WRITE(NRITE,940)RESFRK
!1              WRITE(NRITE,1200) CHMASS
!2              WRITE(NRITE,1300)
!3              WRITE(NRITE,1400)
!4              WRITE(NRITE,1500)
!5              WRITE(NRITE,1550)
!6              DO 12 I=1,NNPTS
!7              FRN(I)=FR(I)/7.5905
!8              RHOU(I)=RHOU(I)*1000.
!9              RHOBA(I)=RHOBA(I)*1000.
!0       12     WRITE(NRITE,1600) TH(I),PR(I),X(I),XDOT(I),FRN(I),QOUT(I),SU(I),
                &DELTAA(I),TUN(I),TBAVA(I),TBNOA(I),RHOU(I),RHOBA(I),EUAVA(I),
                &EBAVA(I),GAM(I)
!1              WRITE(NRITE,1700)
!2       1700   FORMAT(///,' IONIZATION      TIME PRESSURE    P/PMAX    RADIUS    NORM
                &ALIZED DISTANCE       X',6X,'TU')
!3              WRITE(NRITE,1800)
!4       1800   FORMAT(3X,'PROBE',7X,'MSEC',4X,'ATM',16X,'CM',8X,'RADIUS   FROM WAL
                &L(MM)',10X,'K')
!5              DO 132 I=1,3
!6              J=I+NNPTS
!7              PRAT=PR(J)/PMAX
!8              FRNP=FR(J)/7.62
!9              DFW=10.0*(7.62-FR(J))
!0       132    WRITE(NRITE,1900)I,TH(J),PR(J),PRAT,FR(J),FRNP,DFW,X(J),TUN(J)
!1       1900   FORMAT(I6,F14.3,F9.3,F8.3,F10.3,F11.3,F12.3,F8.3,F7.1)
!2              WRITE(NRITE,2000)THMAX,PMAX,TMAX
!3       2000   FORMAT(3X,'MAX TIME=',F7.2,' MAX PRES.=',F6.2,' MAX TU=',F6.2)
!4              RMEAN=(FR(NNPTS+1)+FR(NNPTS+2)+FR(NNPTS+3))/3.
!5              SUM=(FR(NNPTS+1)-RMEAN)**2.+(FR(NNPTS+2)-RMEAN)**2.+(FR(NNPTS+3)-
                &RMEAN)**2.
!6              RMSIPR=10.0*(SQRT(SUM/3.))/1.0
!7              WRITE(NRITE,2050) RMSIPR
!8              WRITE(NRITE,2100)PBP
!9              WRITE(NRITE,2200)PTBP
!0              WRITE(NRITE,2250)PTBPA
!1              WRITE(NRITE,2300)PTE
!2       7359   CONTINUE
!3              IF(NLA)8850,8850,8851
!4       8851   CONTINUE
!5              WRITE(NRITE,2400)FRPR
!6              WRITE(NRITE,2500)RADER
!7       8850   CONTINUE
!8              IF(ANONE .EQ. AANONE) GO TO 7007
!9              OPEN(UNIT=LREDUC,NAME=NREDUC)
'0              WRITE(LREDUC,6010) (NRAW(I),I=5,10) ,I1,I2,I3,ITIM
'1       6010   FORMAT(' RAW DATA FILE ',6A1,3X,I2,'/',I2,'/',I2,6X,4A2)
'2              WRITE(NRITE,6011)(NREDUC(I),I=5,10)
'3       6011   FORMAT(' REDUCED DATA TO FILE ',6A1)
'4              CALL IDATE( I1,I2,I3)
'5              CALL TIME (ITIM)
'6              WRITE(LREDUC,6012) I1,I2,I3,ITIM
'7       6012   FORMAT(' REDUCTION PERFORMED ',I2,'/',I2'/',I2,6X,4A2)
```

```
FORTRAN IV-PLUS V02-51          15:45:27   20-SEP-79           PAGE 14
FLAME.FTN          /TR:BLOCKS/WR

0478    7007  CONTINUE
0479          WRITE(LREDUC,4000)FNAM
0480    4000  FORMAT(3X,20A4)
0481    4001  FORMAT(4(1X,E10.3),I3)
0482          DO 4002 I=1,NNPTS
0483    4002  WRITE(LREDUC,4003)PR(I),TUN(I),RHOU(I),SU(I),TBNOA(I),FRN(I),
             &TH(I),DELTAA(I),X(I),TBAVA(I),XDOT(I)
0484    4003  FORMAT(11(1X,E11.4))
0485          CLOSE(UNIT=LREDUC)
0486          DO 5321 I=1,NNPTS
0487          IF(X(I).GT. 0.8) GO TO 5322
0488    5321  CONTINUE
0489    5322  NFIT=I-1
0490          IF(TNOT-370) 121,122,122
0491    121   TMFA(1)=450
0492          TMFA(2)=550
0493          NCOR=2
0494          TNEXT(1)=400.
0495          TNEXT(2)=500.
0496          NNEXT=2
0497          GO TO 125
0498    122   IF(TNOT-450) 123,124,124
0499    123   TMFA(1)=450
0500          TMFA(2)=550
0501          NCOR=2
0502          TNEXT(1)=500.
0503          NNEXT=1
0504          GO TO 125
0505    124   TMFA(1)=550
0506          NNEXT=0
0507          NCOR=1
0508    125   DO 126 I=1,NCOR
0509          TUNOT=TMFA(I)
0510          CALL SUFIT(SU,TUN,TUNOT,SUO,ALFA,NFIT)
0511    126   WRITE(NRITE,2600) TUNOT,SUO,ALFA
0512    2600  FORMAT(//,3X,'SU=SUO*(T/TO)**ALFA',5X,'TO=',F5.1,5X,'SUO=',F5.1,
             &5X,'ALFA=',F5.2)
0513          IF(NNEXT .EQ. 0) GO TO 7362
0514          DO 7360 I=1,NNEXT
0515          DO 7361 J=1,NOUT
0516          IF(TNEXT(I)-TU(J)) 7363,7364,7365
0517    7365  GO TO 7361
0518    7364  PNEXT(I)=PN(J)
0519          GO TO 7360
0520    7363  PNEXT(I)=PN(J-1)+(PN(J)-PN(J-1))*(TNEXT(I)-TU(J-1))/(TU(J)-TU(J-1
             &))
0521          GO TO 7360
0522    7361  CONTINUE
0523    7360  CONTINUE
0524          DO 7366 I=1,NNEXT
0525    7366  WRITE(NRITE,2700)PNEXT(I),TNEXT(I)
0526    2700  FORMAT(5X,'PRESS.=',F8.3,3X,'TEMP.=',F8.1)
0527    7362  CONTINUE
0528    101   FORMAT(4F10.0)
0529    103   FORMAT(15(I4,1X))
```

```
30     200   FORMAT(6F10.4)
31     300   FORMAT(4F10.0)
32     400   FORMAT(4F10.0)
33     600   FORMAT(1H1,////,20A4,//)
34     700   FORMAT(10X,'ENTHALPY COEFFICIENTS ARE:')
35     900   FORMAT(//,10X,'COMBUSTION BOMB VOLUME IS:',F16.4,5X,'CC')
36     910   FORMAT(10X,'INITIAL PRESSURE IS:',F22.4,4X,'ATM')
37     920   FORMAT(10X,'INITIAL TEMPERATURE IS:',F19.4,6X,'K')
38     930   FORMAT(10X,'EQUIVALENCE RATIO IS:',F21.4)
39     940   FORMAT(10X,'RESIDUAL FRACTION IS:',F21.3)
40    1200   FORMAT(//,5X,'MASS OF MIXTURE IS',F15.3,'GM')
41    1300   FORMAT(///,2X,'TIME',4X,'PRES',6X,'X',5X,'XDOT',1X,'NORMALIZE',1X,
          &' CUM.',1X,'BURNING',1X,'DELTA',5X,'TU',4X,'TBAV',1X,'ADIABATIC',1
          &X,'RHOU',4X,'RHOB',4X,'EUAV',4X,'EBAV',4X,'GAMMA U')
42    1400   FORMAT(32X,'FLAME',4X,'QOUT',2X,'VELOCITY',2X,5X,18X,'FLAME')
43    1500   FORMAT(32X,'RADIUS',42X,'TEMP')
44    1550   FORMAT(1X,'MSEC',4X,'ATM',12X,'PER MS',10X,'CAL/GM',2X,'CM/SEC',3X,
          &' CM  ',4X,'K',7X,'K',6X,'K',6X,'KG/M3',3X,'KG/M3',2X,'CAL/GM',2X
          &,'CAL/GM')
45    1600   FORMAT(2X,F5.1,2F7.3,2F8.3,F8.3,F8.2,F9.5,3F8.0,2F9.3,2F8.1,F8.3)
46    2050   FORMAT(//,3X,'RMS OF RADII WHEN IONIZATION PULSES OCCUR=',F8.5,'
          & MM')
47    2100   FORMAT(//,3X,'BALANCING PRESSURE=',F27.3,' ATM')
48    2200   FORMAT(3X,'TRANSDUCER PRES. WHEN SWITCH IS CLOSED=',F7.3,' ATM')
49    2250   FORMAT(3X,'TRANSDUCER PRES. INCLUDING CORRECTION=',F8.3,' ATM')
50    2300   FORMAT(3X,'PERCENTAGE ERROR=',F9.2)
51    2400   FORMAT(//,3X,'RADIUS OF FLAME FRONT(USING LASER)=',F7.3,' CM')
52    2500   FORMAT(3X,'DELTA RADIUS/RADIUS OF LASER  =',F14.3,' %')
53           END
```

```
RAN IV-PLUS V02-51          15:43:56    20-SEP-79              PAGE 1
ISP.FTN      /TR:BLOCKS/WR

C********************************************************************************
C
C     SUBROUTINE TRANSP
C
C     PURPOSE:
C       TO CALCULATE VISCOSITY,FROZEN THERMAL CONDUCTIVITY OF A
C       HOMOGENEOUS MIXTURE OF CARBON DIOXIDE,WATER,CARBON MONOXIDE,
C       HYDROGEN,OXYGEN,AND FUEL.AND DIFFUSIVITY COEFFICIENT OF
C       FUEL AND AIR.
C
C     USAGE:
C       CALL TRANSP(SIGMA,EPOVRK,X,T,P,VISC,THCOND,DIFFUS)
C
C     DESCRIPTION OF PARAMETERS:
C       GIVEN:
C       SIGMA - MOLECULAR DIAMETER OF FUEL FOR A LENNARD-JONES (12-6)
C               POTENTIAL (ANGSTROMS)
C       EPOVRK- DEPTH OF POTENTIAL WELL DIVIDED BY BOLTZMAN,S CONSTANT
C               FOR THE LENNARD-JONES (12-6) POTENTIAL OF THE FUEL
C               (DEG K)
C       X     - COMPOSITION VECTOR OF DIMENSION SEVEN
C       X(1)  - CARBON DIOXIDE MOLE FRACTION
C       X(2)  - WATER VAPOR MOLE FRACTION
C       X(3)  - CARBON MONOXIDE MOLE FRACTION
C       X(4)  - HYDROGEN MOLE FRACTION
C       X(5)  - OXYGEN MOLE FRACTION
C       X(6)  - NITROGEN MOLE FRACTION
C       X(7)  - FUEL MOLE FRACTION
C       T     - TEMPERATURE OF THE MIXTURE (DEG K)
C       P     - PRESSURE OF THE MIXTURE (ATM)
C       GIVEN IN COMMON AREA/FUEL/:
C       AF(I) - 6 DIMENSIONAL VECTOR OF ENTHALPY COEFFICIENTS SUCH THAT
C               THE ENTHALPY OF FUEL VAPOR AS A FUNCTION OF TEMPERATURE
C               (T DEG K) IS GIVEN BY:
C               H(T)=AF(1)*ST+(AF(2)*ST**2)/2+(AF(3)*ST**3)/3
C                 +(AF(4)*ST**4)/4-AF(5)/ST+AF(6)
C               WHERE ST=T/1000 AND H(T)= <KCAL/MOLE>
C               THIS PROGRAM ASSUMES THAT FUNCTION H(T) IS VALID OVER
C               THE FOLLOWING TEMPERATURE RANGE: 300 < T < 1500
C               ENTHALPY DATUM STATE IS T=0 ABSOLUTE WITH O2,N2,AND
C               H2 GASEOUS AND C GRAPHITE.
C       ENW   - AVERAGE NUMBER OF NITROGEN ATOMS PER FUEL MOLECULE
C       CX    - AVERAGE NUMBER OF CARBON ATOMS PER FUEL MOLECULE
C       HY    - AVERAGE NUMBER OF HYDROGEN ATOMS PER FUEL MOLECULE
C       OZ    - AVERAGE NUMBER OF OXYGEN ATOMS PER FUEL MOLECULE
C       QLOWER- LOWER HEATING VALUE (KCAL/G)
C
C     RETURNS:
C       VISC  - VISCOSITY OF THE MIXTURE (G/CM-SEC) OR (POISE)
C       THCOND- FROZEN THERMAL CONDUCTIVITY OF THE MIXTURE
C               (CAL/CM-SEC-DEG K)
C       DIFFUS- BINARY DIFFUSION COEFFICIENT OF FUEL AND AIR(CM**2/SEC)
C
C     REMARKS:
C       1) POLAR MOLECULES WATER AND IN SOME CASES FUEL (E.G. CH3OH)
```

```
       C            ARE TREATED THE SAME AS NON-POLAR MOLECULES
       C         2) DIFFUSION COEFFICIENT OF THE MIXTURE IS APPROXIMATED AS
       C            BINARY DIFFUSION COEFFICIENT OF FUEL AND AIR
       C         3) CODED BY HAMEED METGHALCHI 253-6647 (ROOM 3-359  MIT)
       C
       C      METHODS AND REFERENCES:
       C         1) R.S.BROKAW :ALIGNMENT CHARTS FOR TRANSPORT PROPERTIES,
       C            VISCOSITY ?,THERMAL CONDUCTIVITY,AND DIFFUSION COEFFICIENTS
       C            FOR NON-POLAR GASES AND GAS MIXTURES AT LOW DENSITY.
       C            NASA TR R-81 1961.
       C         2) R.A.SVEHLA :ESTIMATED VISCOSITIES AND THERMAL CONDUCTIVITIES
       C            OF GASES AT HIGH TEMPERATURES. NASA TR R-132 1962.
       C         3) A.A.WESTENBERG :PRESENT STATUS OF INFORMATION ON TRANSPORT
       C            PROPERTIES APPLICABLE TO COMBUSTION RESEARCH.
       C            COMBUSTION & FLAME VOL. 1 #3 1957 P346
       C         4) DANON & ADMUR, I.J OF CHEM. PHYS. VOL. 50 P.4178 1969
       C
       C*******************************************************************
01             SUBROUTINE TRANSP(SIGMA,EPOVRK,X,T,P,VISC,THCOND,DIFFUS)
02             REAL*4 LMMIX1,LMMIX2,LMBDA1(7),LMBDA2(7),M(7),MJ,MI,MAIR
03             DIMENSION A(6,7,2),A1(42),A2(42),ETA(7),SIGMA1(7),EPS(7),CP(7),
       &          X(7)
04             EQUIVALENCE (A1(1),A(1,1,1)),(A2(1),A(1,1,2))
05             COMMON/FUEL/AF(6),ENW,CX,HY,OZ,QLOWER
       C
06             DATA A1/11.94033,2.098581,-0.47029,.037363,-.589447,-97.1418,
       1          6.139094,4.60783,-.9356009,6.669498E-02,.0335801,-56.62588,
       2          7.099556,1.275957,-.2877457,.022356,-.1598696,-27.73464,
       3          5.55568,1.787191,-.2881342,1.951547E-02,.1611828,.76498,
       4          7.865847,.6883719,-.031944,-2.68708E-03,-.2013873,-.893455,
       5          6.807771,1.453404,-.328985,2.561035E-02,-.1189462,-.331835,
       6          6*0.0/
07             DATA A2/4.737305,16.65283,-11.23249,2.828001,6.76702E-03,-93.75793
       7          ,7.809672,-.2023519,3.418708,-1.179013,1.43629E-03,-57.08004,
       8          6.97393,-.823819,2.942042,-1.176239,4.132409E-04,-27.19597,
       9          6.991878,.1617044,-.2182071,.2968197,-1.625234E-02,-.118189,
       &          6.295715,2.388387,-.0314786,-.3267433,4.35925E-03,.103637,
       -          7.092199,-1.295825,3.20688,-1.202212,-3.457938E-04,-.013967,
       $          6*0.0/
08             DATA SIGMA1/3.941,2.641,3.69,2.827,3.467,3.798,0.0/
09             DATA EPS/195.2,809.1,91.7,59.7,106.7,71.4,0.0/
10             DATA M/44.01,18.02,28.01,2.016,32.,28.02,0.0/,R/1.9872/
11             DATA MAIR/28.97/,SGMAIR/3.689/,EPSAIR/84./
       C
       C            STATEMENT FUNCTIONS FOR COLLISION INTEGRALS OMEGA(1,1)*,
       C            OMEGA(2,2)*,PHI(I,J),ANDPSI(I,J)
       C
12             OMEGA1(TSTAR)=AMAX1(1.464*TSTAR**(-0.493),1.145*TSTAR**(-0.177))
13             OMEGA2(TSTAR)=AMAX1(1.220*TSTAR**(-.1600),1.610*TSTAR**(-0.450))
14             PHI(ETAI,ETAJ,MI,MJ)=(1.+(ETAI/ETAJ)**0.5*(MJ/MI)**0.25)**2
       &                       /(2.*SQRT(2.*(1.+MI/MJ)))
15             PSI(PHIIJ,MI,MJ)=PHIIJ*(1.+2.41*(MI-MJ)*(MI-0.142*MJ)/(MI+MJ)**2)
       C
       C            CALCULATE THE VISCOSITY AND THERMAL CONDUCTIVITY OF THE
       C            INDIVIDUAL SPECIES
```

```
TRAN IV-PLUS V02-51          15:43:56    20-SEP-79           PAGE 3
NSP.FTN       /TR:BLOCKS/WR

      C
6             IR=1
7             IF(T.LT.500.) IR=2
8             ST=T/1000.
9             DO 1 I=1,6
0             A1(I+36)=AF(I)
1        1    A2(I+36)=AF(I)
2             M(7)=14.*ENW + 12.*CX + HY + 16.*OZ
3             SIGMA1(7)=SIGMA
4             EPS(7)=EPOVRK
5             DO  2 I=1,7
6             IF(X(I).EQ.0.) GO TO 2
      C
      C           SINCE FOR MOST FUELS THE ENTHALPY COEFFICIENTS ARE VALID ONLY
      C           FOR T<1500, WE ASSUME CP(7)=CP(7) EVALUATED AT T=1500 FOR
      C           THOSE CASES WHERE T>1500.
      C
7             IF(I.EQ.7 .AND. ST.GT.1.5) ST=1.5
8             CP(I)=((A(4,I,IR)*ST+A(3,I,IR))*ST+A(2,I,IR))*ST+A(1,I,IR)
      &          +A(5,I,IR)/ST**2
9             TSTAR=T/EPS(I)
0             ETA(I)=26.693E-06*SQRT(M(I)*T)/SIGMA1(I)**2/OMEGA2(TSTAR)
1             LMBDA1(I)=3.75*R*ETA(I)/M(I)
2             LMBDA2(I)=0.88*(0.4*CP(I)/R-1.)*LMBDA1(I)
3        2    CONTINUE
      C
      C           CALCULATE VISCOSITY AND THERMAL CONDUCTIVITY OF THE MIXTURE
      C
4             ETAMIX=0.
5             LMMIX1=0.
5             LMMIX2=0.
7             DO 4 I=1,7
3             IF(X(I).EQ. 0.) GO TO 4
9             DEN1=1.0
0             DEN2=1.0
1             DO 3 J=1,7
2             IF(J .EQ. I .OR. X(J).EQ.0.) GO TO 3
3             DUMMY=PHI(ETA(I),ETA(J),M(I),M(J))
4             DEN1=DEN1+DUMMY*X(J)/X(I)
5             DEN2=DEN2+PSI(DUMMY,M(I),M(J))*X(J)/X(I)
5        3    CONTINUE
7             ETAMIX=ETAMIX+ETA(I)/DEN1
3             LMMIX1=LMMIX1+LMBDA1(I)/DEN2
9             LMMIX2=LMMIX2+LMBDA2(I)/DEN1
0        4    CONTINUE
1             VISC=ETAMIX
2             THCOND=LMMIX1+LMMIX2
      C
      C         CALCULATE DIFFUSIVITY
      C
3             SIG=(SGMAIR+SIGMA1(7))/2.
4             EPVRK=SQRT(EPSAIR*EPS(7))
5             TSTAR=T/EPVRK
5             DIFFUS=2.628E-03*(SQRT((T**3)*(M(7)+MAIR)/(2.*M(7)*MAIR))
      &            /(P*(SIG**2)*OMEGA1(TSTAR)))
```

```
FORTRAN IV-PLUS V02-51        15:43:56     20-SEP-79              PAGE 4
TRANSP.FTN        /TR:BLOCKS/WR

0057          RETURN
0058          END
```

```
C****************** VERSION 1.0 *** 4/23/79 *******************************
C
C        SUBROUTINE PPDTCL
C
C        PURPOSE:
C            TO CALCULATE  PDOT AT CONSTANT INCREMENT OF UNBURNED
C                GAS TEMPERATURE
C
C        USAGE:
C            CALL PPDTCL(P,TH,THN,T,TINC,NPTS,NDP,PN,PDOT,TN,NNPTS,PINF,
C                       TIMIN,EXPNT)
C
C        DESCRIPTION OF PARAMETERS:
C         GIVEN :
C            P     -PRESSURE
C            TH    -TIME (MSEC)
C            T     -UNBURNED GAS TEMPERATURE K
C            TINC  -TEMPERATURE INCREMENT K
C            NPTS  -NUMBER OF DATA POINTS
C            NDP   -DEGREE OF POLYNOMIAL WHICH FITS THE PRESSURE DATA
C
C         RETURNS:
C            THN   -TIME(MSEC)
C            PN    -PRESSURE
C            TN    -UNBURNED GAS TEMPERATURE K
C            PDOT  -TIME DERIVATIVE OF PRESSURE
C            NNPTS -NUMBER OF NEW ARRAYS OF DATA POINTS
C            PINF  -PRESSURE AT INFLECTION POINT (ATM)
C            TIMIN -TIME AT INFLECTION POINT
C            EXPNT -THE EXPONENT FOR THE FITTED CURVE FOR PRESSURE
C                   (P/PNOT=1+((PINF-PNOT)/PNOT)*(T/TIMIN)**EXPNT
C
C        SUBROUTINE REQUIRED:
C            HGASJO
C
C        METHOD:
C            FIT THE PRESSURE DATA LOCALLY TO A POLYNOMIAL OF DEGREE NDP
C            WITH A WEIGHTING FUNCTION OF W=EXP(-(T(I)-TN)**2/2(TINC/2)**2)
C            WHERE TN(I)=T(1)+(N-.5)*TINC
C
C        REMARKS:
C            IN CASE OF PROBLEM CONTACT HAMEED METGHALCHI 3-359 M.I.T.
C            AT  253-6647
C
C*****************************************************************************
        SUBROUTINE PPDTCL(X,TH,THN,T,TINC,NPTS,NDP,XN,XDOT,TN,NNPTS,
     &                  PINF,TIMIN,EXPNT)
        DIMENSION X(NPTS),T(NPTS),XDOT(30),C(3,5),R(260),XN(30),
     &          S(260),TH(NPTS),TN(30),THN(30)
        COMMON XINT(260),DELTDP(260)
C
C        CALCULATE CONSTANT INCREMENT OF TEMPERATURE
C
        DO 1 I=1,NPTS
        FI=I
```

```
0006            TN(I)=T(1)+(FI-.5)*TINC
0007            IF(TN(I)-T(NPTS)) 1,2,3
0008      1     CONTINUE
0009      2     NNPTS=I
0010            GO TO 4
0011      3     NNPTS=I-1
0012      4     CONTINUE
          C
          C
          C     FIND THE CORRESPONDING TIMES TO THE NEW TEMPERATURE ARRAY
          C
0013            DO 17 I=1,NNPTS
0014            DO 14 J=1,NPTS
0015            IF(TN(I)-T(J)) 16,15,14
0016     15     THN(I)=TH(J)
0017            GO TO 17
0018     16     THN(I)=TH(J-1)+(TN(I)-T(J-1))*(TH(J)-TH(J-1))/(T(J)-T(J-1))
0019            GO TO 17
0020     14     CONTINUE
0021     17     CONTINUE
          C
          C     FIT DATA TO POLYNOMIALS OF DEGREE NDP
          C
0022            DO 5 I=1,NNPTS
0023            K1=2*NDP+1
0024            S(1)=0.0
0025            DO 6 J=1,NPTS
0026            DELTDP(J)=TH(J)-THN(I)
0027            XINT(J)=2.71828**(-2*(T(J)-TN(I))**2/(TINC**2))
0028      6     S(1)=S(1)+XINT(J)
0029            DO 7 K=2,K1
0030            S(K)=0.0
0031            DO 7 J=1,NPTS
0032      7     S(K)=S(K)+XINT(J)*DELTDP(J)**(K-1)
0033            K2=NDP+1
0034            R(1)=0.0
0035            DO 8 J=1,NPTS
0036      8     R(1)=R(1)+X(J)*XINT(J)
0037            DO 9 K=2,K2
0038            R(K)=0.0
0039            DO 9 J=1,NPTS
0040      9     R(K)=R(K)+(DELTDP(J)**(K-1))*XINT(J)*X(J)
0041            DO 10 N=1,K2
0042            DO 10 J=1,K2
0043     10     C(N,J)=S(N-1+J)
0044            K3=NDP+2
0045            DO 11 N=1,K2
0046     11     C(N,K3)=R(N)
          C
          C     CALL SUBROUTINE HGASJO TO SOLVE NDP LINEAR EQUATIONS
          C
0047            CALL HGASJO(C,K2)
0048            XN(I)=C(1,1)
0049            XDOT(I)=C(2,1)
0050      5     CONTINUE
0051            DO 12 I=2,NNPTS
```

```
0052              IF(XDOT(I).LT.XDOT(I-1)) GO TO 13
0053        12    CONTINUE
0054              GO TO 18
0055        13    PINF=XN(I-1)
0056              TIMIN=THN(I-1)
0057              PDTINF=XDOT(I-1)
0058              EXPNT=TIMIN*PDTINF/PINF
0059              GO TO 19
0060        18    PINF=XN(NNPTS)
0061              TIMIN=THN(NNPTS)
0062              PDTINF=XDOT(NNPTS)
0063              EXPNT=TIMIN*PDTINF/PINF
0064        19    CONTINUE
0065              RETURN
0066              END
```

METHANOL   4:25 P.M. 8/3/79

      ENTHALPY COEFFICIENTS ARE:
  -2.7058   44.1677 -27.5009   7.2193   0.2100 -42.9501

        COMBUSTION BOMB VOLUME IS: 1853.3333   CC
        INITIAL PRESSURE IS: 1.0000   ATM
        INITIAL TEMPERATURE IS: 298.0000   K
        EQUIVALENCE RATIO IS: 1.2000
        RESIDUAL FRACTION IS: 0.000

    MASS OF MIXTURE IS   2.220GM

TIME	PRES	X	XDOT	NORMALIZE FLAME RADIUS	CUM. QOUT	BURNING VELOCITY	DELTA	TU	TBAV	ADIABATIC FLAME TEMP	RHOU	RHOB	EUAV	EBAV	GAMMA U
MSEC	ATM		PER MS		CAL/GM	CM/SEC	CM	K	K	K	KG/M3	KG/M3	CAL/GM	CAL/GM	
9.24	1.088	0.009	0.003	0.411	0.011	47.57	0.00035	305.	2162.	2116.	1.274	0.162	-168.3	-310.7	1.360
13.76	1.293	0.031	0.007	0.585	0.053	45.45	0.00140	319.	2213.	2126.	1.447	0.188	-165.6	-293.4	1.357
16.54	1.526	0.056	0.012	0.679	0.105	48.63	0.00239	333.	2251.	2135.	1.636	0.218	-163.0	-280.7	1.355
18.60	1.783	0.085	0.017	0.742	0.163	51.03	0.00321	347.	2289.	2145.	1.834	0.252	-160.3	-270.6	1.352
20.37	2.077	0.118	0.022	0.790	0.231	52.37	0.00394	361.	2310.	2154.	2.054	0.289	-157.6	-260.3	1.349
21.96	2.408	0.155	0.028	0.828	0.308	54.00	0.00457	375.	2338.	2164.	2.293	0.331	-154.8	-250.5	1.346
23.38	2.781	0.198	0.035	0.858	0.392	56.28	0.00508	389.	2364.	2174.	2.553	0.378	-152.1	-241.1	1.343
24.69	3.191	0.245	0.041	0.884	0.485	56.65	0.00550	403.	2386.	2183.	2.827	0.430	-149.3	-232.6	1.340
25.93	3.650	0.298	0.049	0.905	0.587	58.41	0.00585	417.	2411.	2193.	3.125	0.487	-146.5	-224.4	1.337
27.13	4.170	0.359	0.059	0.924	0.703	60.99	0.00616	431.	2433.	2203.	3.454	0.551	-143.7	-216.3	1.334
28.21	4.729	0.424	0.069	0.940	0.822	63.55	0.00637	445.	2454.	2213.	3.794	0.619	-140.8	-208.9	1.331
29.24	5.359	0.499	0.085	0.954	0.954	68.48	0.00655	459.	2474.	2223.	4.169	0.696	-137.9	-201.7	1.329
30.17	6.058	0.582	0.108	0.967	1.095	77.54	0.00667	473.	2493.	2233.	4.572	0.780	-135.0	-194.7	1.326
30.97	6.825	0.673	0.130	0.978	1.241	93.48	0.00673	487.	2512.	2242.	5.003	0.872	-132.1	-188.0	1.323
31.73	7.691	0.777	0.143	0.988	1.395	81.84	0.00680	501.	2530.	2252.	5.481	0.976	-129.4	-181.3	1.325
32.52	8.592	0.885	0.117	0.997	1.588	60.36	0.00690	515.	2547.	2261.	5.956	1.083	-126.4	-175.3	1.321

IONIZATION PROBE	TIME MSEC	PRESSURE ATM	P/PMAX	RADIUS CM	NORMALIZED DISTANCE RADIUS	FROM WALL(MM)	X	TU K
1	32.670	8.730	0.960	7.577	0.994	0.428	0.902	517.1
2	32.220	8.257	0.908	7.545	0.990	0.750	0.845	510.2
3	32.150	8.172	0.899	7.538	0.989	0.819	0.835	509.7

MAX TIME= 33.73 MAX PRES.= 9.09 MAX TU=522.23

  RMS OF RADII WHEN IONIZATION PULSES OCCUR= 0.17022 MM

  BALANCING PRESSURE=   7.755 ATM
  TRANSDUCER PRES. WHEN SWITCH IS CLOSED= 8.098 ATM
  TRANSDUCER PRES. INCLUDING CORRECTION=   7.963 ATM
  PERCENTAGE ERROR=   2.74

  RADIUS OF FLAME FRONT(USING LASER)= 6.443 CM
  DELTA RADIUS/RADIUS OF LASER =   0.326 %
REDUCED DATA TO FILE MET003

  SU=SUO*(T/TO)**ALFA   TO=450.0   SUO= 69.6   ALFA= 1.27
    PRESS.= 3.098   TEMP.= 400.0
    PRESS.= 7.603   TEMP.= 500.0

FIG. I.1   A Typical Computer Result Showing Laminar Burning Velocity as a
           Function of Measured Pressure for Methanol-Air Mixture of
           Equivalence Ratio of 1.2 with Initial Pressure of 1 Atm and
           Initial Temperature of 298 K